

REVIEW

Smart materials for drug delivery and cancer therapy

Yao Yang¹ | Weiwei Zeng¹ | Ping Huang¹ | Xiaowei Zeng¹ | Lin Mei^{1,2} ¹ Institute of Pharmaceutics, School of Pharmaceutical Sciences (Shenzhen), Sun Yat-sen University, Shenzhen, China² Tianjin Key Laboratory of Biomedical Materials, Key Laboratory of Biomaterials and Nanotechnology for Cancer Immunotherapy, Institute of Biomedical Engineering, Chinese Academy of Medical Sciences & Peking Union Medical College, Tianjin, China**Correspondence**

Xiaowei Zeng, Institute of Pharmaceutics, School of Pharmaceutical Sciences (Shenzhen), Sun Yat-sen University, Shenzhen 518107, China.

Email: zengxw23@mail.sysu.edu.cn

Lin Mei, Tianjin Key Laboratory of Biomedical Materials, Key Laboratory of Biomaterials and Nanotechnology for Cancer Immunotherapy, Institute of Biomedical Engineering, Chinese Academy of Medical Sciences & Peking Union Medical College, Tianjin 300192, China.

Email: meilin7@mail.sysu.edu.cn

[The copyright line for this article was changed on 31 March 2021 after original online publication.]

Funding information

National Natural Science Foundation of China, Grant/Award Numbers: 31922042, 81771966, 32071342; Guangdong Special Support Program, Grant/Award Number: 2019TQ05Y209; Fundamental Research Funds for the Central Universities, Grant/Award Number: 19ykzd31

Abstract

Until now, enormous smart materials have been engineered with endogenous stimulators such as pH, reactive oxygen species, glutathione, hypoxia and enzyme, or exogenous stimulators such as temperature, light, ultrasound, radiation, and magnetic field in drug delivery. As footstone of stimuli-responsive nanocarriers, endogenous/exogenous responsive smart materials possess many properties, such as responding ability to specific triggers, controlled drug release, long blood circulation, increased tumor accumulation, “ON-OFF” switch activities, enhanced diagnostic accuracy, and therapeutic efficacy. Smart materials have attracted considerable attention because they provide likelihood strategy for individualized and comprehensive therapy. In this review, significant research achievements of smart materials responsive to different triggers including their synthesis and formulation mechanism, responsive mechanism, applications, multiple functions are summarized and discussed separately. We primarily focus on the studies in the past few years (2017–2020). The current situation and remaining challenges of stimuli-sensitive materials-based nanocarriers for clinical translation are discussed rationally at the end. It is hope that this timely and overall review would provide some helpful information for researchers in this field.

KEY WORDS

cancer therapy, drug delivery, exogenous triggered, smart materials, tumor microenvironment responsive

1 | INTRODUCTION

The engineered materials used for spatially and/or temporally controlled drug release were first carried out in the 1970s.¹ More recently, the smart materials for stimuli-responsive applications of drug delivery, diagnostics,

theranostics, tumor imaging, and biomedical devices have obtained growing development.^{2–5} A major research focus is smart materials for cancer drug delivery. These smart materials are inspired to meet the demands of the booming nanocarriers that act as promising drug delivery vehicles to tumors. Because the endogenous/exogenous responsive

This is an open access article under the terms of the [Creative Commons Attribution License](#), which permits use, distribution and reproduction in any medium, provided the original work is properly cited.

© 2021 The Authors. *VIEW* published by Shanghai Fuji Technology Consulting Co., Ltd, authorized by Professional Community of Experimental Medicine, National Association of Health Industry and Enterprise Management (PCEM) and John Wiley & Sons Australia, Ltd.

smart materials-based nanocarriers under rational design and implementation with tumor-specific drug delivery ability can surmount their barriers during circulation or in tumors, avoiding protein corona, enzymatic degradation, cargos leakage or burst release in undesired healthy tissues, prolonging blood circulation, as well as increasing tumor accumulation, etc.^{6,7} Thus, the stimuli-sensitive nanocarriers possess desired and controlled cargo delivery, release, and activation in specific regions, facilitating powerful antitumor activities without harmful side effects on normal sites.^{8–10}

Typical stimulators applied to smart materials for cancer drug delivery include endogenous stimulators such as pH, reactive oxygen species (ROS), glutathione (GSH), hypoxia and enzyme, or exogenous stimulators such as temperature (T), light, ultrasound (US), radiation, and magnetic field.^{11,12} These smart materials with biocompatibility and degradability would show dramatic conformational changes when they response to mild physical/chemical.¹³

Generally, endogenous-triggered smart materials for drug delivery are always synthetic bioresponsive polymers that can be deconstructed into functional motifs with biological sensitivities and assistant structures such as polyethylene glycol (PEG) shell, targeting moieties and hydrophobic units. These smart polymers can be further conducted into nanocarriers or prodrugs via appropriate fabrication methodologies. And the main drug release mechanism of the formed bioresponsive nanocarriers or prodrugs can be summarized as endogenous-triggered carrier solubility change, endogenous-triggered carrier cleavage, or endogenous-triggered prodrug linker cleavage.

Comparing with endogenous-triggered smart materials, exogenous-triggered smart materials have their advantages of being stimulated at a desired time, location, and/or dose.¹⁴ The pathophysiological features can be highly heterogeneous. And features of patients might vary from each other. Therefore, it is difficult for endogenous-triggered smart materials to develop drug delivery system (DDS) with predictable release kinetics and artificially controlled release after administration. The exogenous-triggered smart materials make it possible to prepare the DDS with real-time modulation of drug levels and can be complementary with the endogenous-triggered smart materials. The united-triggered DDS could repeatedly switch drug release on and off and enable pathophysiological-sensitive drug release. This makes possible the time, location, intensity, and duration-controlled drug delivery, resulting in better match to the actual needs of the patients. Furthermore, exogenous-triggered smart materials-based DDSs induce additional therapeutic effects such as photothermal

therapy (PTT), photodynamic therapy (PDT), and sonodynamic therapy (SDT), as well as imaging abilities such as fluorescence imaging (FLI), photoacoustic imaging (PAI), US, and magnetic resonance imaging (MRI).¹⁵

As the fast-growing smart materials involve a wide range of applications, this review specially focuses on the latest progress and achievements of smart materials in drug delivery that is sensitive to either endogenous or exogenous stimuli. Different stimuli-responsive strategies and design principles of materials have been presented and discussed in detail. This review is expected to clearly summarize the examples of smart materials in drug delivery and provide an overview on their current knowledge and perspectives.

2 | ENDOGENOUS-TRIGGERED SMART MATERIALS

The physiological parameters of tumor microenvironment (TME), such as pH, ROS, GSH, hypoxia, and enzyme, often vary from that of the normal tissues and intracellular compartment.^{16,17} These physiological variations are attractive targets to design bioresponsive materials for controlled drug release or even multistage drug delivery.

2.1 | pH-responsive smart materials

Compared with normal tissues, tumor tissues have a special microenvironment due to the differences in vascular structure, proliferation, and metabolism. A pH gradient exists between the tumor tissues and the normal sites. The pH of normal tissues and blood is about 7.4, while the pH of tumor extracellularly shows weak acidity (pH = 6.5–7.2), and the acidity of intracellular endosomes (5.0–6.5) and lysosomes (4.5–5.0) is lower. This is mainly due to the high glycolysis rate at the tumor sites that produces much lactic acid, which is known as the Warburg effect.¹⁸ To maintain the normal survival of tumor cells, acid is expelled to the outside of the cell, resulting in an environment of outer acid and inner base. Based on this, we can achieve the targeted release and targeted therapy of drugs. The special pH in the TME has become an effective target for drug delivery and controlled release. Drug delivery platforms for chemotherapy, gene therapy, PTT, or combinations of multiple therapies through pH responsive materials have shown great potential.^{19,20} In recent years, many pH-sensitive DDSs have been developed for tumor microenvironmental response, which can be divided into the following three categories. And the examples of them were summarized in Table 1.

TABLE 1 pH-responsive materials for drug delivery of cancer therapeutics

pH-sensitive sites	Function	Cargos	Linked materials	Nanocarriers	Ref.
Name and structure					
Acid sensitive bonds					
Imine bond 	Prodrug and carrier	Dox	BSA, benzaldehyde	nBSA-Dox nanocapsule	22
Ortho ester bond 	Prodrug	Rutin, DHA, HCPT	GLP, CPBA, DPA [†]	Self-assembled nanoparticles of RCGDDH	23
Hydrazone bond 	Prodrug	Dox	DEX, POEGMA	Self-assembled micelles of DOM@DOX	24
Acetal/ketal bond 	Nanoexpansion carrier	-	TPPC6MA, TTMA, POEGMA	Self-assembled micelles of POEGMA-b-[TPPC6MA-co-PTTMA]	25
Amide bond 	Carrier	CPT-11	Gal-P123, DC, mesoporous silica	GPDC-MSNs	26
Protonation and deprotonation					
Carboxyl 	Carrier	PTX	Chitosan, anisamide	Self-assembled micelles of a-OMPC	32
Imidazole 	Prodrug	NLG919	RGD, histidine	NLG-RGD NI	34
Polyacrylic acid	Structure changeable carrier	Erlotinib	Au NCs	P _A Au NCs	33
PLL-DMA	Charge-reversal carrier	p53 DNA	PEI, PLL-DMA	Microneedle patch of PCL and PEM	37
Peptides	Nanotransformer	Cypate	MEL [†] , HA	Self-assembled nanocomplexes MEL [†] /Cypate@HA	40
PDA					
	Dual drugloading carrier	DTX, BTZ	CA-PLGA, PDA, NH ₂ -PEG-FA	DTX-loaded CA-PLGA@PDA-PEG-FA+BTZ/NPs	45
	High-stability carrier	DOX, P-gp siRNA	BP, PDA, Apt	BP NSs	46
	Gatekeeper	DOX	Mesoporous silica, PDA, PEG-FA	MSNs	47

[†]Abbreviations: DPA, dithiodipropionic acid; MEL, melittin.

[‡]The bold words are prodrug in the DDS.

2.1.1 | Acid-sensitive bonds

When the carrier is constructed with acid-sensitive chemical bonds, H⁺-sensitive imine bond,^{21,22} ortho ester bond,²³ hydrazone bond (HDZ),²⁴ oxime bond, acetal/ketone bond,²⁵ amide bond,²⁶ and so on, are usually introduced into the system. Under normal physiological conditions, the drug carrier system remains stable. But when it reaches the tumor site, these acid-sensitive chemical bonds will break, causing drug release or partial carrier

separation. The HDZ is a common construction linker for pH-responsive drug delivery carriers. At pH 7.4, the HDZ hydrolyzes slowly and remains relatively stable, but a large amount of hydrolyzation occurs in the presence of endosomes or lysosomes. Zhang et al designed a bottlebrush-architecture carrier prodrug (DOM@DOX) based on dextran (DEX) polysaccharide that has abundant hydroxyl groups to realize wide chemical modifications. The anticancer drug doxorubicin (DOX) was connected to the DEX skeleton by the pH-sensitive

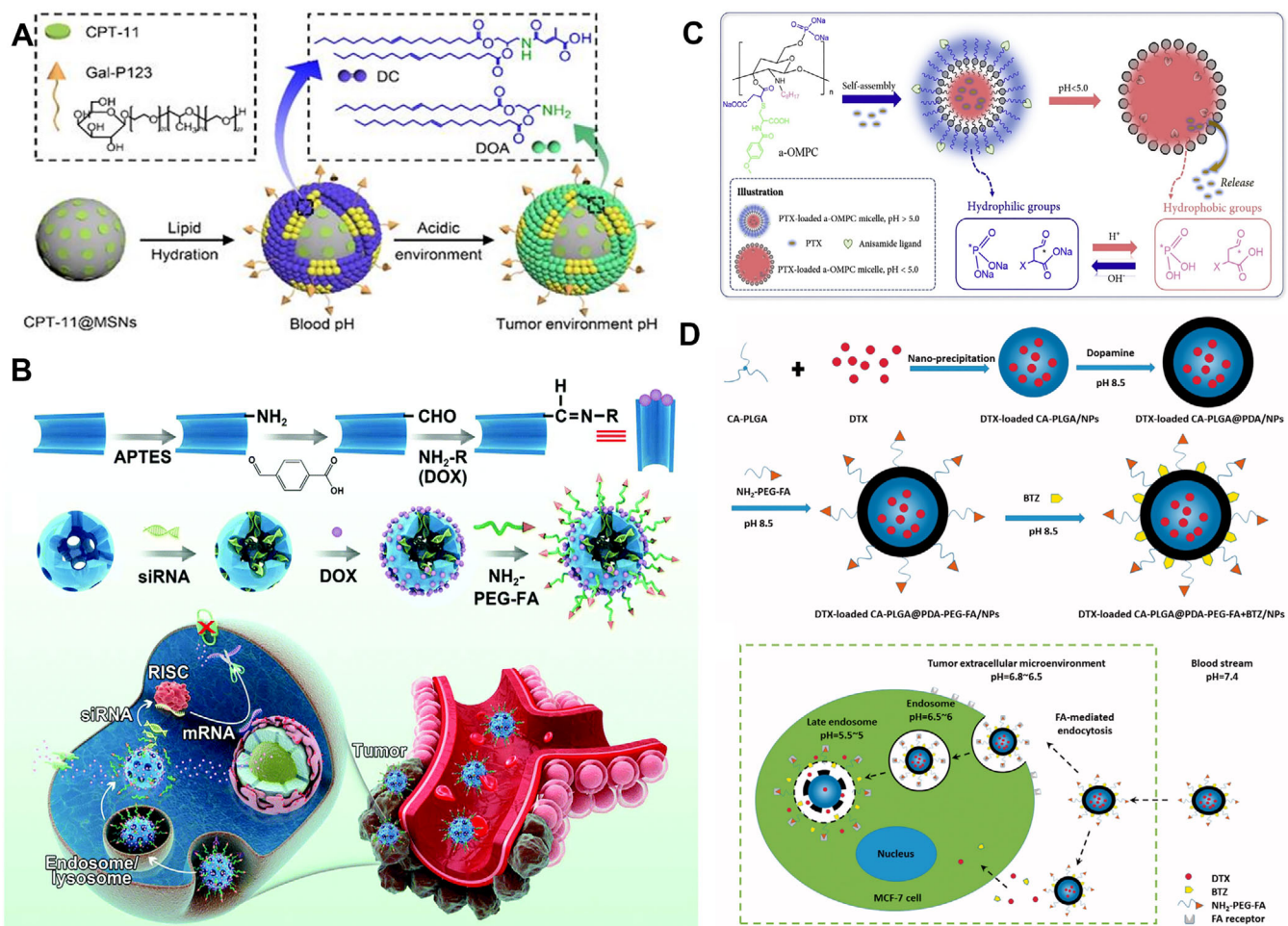


FIGURE 1 Several pH-responsive smart materials. (A) Schematic diagram of the structure and pH sensitivity of CPT-11@GPDC-MSNs. Reproduced with permission.²⁶ Copyright 2020, IJSP International Publisher. (B) Schematic illustration of the interaction between DOX and benzaldehyde, and the synthesis route of MSNs-siRNA@DOX-PEG-FA. Reproduced with permission.²⁸ Copyright 2017, Royal Society of Chemistry. (C) Schematic representation of self-assembled PTX-aM and pH-induced protonation of phosphate and carboxylate. Reproduced with permission.³² Copyright 2020, Elsevier. (D) Technological preparation process and pH-triggered intracellular release of DTX-loaded CA-PLGA@PDA-PEG-FA+BTZ/NPs. Reproduced with permission.⁴⁵ Copyright 2017, Taylor & Francis Inc

HDZ.²⁴ In addition, Li et al constructed lipid-coated nanoparticles (GPDC-MSNs) by a pH-sensitive lipid (2E)-4-(dioleostearin)-amino-4-carbonyl-2-butenonic (DC) containing amide bonds for enhanced hepatocellular carcinoma (HCC) therapy (Figure 1).²⁶ The nanoparticles were loaded with the anticancer drug irinotecan (CPT-11), with Gal-P123 (galactosyl-conjugated PEO-PPO-PEO) for HCC targeting. Under the acidic environment of tumor, the citraconic amide in DC hydrolyzes, facilitating cellular uptake. Further dissociation of lipid layer in the cell led to the explosive release of drug, which had better anti-tumor effect and lower systemic toxicity. Acid-sensitive chemical bonds are also widely used in polymer design. For example, Ma et al²⁷ constructed a three-segment prodrug polymer PMPC-b-P[MPA(Cap)-co-TPMA]-PAEMA(PMMTA_b-Cap), in which the outer hydrophilic block poly(2-methacryloyloxyethyl phosphorylcholine)

(PMPC) was connected to the inner block via a pH-sensitive benzoyl imide bonds, revealing strong biocompatibility and antiprotein adsorption due to the presence of zwitterionic phosphorylcholine. In such drug-carrying systems, in addition to wrapping the drug in a carrier, the drug itself can also act as a gated molecule. For example, Cheng et al designed a pH-responsive mesoporous silicon dioxide delivery system with drug self-gating (Figure 1B).²⁸ The amino groups of chemotherapy drug DOX and the benzaldehyde-modified mesoporous silica nanoparticles (MSNs) were connected through the benzoic acid-imine bond to control the MSNs hole exports. At the same time, P-gp siRNA was encapsulated in nanoparticles. In tumor acidic environment, the benzoic-acid-imine bond became sensitive and fractured, and then DOX and siRNA were released from this system, making the drug DOX itself as the gatekeeper. In addition, the nanoparticles were

modified with poly(ethylene glycol)-folic acid (FA) to enhance the targeting of drug therapy. As a result, this resulted in a “four in one” multifunctional nanodelivery system, reducing the potential harm of introducing other materials to hole closing, and showing great potential for cancer treatment. Recently, there have been some studies on the use of natural compounds, which was modified by acid-sensitive chemical bonds to serve as carriers for drug delivery to treat tumors.^{23,29} Dan et al used ganoderma lucidum polysaccharide (GLP) as a carrier to deliver rutin for cancer treatment. Rutin was linked to GLP via boric acid ester bond, simultaneously loading with two other anticancer drug, dihydroartemisinin (DHA), and 10-hydroxy camptothecin (HCPT).²³ The nanoparticle possessed acid responsive property. When it reached the tumor acid environment, its boric acid ester bond ruptured and rutin was released firstly. Moreover, on account of the anticancer activity of the carrier material GLP, experiments *in vivo* and *in vitro* showed that the DDS had minor side effects and could effectively kill the tumor cells. Due to the natural source, good safety, and biocompatibility of GLP, it has broad prospects for drug delivery.

2.1.2 | Protonation and deprotonation

Protonation/deprotonation is another strategy commonly used in DDSs. Carrier materials usually contain amino, carboxyl, sulfanilamide, nitrogen heterocyclic, etc.³⁰ In the tumor acidic pH environment, because of protonation and deprotonation, it will lead to charge shift,³¹ hydrophilic/hydrophobic change,³² swelling,³³ dissociation,³⁴ or solubility change,³⁵ then the binding force between the drug and the carrier is reduced, resulting in drug release. Because the positively charged delivery systems are accessible to adsorb and remove by phagocytic cells, these delivery systems are usually negatively charged or electrically neutral. Under normal physiological environment, they enable themselves with “invisible effect.” The excellent characteristic extends the cycle time and the half-life of the drugs. While under the stimulation of tumor site, it promotes the release of drugs and cellular internalization, improving the efficiency of the permeability and drug therapy.³⁶ Li et al designed an acidic microenvironment-responsive microneedle patch for gene therapy of subdermal tumors.³⁷ The p53 expression plasmid (p53 DNA) and the polymer dimethylmaleic anhydride-modified polylysine (PLL-DMA) composed pH-responsive polyelectrolyte multilayers (PEM). PLL-DMA is a widely used material with acid-responsive charge shift.³⁸ Under acidic environment, PLL-DMA reversed charge, which led to the

transition-layer collapse and promoted the rapid release of p53 DNA from the outermost layer. The microneedle patch could well penetrate the cuticle layer and show good inhibition rate on tumor growth. The design of this new drug delivery platform provides a great reference for the delivery of other biological macromolecules for tumor treatment. In addition to PLL-DMA, many other polymers usually protonate or deprotonate as acid-sensitive materials, too, such as poly(2-diisopropylamino) ethyl methacrylate (PDPAEMA), poly(4-vinyl pyridine) (P4VP), poly(2-azepane ethyl methacrylate) (PAEMA), poly(benzimidazole ethyl methacrylate) (PBM), etc.³⁹ Chitosan is a kind of polysaccharide with positive charge. It is considered as a promising backbone material for preparing amphiphilic polymers because of its unique biological characteristics. Qu et al synthesized an anisamide-conjugated N-octyl-N, O-maleoyl-O-phosphoryl chitosan (a-OMPC), which can self-assemble into amphiphilic micelles loaded with paclitaxel (PTX) (PTX-aM), showing pH responsiveness and targeting property (Figure 1C).³² When pH < 5.0, due to the protonation of phosphate/carboxylate, the hydrophobicity of the micelles increased, leading to the rapid release of PTX. Because of the simultaneous existence of amino and carboxyl groups in the protein peptides, they can also be modified and transformed for delivery through this strategy. In one study, Jia et al reported an intelligently form-switching nanotransformer MEL/Cypate @HA for therapeutic peptide delivery.⁴⁰

2.1.3 | Polydopamine (PDA)

Apart from the above two types of DDSs, there is a special pH-responsive smart material. PDA, a mussel-inspired material, which has good biocompatibility, adhesion, and photothermal conversion efficiency, can spontaneously form a copolymer film on the material surface. Under alkaline conditions, dopamine reacts with other catechins by oxidation, and the product then reacts with quinones to form PDA.^{41–43} In addition, PDA has an special pH sensitivity and can degrade in acidic environment, making it a good acid-sensitive material.⁴⁴ Although the degradation mechanism of PDA is still unclear, it has become a good drug delivery vehicle.⁴¹ Drug delivery platforms such as polymeric nanoparticles, black phosphorus (BP) nanocapsules, and manganese dioxide nanoparticles modified with PDA as the surface coating has improved stability, reduced the early release of drugs, and enhanced the effect of tumor treatment.^{45–47}

Zeng et al used a simple PDA modification method on the BP and designed a multifunctional codeelivery system.⁴⁶ The surface of PDA also contains

a large number of amino groups and hydroxyl groups, which can be modified with amines or thiols via Michael addition reaction or Schiff base reaction.^{48–50} Nie et al formed a star-shaped copolymer cholic acid-poly(lactide-co-glycolide) nanoparticles (CA-PLGA/NPs) with the anticancer drug docetaxel (DTX) in the package, coating with dopamine (Figure 1D).⁴⁵ The amino-poly(ethylene glycol) FA ($\text{NH}_2\text{-PEG-FA}$) and another anticancer drug, bortezomib, were then combined on the PDA coating for active targeting and anticancer enhancement, respectively. This dual DDS for breast cancer treatment provides a reference for enhanced chemotherapy due to the acid sensitivity of PDA and the coupling mechanisms it provides.

In a recent study, hollow mesoporous manganese dioxide (MnO_2) nanoparticles encapsulated the photosensitizer chlorin e6 (Ce6), which was then coated by PDA and modified by FA ($\text{MnO}_2@\text{Ce6@PDA-FA NPs}$).⁴⁷ This multifunctional platform combines PDT with PTT and greatly inhibits tumor growth. In a word, PDA possesses many fascinating properties and will have further development.

2.2 | Redox-triggered smart materials

ROS is generally consisted of the hydrogen peroxide (H_2O_2), superoxide anion (O_2^-), and hydroxyl radicals.⁵¹ Appropriate levels of ROS play important roles in the regulation of biological system by continually generating and eliminating.⁵² Mitochondrial malfunction, oncogenic stimulation, and increased metabolic activity would increase the ROS stress in cancer cells.⁵³ The ROS generation causes DNA-damaging development of drug-resistance occurrence that promotes cancerization and increases the cure difficulty. But it also provides new strategies for the treatment of cancer through ROS-mediated mechanisms. Thus, numerous ROS-triggered smart materials have been developed and applied in cancer treatment, and few cases are listed in Table 2. These materials mainly target hydrogen peroxide (H_2O_2) and hydroxyl radicals. As summarized in Table 2, major classes of ROS-responsive materials are thioether, thioketal, and arylboronic ester-based. Besides, diselenide, aminoacrylate, and other groups-based smart materials could also be seen in many works. These smart materials often self-assembled to amphiphilic nanomicelles and serve as prodrug or drug carrier.

In oxidative conditions, phase transition of thioether-containing polymers from hydrophobic sulfide to more hydrophilic sulfoxide or sulfone can be often observable.⁵² The drug release was attributed to ROS-induced carrier solubility change.^{54,55} Cheng et al made a delicacy design, and in this work, they fabricated a ROS-responsive free

blockage on the internal surface nanopores of MSNs.⁵⁶ In detail, the hydrophobic phenyl sulfide groups that contain thioether were modified on the internal surface nanopores of MSNs. Once stimulated by endogenous ROS of tumor cells, hydrophobic phenyl sulfide groups were oxidized into hydrophilic molecules. Thus, the nanopores would release DOX gradually with the wetting behavior change. Thioether-linked materials containing ester bonds adjacent to either side of the sulphur atom are always applied to the design of prodrug.^{57,58} Because these thioether-containing polymers possess not only the ROS-induced solubility switch ability but also further hydrolysis cleavage of the proximal ester bond. For example, Wang et al developed a self-strengthened oxidation-responsive prodrug-based polymeric micelles (LPC/PTX-S-LA PMs).⁵⁹ β -lapachone (LPC) could generate a considerable amount of ROS by activated tumor-overexpressed NQO1 (quinone oxidoreductase-1)-mediated redox cycle. Thus, endogenous high ROS levels and NQO1-generated ROS in tumor cells facilitate PTX-S-LA to release PTX synergistically for cancer chemotherapy. Thioethers were gifted dual redox-responsive ability of ROS and GSH, and several dual redox-responsive materials were successfully developed.^{54,60} As shown in Figure 2A, Yin et al first used the dual-responsive bonds of ROS and GSH to link polymers as amphiphilic block copolymer prodrugs (GR-BCPs).⁶⁰ Moreover, GR-BCPs were compared with R-BCPs and G-BCPs, results showed that there was no significant difference in blood circulation and tumor accumulation among them but GR-BCPs showed the most efficient antitumor activity with few side effects. Selenide-/telluride-containing materials share the similar design ideas with thioether.^{61–63} Yu et al prepared the nanoparticles by self-assemble amphiphilic copolymers that composed of a PEG segment and a selenide-containing hydrophobic polycarbonate segment with a small fraction of coumarin-modified chromophore. Upon encounter with the high ROS level of cancer cells, the hydrophobic polycarbonate segment would change to hydrophilic with drug release, and was accompanied by the coumarin-modified chromophore practicing fluorescence decrease. Therefore, these amphiphilic copolymers made system could reveal the internal fate of nanoparticles (integrity change and drug release) and endogenous ROS-level change.

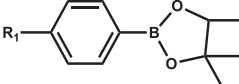
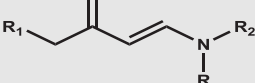
Thioketal-containing polymers are another important type of ROS-responsive smart materials. These thioketal were specially cleaved by endogenous ROS to two thiols, causing the intelligent materials crushed into pieces and drug release from nano system or prodrug.^{64–68} For instance, Wang et al developed an ROS-sensitive amphiphilic polymeric micelle system with degradable thioketal linkages that efficiently coloaded DOX and

TABLE 2 ROS-responsive materials for drug delivery of cancer therapeutics

ROS-sensitive linkers	Function	Cargos	Linked materials	Nanocarriers	Ref.
Thioether R_1-S-R_2	Solubility change carrier	DOX, NO	PEG, GSNO [†] (NO donor)	Self-assemble nanomicelles of PEG-PPS [†] -GSNO	54
	Free-blockage drug release	DOX	Mesoporous silica	MSNs	56
	Prodrug	CTX [†] , pyropheophorbide a	Oleic acid (OA), CTX	Self-assemble nanomicelles of OA-S-CTX and DSPE [†] -PEG _{2K}	57
	Prodrug	DTX, LPC	Linoleic acid (LA), DTX	Self-assemble nanomicelles of LA-S-DTX and DSPE-PEG _{2K}	58
	Prodrug	PTX	LA, PTX	Self-assemble nanomicelles of LA-S-PTX and PEG-PDLLA [†]	59
	Prodrug and carrier	CPT	CPT, PEG	Self-assemble nanomicelles of PEG-PGRCPT-CPT	60
Selenide R_1-Se-R_2	Solubility change carrier	PTX, Cisplatin	PEG, coumarin	Self-assemble nanomicelles of copolymers composed of PEG and selenide-containing hydrophobic polycarbonate	62
Telluride R_1-Te-R_2	Interaction change between Te and Pt	Cisplatin	PEG	Self-assemble nanomicelles of PEG-PUTe-PEG	63
Thioketal 	Self-cleavage carriers	DOX, IR780	PEG	Self-assemble nanomicelles of PEG-PTK	68
	Self-cleavage carriers	DOX, PhA	PEG, stearamine (C18)	Self-assemble nanomicelles of PEG-TK-C18	83
	Light-triggered size-reducing carriers	CPT, Ce6	Ce6, cyclic phosphate monomer	Self-assemble nanomicelles of a hyperbranched polyphosphoester containing TK and Ce6	69
	Formulation stability assistance	DOX	pLys [†]	Self-assemble nanomicelles of PEG-pLys-pBla [†]	70
	Prodrug	DOX, Ce6	DOX, PPE [†]	Self-assemble nanomicelles of PPE-TK-DOX	71
	Prodrug	PTX	PTX	Red blood cell membrane-camouflaged nanoparticles	72

(Continues)

TABLE 2 (Continued)

ROS-sensitive linkers	Function	Cargos	Linked materials	Nanocarriers	Ref.
	Prodrug	DOX, <u>Ce6</u>	DOX, PEG-PBC [†]	Self-assemble nanomicelles of PEG-PBC-TK-DOX	67
Arylboronic ester	Self-cleavage carriers	DNA		Condense polyplexes of DNA and polysulfoniums	77
	Prodrug	PTX	PTX, PEG	Self-assemble nanomicelles of PEG-B-PTX	76
	Self-cleavage carriers	DOX	PEG	Self-assemble nanomicelles of mPEG-b-P(PA-altGPBAe) [†]	74
		TPZp [†] , <u>Ce6</u>	PEG	Self-assemble nanomicelles of mPEG-PBBA [†]	75
Aminoacrylate	Prodrug	PTX, <u>bodipy</u>	PTX, bodipy	Self-assembled nanoparticles of PEG-PGA [†] -β-CD	81
					
Diselenide	Self-cleavage carriers	DTX, LPC	pullulan polysaccharide	Crosslinked nanoparticles of pullulan polysaccharide diselenide	79
R₁—Se—Se—R₂					

[†]Abbreviations: CTX, Cabazitaxel; DSPE, 1,2-distearoyl-sn-glycero-3-phosphoethanolamine; GSNO, S-nitrosoglutathione; (mPEG-b-P(PA-altGPBAe), poly(ethylene glycol)-block-poly(phthalic anhydride-alter-glycidyl propargyl ether); PLLA, poly (D, L-lactic acid); PBC, polycarbonate; pBla, poly(N6-carbobenzoxy-L-lysine); pLys, poly(N6-carbobenzoxy-L-lysine); PPE, polyphosphoester; PPS, poly (propylene sulfide); TPZp, hydrophobic TPZ prodrug; PBBA, poly(4-(hydroxymethyl)-phenylboronic acid pinacol ester).

[‡]The bold words are prodrugs in the DDS.

[§]The underlined words are photosensitizers.

IR780 (a cyanine dye with strong absorption at 780 nm). Some hyperbranched ROS-responsive size-reducing polymers containing thioketal were also designed for preparing of nano DDS.^{65,66,69} Among these works, Hua Jin and coworkers synthesized the ROS-responsive amphiphilic hyperbranched polyphosphoesters (PPEs) by self-condensing ring open polymerization of a novel cyclic phosphate monomer (CPM, as seen in Figure 2B).⁶⁹ And then the drug-loaded nanoparticles were obtained through self-assembly of this amphiphilic hyperbranched PPE. These obtained nanoparticles would experience dual light and ROS-triggered size-reducing after administration. In the work of Zhang et al, the ROS-responsive thioketal cross-linker served as the formulation stability assistance and the fast drug release *in situ* implementation layer.⁷⁰ In detail, the thioketal-containing cross-linker, N-hydroxysuccinimide ester, was constructed for cross-linking with the amphiphilic micelles' interlace sites.

The ROS-responsive thioketal linker is applied in the designing of the prodrugs too.^{67,71,72} Pei et al designed a photosensitive prodrug called PPE-TK-DOX. In this work, DOX was conjugated to the branch chain of PPE via a thioketal linker, which simultaneously encapsulated the photosensitizer Ce6 during self-assembly. The obtained Ce6@PPE-TK-DOX nanoparticles could maintain ROS-activated locoregional drug release and realize specific chemotherapy in fighting cancer.

Thioether and thioketal are the commonest moieties applied to fabricate ROS-responsive polymers. Given the fact above, Xu et al synthesized three amphiphilic copolymers including mPEG-poly(ester-thioether), mPEG-poly(thioketal ester), and mPEG-poly(thioketal-ester-thioether) and investigated their ROS-responsive ability as drug nanocarriers.⁷³ The results showed that mPEG-poly(ester-thioether) nanoparticles present the highest ROS sensitivity and fastest drug release rate,

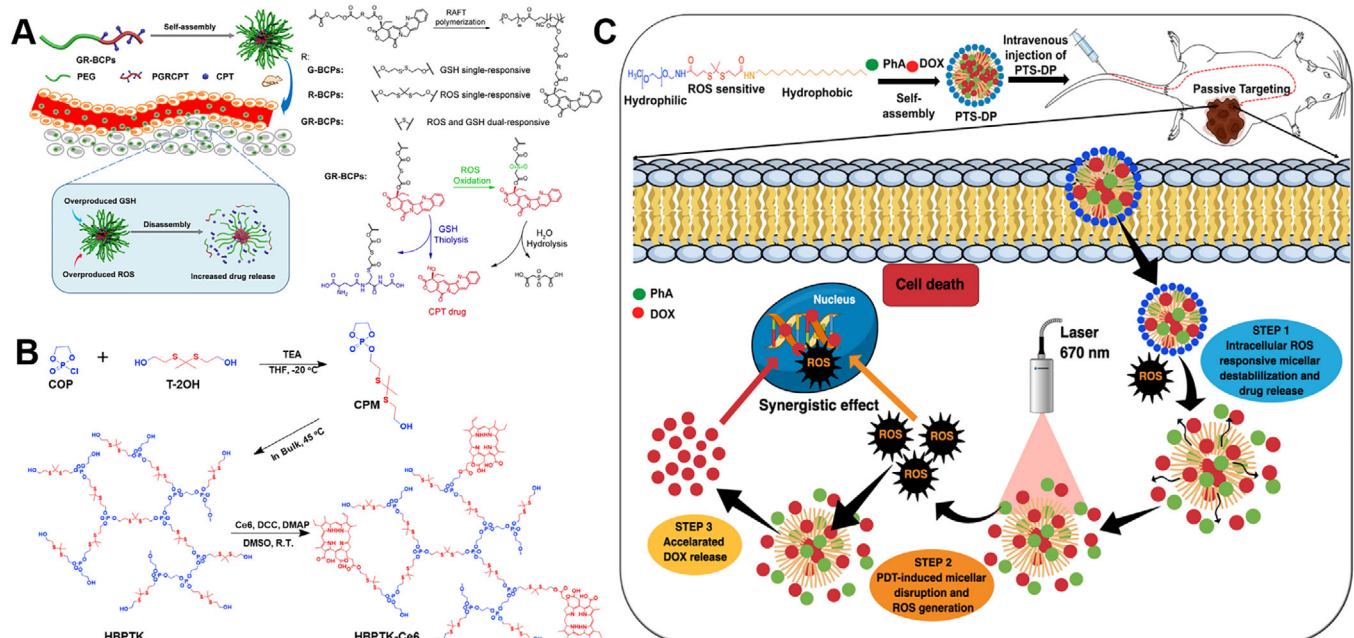


FIGURE 2 (A) Synthetic routes and drug release mechanism of G-BCPs, R-BCPs, and GR-BCPs micelles. Reproduced with permission.⁶⁰ Copyright 2020, American Chemical Society. (B) The synthesis of the light-triggered ROS-responsive hyperbranched polyphosphoester. Reproduced with permission.⁶⁹ Copyright 2019, Elsevier. (C) Schematic illustration of ROS cascade responsive drug release of PTS-DP for enhanced locoregional chemo-photodynamic therapy. Reproduced with permission.⁸³ Copyright 2020, Elsevier

whereas the mPEG-poly(ester-thioether) nanoparticles-loaded DOX possessed the most effective anticancer activity *in vitro*. Comparing to the control nanoparticles, each kind of ROS-responsive nanoparticle displayed higher cellular uptake activity and anticancer efficacy.

Arylboronic ester, one more frequently used ROS-responsive bond, has caught the attention of researchers and been applied to conduct the ROS-sensitive delivery materials. It is generally believed that this could be oxidized by H_2O_2 and generated phenol, which thereafter experienced a quinone-methide rearrangement with degradation of polymer side chains or backbones.⁷⁴ Various efforts have been devoted to develop arylboronic ester containing ROS-responsive polymers for drug delivery. Same as thioketal linker, arylboronic ester ROS-responsive polymers always assembled themselves as self-cleavage nanocarriers^{74,75} or prodrug.⁷⁶ In the work of Zhu et al, while different, polysulfoniums that contain cationic unit and arylboronic ester would interact with anionic DNA and condense into nanosized polyplexes.⁷⁷ The polyplexes were efficiently crushed to release DNA in the presence of ROS. Thus, not only quickly release of DNA but also effective gene transcription process could be realized.

The other ROS-responsive units include diselenide,^{78–80} aminoacrylate,⁸¹ cerium oxide,⁸² etc. Diselenide bonds shared similar design scheme with thioketal and arylboronic ester. For aminoacrylate, Chen et al constructed

an interesting supramolecular system of PEG-PGA- β -CD, which was prepared by conjugated β -CD onto poly-l-glutamic acid (PGA) moieties of PEG-PGA, with adamantane-modified PTX or bodipy enclosed into the cavities of the β -CD.⁸¹ In this system, β -CD was employed as a model host, and the two adamantane-modified molecules were served as guests. The most notably feature of this host-guest strategy was easily to modulate the ratio of photosensitizer and ROS-sensitive prodrug for maximum combination therapy. Zhu et al developed hybrid semiconducting polymer nanoparticles (SPNs) of poly(cyclopentadithiophene-altbenzothiadiazole) (PCPDGTBT) and cerium oxide nanoparticle (nanoceria).⁸² The nanoceria could switch oxidation states between III and IV (Ce^{3+}/Ce^{4+}) based on neutral and acidic pH conditions making it act as a smart regulator of ROS scavenger in normal tissues and converter in tumor areas, respectively. PCPDGTBT worded as a near-infrared (NIR) fluorescence agent and photosensitizer. Therefore, the SPN possessed phototherapy enhancement in the acidic TME and side effect decrease in normal tissues.

ROS-responsive DDSs were often combined with PDT.^{57,61,64–68} PDT is a therapeutic technique that involves the illumination on photosensitizers with appropriate light to generate excess ROS for cancer therapy.⁶⁵ These ROS and PDT dual-responsive systems were always achieved by codelivery photosensitizer, such as Ce6,^{65,66,69} pheophorbide A (PhA),^{83,84} IR780,⁶⁸ and bodipy.⁸¹ In these

systems, excess generating ROS by PDT would strengthen the effectiveness and specificity of ROS-responsive smart materials. Like the work of Uthaman et al, photoactivatable nanomicelles with the properties of tumor tropism enhancement and ROS-responsive cascaded drug release were developed for locoregional chemo-PDT.⁸³ As showed in Figure 2C, the DOX would experience three steps of release. The initial step was intracellular ROS-induced release. The following was PDT-induced micelles disruption and locoregional ROS generation. And the last accelerated release step was *in situ* rapid dissociation of thioketal linkage.

2.2.1 | GSH

The GSH-responsive materials have widely been applied for tumors drug delivery by taking advantage of the distinctly different GSH levels between normal regions and tumor areas. More specifically, it is found that the GSH concentrations are two to three orders of magnitude higher in cytosol (1-11 mM) than in extracellular fluid (eg, 2-20 μ M in plasma),^{85,86} besides, studies have revealed that tumor tissues possess the higher GSH concentration than normal tissues within a rodent model.⁸⁷ GSH-responsive materials include disulfide bond,⁸⁸⁻⁹² GSH-responsive materials include diselenide linkage,⁹³ metal-based (eg, Mn, Cu, Fe, Co)^{94,95} nanoparticles, platinum (IV) (Pt(IV)) prodrug,⁹⁶ etc.

Many GSH-responsive materials contain disulfide bond, because disulfides could transform to thiols in the presence of GSH (work as a reducing agent).⁹⁷ As seen in Table 3, these disulfides could be classified as linear polymers, cross-linked polymers, hyperbranched polymers, star-shaped polymers,¹⁰⁵ disulfide conjugate, dendrimer,¹⁰⁷ disulfide/tetrasulfide-containing MOSNs,¹⁰⁹⁻¹¹¹ surface disulfide-anchored MSNs^{12,300} and so on.

Linear polymers are the most common disulfide-containing GSH-responsive materials. Basically, existing organic polymers (eg, PEG, HA)⁹⁸⁻¹⁰⁰ were linked by one disulfide bond or novel organic polymers were synthetized by polymerization (multiple disulfide bonds).¹⁰¹⁻¹⁰² Deng et al constructed the nanoparticles with Ds-sP (PEG-s-s-1,2-distearoyl-sn-glycero-3-phosphoethanolamine-N-[amino-(polyethylene glycol)-2000] that loaded with endoplasmic reticulum targeting photosensitizer efficiently for GSH-sensitive ER-targeting PDT strategy and augmented immunotherapy effect. In a recent study, a GSH-responsive hydroxycamptothecin-based polyprodrug (named polyHCPT) was synthesized by the copolymerization of HCPT and 2,2'-dithiodiethanol.¹⁰² Lipid PEG was added in the polyHCPT to form polyprodrug nanoparticles

TABLE 3 GSH-responsive materials for drug delivery of cancer therapeutics

GSH-sensitive compounds	Structure	Reduction reaction	
Disulfides	Linear polymers, ^{92,98-102} cross-linked polymers, ^{90,274} hyperbranched polymers, ¹⁰⁴ star-shaped polymers, ¹⁰⁵ disulfide conjugate, ^{91,106,299} dendrimer, ¹⁰⁷ disulfide/tetrasulfide-containing MOSNs, ¹⁰⁹⁻¹¹¹ surface disulfide-anchored MSNs ^{12,300}	$R_1-S-S-R_2 + GSH \longrightarrow R_1-SH + R_2-SH + GSSG$	
Disselenides ^{93,113}	$R_1-Se-Se-R_2$	$R_1-Se-Se-R_2 + GSH \longrightarrow R_1-SeH + R_2-SeH + GSSG$	
Pt (IV) prodrugs ¹¹⁵⁻¹¹⁸	$\begin{array}{c} R_1 \\ \\ H_2N \cdots \cdots Pt \cdots \cdots Cl \\ \\ H_2N \cdots \cdots Cl \end{array}$	$\begin{array}{c} R_1 \\ \\ H_2N \cdots \cdots Pt \cdots \cdots Cl \\ \\ H_2N \cdots \cdots Cl \end{array} + GSH \longrightarrow \begin{array}{c} H_2N \cdots \cdots Pt \cdots \cdots Cl \\ \\ H_2N \cdots \cdots Cl \end{array} + GSSG$	$Mn^{4+}/Fe^{3+}/Cu^{2+}/Co^{3+} + GSH \longrightarrow Mn^{2+}/Fe^{2+}/Cu^{+}/Co^{2+} + GSSG$
Metal-based nanoparticles ^{94,95,119-121}	Oxide compound of Mn, Cu, Fe, Co		

containing another drug of B-cell lymphoma 2 siRNA for synergistic cancer therapy.

The other shapes of GSH-responsive polymers possessed multiple disulfide bonds on different branched chains of the polymers. Researchers copolymerized hexachlorocyclotriphosphazene with GSH-sensitive molecules (bis-(4-hydroxyphenyl)-disulfide) to form cross-linked polyphosphazene (PPZ) as pH/GSH dual-stimuli-responsive materials. PPZ is an inorganic-organic hybrid polymer. It contained the polymeric backbone chain of alternating nitrogen and phosphorus atoms ($-P=N-$), and two side groups linked to each phosphorus atom.¹⁰³ These multifunctional cross-linked PPZ possessed excellent coating property on various nanomaterials. In this work, the pH/GSH dual-stimuli-responsive PPZ was coated on superparamagnetic Fe_3O_4 nanoclusters to form discrete nanoparticles for chemo-PDT. A hyperbranched GSH-responsive polymeric prodrug (HPAA-MTX) composed of methotrexate (MTX) and cationic poly(amido amine) (HPAA) was designed and synthesized for cancer treatment.¹⁰⁴ And HPAA was synthesized by polymerization with N,N'-bis(acryloyl) cystamine and 1-(2-aminoethyl) piperazine via Michael addition reaction as hyperbranched GSH responder. In the reporting of Shang et al, four linear GSH-responsive copolymers were anchored on a tetraphenylsilane core to form a star-shaped polymer with FA capped at each end of the four arms.¹⁰⁵ The star-shaped GSH-responsive polymers were prepared as tumor-targeting nanodrug carriers.

Disulfide conjugate and dendrimer of GSH-responsive materials are usually low-molecular-weight amphiphilic prodrug. Disulfide conjugate always links two macromolecules (eg, drugs, photosensitizers) through disulfide bond. Recently, a GSH-responsive paclitaxel-ss-berberine conjugate was synthesized and self-assembled to the nanomedicine for synergistic cancer treatment.¹⁰⁶ Tang et al developed a GSH-responsive amphiphilic dendritic prodrug with quantitative and high drug loading.¹⁰⁷ In this case, sorafenib was attached to the four disulfide-containing arms of short PEG chain via Michael Addition reaction, and the formative dendritic GSH-responsive prodrug could self-assemble into nanoparticles.

There are two strategy prepare GSH-responsive organosilica nanoparticles. One is the tetraethyl orthosilicate reacted with bis[3-(triethoxysilyl) propyl] disulfide or bis[3-(triethoxysilyl) propyl] tetrasulfide for several hours in certain condition to obtain disulfide or tetrasulfide containing MOSNs, respectively.¹⁰⁸ For instance, researchers first reported the tetrasulfide-containing MOSNs coloaded antigen protein (ovalbumin) and a toll-like receptor 9 agonist as a promising delivery platform for cancer immunotherapy.¹⁰⁹ However, these systems showed a limitation of low drug loading capacity. Hence,

Moghaddam et al developed a hollow disulfide-containing MOSNs by removing the dense Stöber core with many features such as high loading efficiency, GSH-responsive degradability, large surface area, low density, and the ability of surface modification.¹¹⁰ Another is to use (3-mercaptopropyl) methyldimethoxysilane (MPDMS) as a single silica source for polymerization and oxidation in NH_4OH as a base catalyst.¹¹¹ But the (3-mercaptopropyl) trimethoxysilane (MPMS)-based MSNs would be used to graft disulfide bond on the surface as surface disulfide-anchored MOSNs. This is because MPMS could form three siloxane bonds and result in silsesquioxane cores with internal and external mercaptopropyl, whereas MPDMS formed two siloxane bonds at most and result in disulfide-containing MSNs with internal disulfide bond and external mercaptopropyl.¹¹¹ For example, in the work of Venkatesan et al, transferrin was anchored on the surface of MPMS-based silica nanoparticles by disulfide bond with DOX loading for tumor target therapy.¹¹²

Diselenide linkage is another GSH-responsive motif used for engineering GSH-sensitive materials that shares similar responsive mechanism with disulfides. A novel GSH-responsive diselenide-based PTX dimeric prodrug (PTXD-Se) was constructed and then encapsulated into self-assemble nanoparticles of amphiphilic polypeptide copolymer to form a biodegradable nano system with high drug loading and GSH-responsive ability.¹¹³ Six paclitaxel-citronellol conjugates containing either thioether bond, disulfide bond, selenoether bond, diselenide bond, carbon bond, or carbon-carbon bond as linkers were synthesized, as shown in Figure 3, to investigate the different influence of sulfur, selenium, or carbon linkers on prodrug nanoassemblies and compare their properties *in vivo* and *in vitro* with each other as ROS- or GSH-responsive cancer therapeutics.¹¹⁴ It was found that the sulfur/selenium/carbon bonds would substantially impact the self-assemble efficiency, stability and pharmacokinetics of prodrug nanoassemblies by different bond angles/dihedral angles, as well as redox-responsive ability reflected via different drug release and cytotoxicity. And, more remarkable, thanks to the multiple therapy advantages compared with other kinds of prodrug nanoassemblies, diselenide bond-linked prodrug nanoassemblies presented the strongest antitumor activity.

Pt(IV) prodrug would be decomposed and reduced into Pt(II) as an effective anticancer drug from the prodrug under treatment high concentration of GSH.¹¹⁵ Compared with Pt(II), Pt(IV) prodrug possesses lower erythrocyte binding rate, longer plasma half-life.¹¹⁶ Furthermore, with the two additional ligands of Pt(IV), Pt(IV) prodrug equipped the prospect of fine-tune desired properties, such as lipophilicity, tumor targeting, and increased cellular uptake with high drug loading.¹¹⁷ In

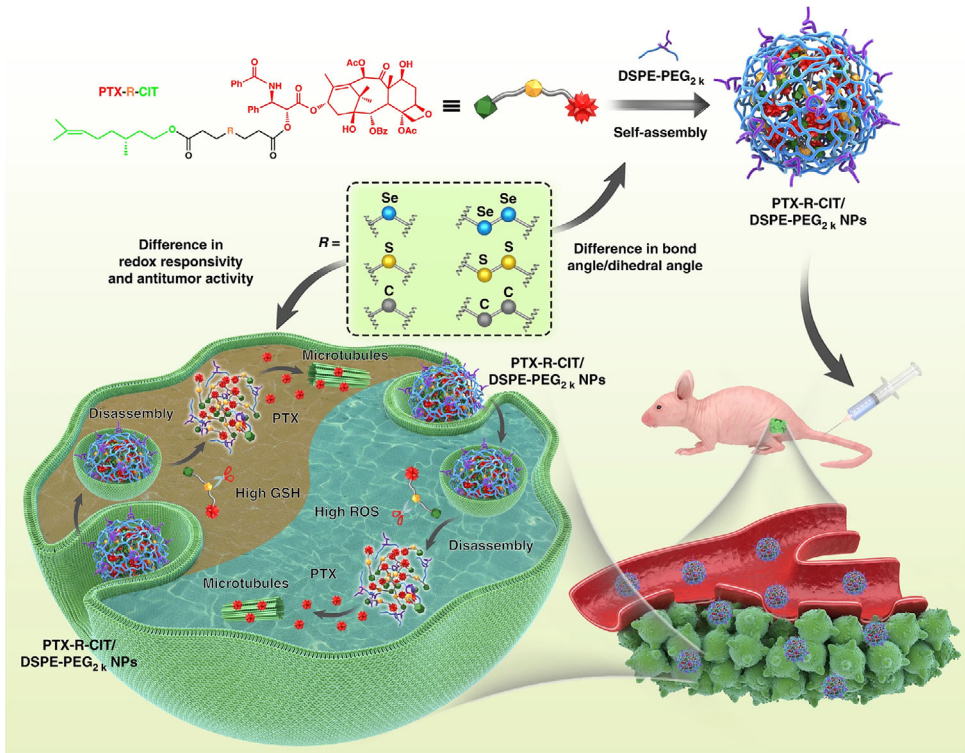


FIGURE 3 Schematic representation. Sulfur/selenium/carbon bond–bridged PTX–CIT prodrug nanoassemblies for cancer therapy. Reproduced with permission.¹¹⁴ Copyright 2019, Nature Publishing Group

a concrete example, the two additional ligands of Pt(IV) were covalently bond with different chain length of aliphatic acid to form analogous octahedral prodrugs named *cis,cis,trans*-[Pt(NH₃)₂Cl₂(OOC-(CH₂)_nCH₃)₂].¹¹⁸ These GSH-responsive Pt(IV) prodrugs with tunable hydrophobicity self-assembled with lipid PEG to be Pt(IV) nanoparticles as a GSH-responsive prodrug platform for effective drug delivery and cancer therapy.

The high-valence metal-based nanoparticles would be decomposed and reduced to release low-valence metal ions and anticancer drug in the acidic and GSH-affluent TME.⁹⁵ Taking MnO₂-based nanoparticles as an example, when the nanoparticles entered the cancer cell, the MnO₂ would be degraded by the high GSH level, resulting in simultaneous consumption of GSH, release of MRI contrast agent Mn²⁺, and activation of chemodynamic therapy.¹¹⁹ Wang et al reported the one-pot synthesis of biocompatible arginine-rich manganese silicate nanobubbles (AMSNs) that were composed of MSNs nanocore, Mn-base nano shell and adopted arginine as a surface capping ligand.¹²⁰ The AMSN degradation during the GSH depletion process caused the release of Mn²⁺ and loaded drugs, resulting in strengthened *T*₁-weighted MRI contrast and chemotherapeutic effects. Recently, a biodegradable MnSiO₃@Fe₃O₄ nanoplatform was constructed by decorated Fe₃O₄ nanoparticles on the MnSiO₃ surface to cover the MnSiO₃ pores effectively and decrease the drug

leakage during the circulation in blood.¹²¹ Owing to the acidic environment and high GSH level in tumor cells, the nanoplatform structure was not stable, resulting in Fe₃O₄ nanoparticles broken into pieces with rapid drug and Mn²⁺ release. Then, the interference between *T*₁ and *T*₂ contrast abilities of the exfoliated Fe₃O₄ and released Mn²⁺ would be decreased, inducing enhanced dual-mode MRI contrast. In addition, the Fe₃O₄ exfoliation would increase the specific surface area of the Fe₃O₄ nanoparticles and enhance the Fenton-like reaction in cancer cells, inducing cell apoptosis.

2.2.2 | Hypoxia

The exponential growth of cancer cells demands continuous supply of nutrient and oxygen. Therefore, irregular tumor microvessels with structural defect are formed in impaired microcirculation, thereby limiting the oxygen diffusion gradients in solid tumors.¹²² Hypoxic regions are formed because of the impaired vasculature networks limiting oxygen diffusion distance within 200 μm in growing tumors. Statistically, 50–60% of solid tumors, especially the tumor interior cells, could be observed hypoxia.¹²³ The hypoxia tumor regions suffer a low oxygen partial pressure (pO₂) (< 2.5 mm of Hg) that decreases from the tumor surface to interior, whereas the healthy cells

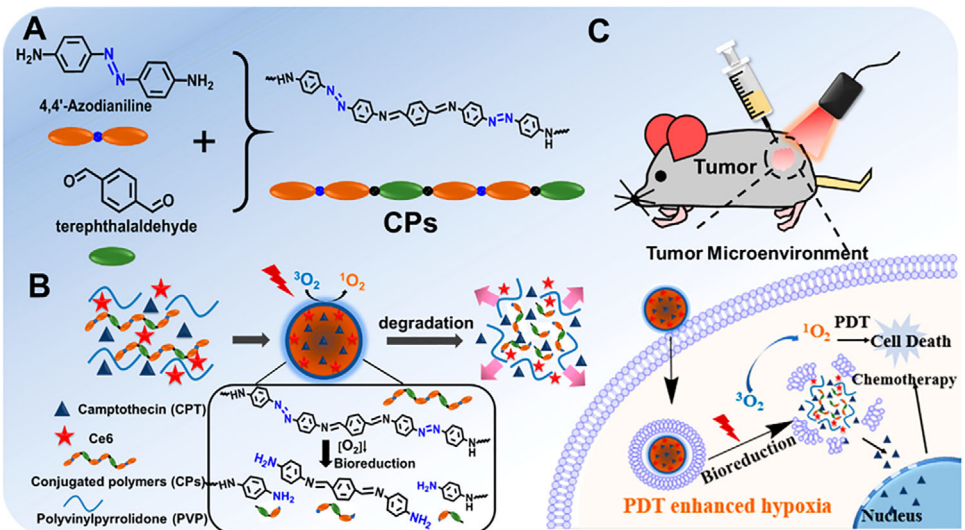


FIGURE 4 Schematic illustration of the hypoxia-responsive drug-delivery system. (A) Formation of CPs. (B) Formation and the responsive drug release mechanism of CPs-CPT-Ce6 NPs. (C) Schematic illustration of the CPs-CPT-Ce6 NPs for ROS generation and hypoxia-responsive drug release to enhance the anticancer efficacy. Reproduced with permission.¹²⁴ Copyright 2018, American Chemical Society

hold a 30–40 mmHg pO₂.¹²⁴ Hypoxia improves the survival of tumor cell not only by enhancing angiogenesis, invasiveness, and metastasis, but also negatively contributing to the cancer therapeutic responses of chemo-, radio-, photodynamic, and ultrasound-therapy leading to poor clinical prognosis.¹²⁵ Yet, for all that, this different physiological cellular state of tumor tissues provokes development of hypoxia-responsive prodrugs and materials for the poorly oxygenated tumor therapy.^{126,127}

Azobenzene derivatives are well-established, hypoxia-responsive linker incorporated in the form of a bioreductive material for tumor drug delivery. There is a first attempt to construct an azoreductase-responsive functional metal-organic framework (MOF) for cancer drug delivery by coordination of Fe³⁺ and azobenzene-4,4'-dicarboxylic acid linkers.¹²⁸ Azoreductase is a typical hypoxia biomarker for targeted reduction and cleavage of azobenzene derivatives. In another work, the azobenzene derivatives of carboxymethyl DEX containing azo bonds are reduced to aniline derivatives by azoreductase under the hypoxic tumor regions with DOX release.¹²⁹ Similarly, azo bond modified polymers such as Azo-PEG,¹³⁰ PEG-Azo-PLGA,¹³¹ PLG-g-mPEG/Azo,¹³² and Ce6-PEG-Azo-PCL¹³³ were synthesized as the hypoxia-responsive moiety of nanocarriers for drug delivery. Recently, researchers also design a novel azobenzene containing conjugated polymers (CPs)-based nanocarriers-loaded Ce6 and CPT as light-enhanced hypoxia-response platform for successive synergistic PDT and chemotherapy.¹³⁴ As illustrated in Figure 4A, the CPs were synthesized through a condensation reaction between the azo bond of 4,4'-azodianiline and terephthalaldehyde. Then, the CPs were mixed with

CPT and Ce6 to prepare nanocarrier by the reprecipitation method in PVP solution (Figure 4B). Upon laser irradiation, the Ce6 would induce PDT and consumed oxygen, which thereafter intensified the local hypoxic for rapid azo bond cleavage with CPT release (Figure 4C). To achieve hypoxia-triggered transforming immunomodulator for cancer immunotherapy, a hypoxia-responsive SO₂ nanocarrier for enhanced immunotherapy assisted by PDT was prepared by mixing the CpG oligonucleotide with Ce6-loaded SO₂ nanoparticles, whose surface was modified with azo bond containing PEG or chitosan.¹³⁵ Another approach might be of interest for tracking the hypoxia-responsive cancer chemotherapy *in vivo*. In this work, an azo-based NIR fluorescent theranostic probe was constructed by covalent bonding of N,N-bis(2-chloroethyl)-1,4-benzenediamine and NIR fluorophore AXPI via azo bond.¹³⁶ When the sensitive probe was exposed to hypoxic conditions, active anticancer drug release and an NIR fluorophore would be turned on, resulting in successful real-time monitoring the drug delivery mice.

Similarly, nitro derivatives are another type of highly hypoxia-responsive materials that were widely exploited for the design of drug carriers and bioreductive prodrugs, including metronidazole,^{137,138} nitroimidazole,^{139,140} 2-nitroimidazole,¹⁴¹ and nitrobenzene.^{142,143} These hydrophobic nitromoieties were introduced into degradable polymers such as PEG-block-poly(L-glutamic acid),¹³⁷ polyethyleneimine,¹³⁹ and HA¹⁴¹ to prepare amphiphilic block copolymer hypoxia-sensitizers. And these hypoxia-sensitizers would be converted to hydrophilic amino compounds in hypoxic conditions. The hypoxic-induced copolymer solubility change caused the destabilization

of nanocarriers and further provoked drug release for chemotherapy. Macromolecules were also used in the hypoxic-responsive nanocarriers. For example, the nitro macromolecules prepared by conjugating 2-nitroimidazole to the head and tail of 1,12-dibromododecane via one-step nucleophilic substitution were incorporated into the phospholipid bilayer containing DSPE-PEG2000 to encapsulate DOX.¹⁴⁰ With the solubility change of the nitro macromolecules under hypoxic conditions, the structure of phospholipid bilayer was destabilized to induce burst release of the encapsulated DOX. Researchers also designed a novel hypoxic radiosensitizer-polyprodrug nanoparticles of angiopep-2-lipid-poly-(metronidazole)_n as hypoxia-responsive drug carrier and significant radiosensitizing effect enhancer on gliomas.¹³⁸ In the work of Shen et al, the Toll-like receptor 7 agonist (imiquimod) was modified with 4-Nitrobenzyl chloroformate (NBCF) as a low molecular prodrug to modulate immunological responses of combretastatin A4, which would induce nitroreductase to curtail its anticancer immunity.¹⁴³ To achieve the hypoxia gradient enhanced tumor penetration effect, Zhen et al developed a nanocarriers containing a core of poly(caprolactone) and a hybrid shell of NBCF-modified polylysine and PEG.¹⁴² These nanocarriers could possess long blood circulation with the help of PEG shield. Upon reaching the tumor, the NBCF degraded at the hypoxia condition, recovering the positively charged amine groups of polylysine on the nanocarriers surface. Remarkable surface positive charge of nanocarriers enabled their penetration into the tumor. With further growing hypoxia of the interior tumor, more positively charged amine groups were recovered from the nanocarriers, resulting in facilitating the deep penetration.

Moreover, tirapazamine (TPZ) is a hypoxia-responsive activated anticancer drug. It is frequently used in many latest designs of hypoxia-sensitive platform.^{126,131,144–146} In the presence of hypoxia, TPZ undergoes the metabolism of an intracellular reductase to form a highly reactive radical species capable of provoking DNA breaks and chromosomal aberrations, leaving cell structural damage and death.¹⁴⁷ However, in aerobic conditions, the generated radical by reductase will be efficiently scavenged by molecular oxygen to reform the parent compound.¹⁴⁸ Tirapazamine significantly enhances radiation-induced hypoxic tumors therapy, presenting dose- and schedule-dependent.¹⁴⁹ Therefore, it is usually combined with radio therapy as hypoxia-activated radio-chemo therapy for cancer.¹⁴⁴ Similarly, TPZ was also used in photo-chemo therapy. For instance, a photothermal-pH-hypoxia-responsive nanoplateform constructed by loading the TPZ and synthesized diethylamino-containing photosensitizer in a melting point tunable eutectic phase change material (LASA).¹⁵⁰ Upon 808-nm laser irradiation, the hyper-

thermia generated by photosensitizer induced LASA melt to release TPZ. Meanwhile, pH-sensitive photosensitizer would turn “off” its charge-transfer state to generate appreciable ¹O₂ for PDT and PTT. More interestingly, Wang et al developed a platform called perfluorocarbon nanoparticles to create a long-lasting and penetrable hypoxia TME for effective delivery and subsequently activation of administered TPZ.¹⁵¹

2.3 | Enzyme-triggered smart materials

Enzymes play important roles in different biological processes, and tumor-associated enzyme dysregulations have frequently applied in the design of smart DDS for medications. Enzyme-responsive materials for drug delivery of cancer therapeutics were partly listed in Table 4. The nanoplateforms composed of enzyme-responsive materials performed their intelligent drug release ability mainly by enzyme-triggered carrier cleavage, enzyme-triggered prodrug cleavage, and enzyme-triggered carrier geometric transformation. As shown in Table 4, protease such as matrix metalloproteinases (MMPs), cathepsin B, proteinase K, protease, and trypsin, etc., esterase (eg, carboxylic-ester hydrolase, phospholipase A2, and butyryl-cholinesterase), hyaluronidase (HAase), heparanase-1,β-Glucuronidase, oxidoreductases (eg, azoreductase, thioredoxin reductase, indoleamine 2,3-dioxygenase 1, and plasma amine oxidase), nuclease, and glutathione S-transferases π were the upregulated enzymes in tumor intracellular or extracellular region, acting as the design basis of *in situ* enzyme-triggered materials. Here, dozens typical enzyme-triggered smart materials were discussed.

Amido bonds are often incorporated for targeting hydrolytic proteases, although they are relatively stable in physiological environments. MMPs, including MMP-2, MMP-7, and MMP-9, mostly overexpressed and abundant in the human tumor sites (extracellular matrix, tumor cells, and tumor vasculatures), acting an important role in tumor progression and metastasis.^{152–154} The upregulated MMPs in the TME were the most frequently applied types of one that serve in the development of intelligently site-specific enzyme-responsive materials. Several MMP-2 responsive materials, for example, enzyme-sensitive cytotoxic peptide-dendrimer conjugates,¹⁵³ cross-linked nature-derived polysaccharides by a peptide linker,¹⁵⁵ and MMP-2-responsive linker-modified gold nanoparticles¹⁵⁶ were produced for tumor therapy. The enzyme-sensitive cytotoxic peptide-dendrimer conjugates of PKT-GPLGIAGQC-PEG₂₀₀₀ were achieved by covalently attaching the three peptides (MMP-2-sensitive peptide-PEG, cytotoxic peptide KLAK, and cell-penetrating peptide TAT) to the three

TABLE 4 Enzyme-responsive materials for drug delivery of cancer therapeutics

Enzyme	Bond type	Structure	Occurrence	Cargo	Ref.
Enzyme-triggered cleavage					
MMPs	MMP-2	Amido bond	PKT-GPLGIAGQC-PEG ₂₀₀₀	TME	KLAK DOX
		PEG ₅₀₀₀ -GPLGVVRGC-Dox-AuNPs			153 156
	MMP-7	CG/AG-PEG-MAL-CGGP ₁ GLAGGC		Individual cells	154
	MMP-9	Fmoc-GP ₁ LGL-DOX		DOX	158
	MMP-2 and MMP-9	polypeptide-LinTT1-PVGLIG-TAT		PTX	152
Cathepsin B		PEG-SS-dendrimer(GFLG)-N = DOX	Tumor lysosomes	DOX	161
		[pHPMA-Gd-PTX(GFLG)-Cy5.5] ₂ -GFLG		PTX, Cy5.5	162
MMP-9 and Cathepsin B		PEG-GGPLGVVRGK, GEM-GFLG	Human pancreatic cancer cells	GEM	163
Proteinase K		PEG-b-F [†] Y _n	Candida albicans	DOX	164
Protease (furin)		(RVRR) ₃ -KLA [†] , (RVRR) ₃ -chlorambucil	Tumor trans-Golgi-body and cell surfaces	KLA, Chlorambucil	165
Trypsin	Carboxylic-ester hydrolase	Poly(casein-g-NIPA [†])	TME	DOX	167
Esterase		Indomethacin-GFFKEH-bicalutamide	Tumor cytosol	Bicalutamide	171
	Phospholipase A2	DSPC/DSPG/DSPE-PEG ₂₀₀₀ [†]	TME	(D-Arg) ₈ -PNA	168
	Butyrylcholinesterase	Choline modified chlorambucil	Tumor extracellular	Chlorambucil	169
HAase		MoS ₂ -PEI-HA	TME and the cell liposomes	DOX	174
		HA-adipic dihydrazide-Ce6		DOX	173
Heparanase-1		Alloferon-heparin/protamine polyelectrolyte complex	Melanoma extracellular	PTX, alloferon-1	177
β-galactosidase		Galactose-Dox	Tumor lysosomes	DOX	178

TABLE 4 (Continued)

Enzyme	Bond type	Structure	Occurrence	Cargo	Ref.
Nuclease	DNase I, nicking enzyme, endonuclease, exonuclease III	Phosphodiester bond	Intracellular	CPT	179
Azoreductase	Azo bond	PBA [†] -PEG-Azo-PCL [‡]	Tumor microsomes	CPT	180
Thioredoxin reductase	Diselenide	RGD-PEG-PUSeSe-PEG-RGD	Tumor intracellular	GEM	181
Indoleamine 2,3-dioxygenase 1	Indoleamine loop	MSNs-Trp-CB[8]-Trp-Fe ₃ O ₄ nanoparticles	Tumor intracellular	DOX	182
Glutathione S-transferases π	Thiol group	HA-DNB-DEA/NO [§]	Intracellular	NO donor	175
Enzyme-triggered carrier geometric transformation					
Alkaline phosphatase	—	D ^D F ^D F ^D F ^D p _Y	Tumor cell surfaces	BAY [†]	185
Plasma amine oxidase	—	(KVK) ₄ D ^D PPTKV _p YKV _p -NH ₂	DOX	DOX	186
Cathepsin B	Amido bond	Ac-VVVVVVKKK-NH ₂	Serum	DOX	187
		CPT _η LVFFGFLG _η pEG _η RGD	Tumor lysosomes	CPT	184

[†]Abbreviations: BAY, BAY 11-7085; DEA/NO, diethylamine NONOate; DNB, 1,5-difluoro-2,4-dinitrobenzene; DSPE-PEG₂₀₀₀, 1,2-di(octadecanoyl) phosphatidylethanolamine-methoxy (poly ethylene glycol); KLA, cell-impermeable antitumor proapoptotic peptide KLAKLAKKLAKLAK; NIPA, N-isopropylacrylamide; PBA, phenylboronic acid; PCL, poly(ϵ -caprolactone).

[‡]The bold words are prodrugs in the DDS.
[§]The underlined words are the enzyme-triggered parts.

branched acryl of poly(amidoamine) (PAMAM) dendrimer, respectively.¹⁵³ The obtained peptide–dendrimer conjugates showed enzyme-trigger cell apoptosis enhancement and deep tumor penetration. In a recently ingenious work, the individual living cell was encapsulated with a shell of MMP-7-responsive polymer for prospective clinical application of cell therapy.¹⁵⁴ As illustrated in Figure 5A, multiple PEG-attached gelatin layers were coated on the surface of individual HeLa or human mesenchymal stem cells through Layer-by-Layer assembly of cationic gelatin-PEG maleimide (CG-PEG-MAL) and anionic gelatin-PEG maleimide (AG-PEG-MAL). Then, the PEG-gelatin layers were cross-linked by click reaction of cysteine-terminated peptide (CGGPLGLAGGC) with both thiol groups on cysteine and MAL groups on PEG-gelatin. The coated cells possessed a long-term stability in the culture period and blood circulation, equipping with increased cell viability, preventable host immunological rejection, and onsite cell release. Battistella et al developed an amphiphilic diblock copolymer (one block containing hydrophobic Toll-like receptor 7 agonists and the other block containing hydrophilic MMP-9 responsive peptides) by ring-opening metathesis polymerization.¹⁵⁵ Subsequent exposure to MMP-9, the self-assemble spherical micelles of amphiphilic diblock copolymers, converted to be immunostimulatory microscale assemblies for immunotherapeutic enhancement. Another MMP-9-responsive material was a DOX prodrug (Fmoc-GPLGL-DOX).¹⁵⁶ DOX prodrug was encapsulated in an amphiphilic copolymers to form an MMP9-DOX-NPs. And the combretastatin A4 (CA4) as a vascular disrupting agent was conjugated with poly(l-glutamic acid)-g-PEG by the Yamaguchi reaction as a nanodrug. With the selectively disrupting immature tumor blood vessels of CA4 nanodrug, MMP9 expression was significantly increased in treated tumors and further boosted the tumor-selective active drug release. In addition, a few peptide linkers are sensitive to both MMP-2 and MMP-9. For instance, PVGLIG was first synthesized and characterized in 2004 and applied in the work of Yao et al.^{152,159}

The other protease-responsive materials for the cathepsin B, proteinase K, protease, and trypsin, whose expression is often elevated at the tumor site, can be seen in many works. The oligopeptide Gly-Phe-Leu-Gly (GFLG) is specifically sensitive to the cathepsin B that is a lysosomal cysteine protease, and it has been utilized as a linker of many prodrugs and polymeric carriers.^{160–162} A typical cathepsin B-responsive materials-based DDS is the self-assemble amphiphilic triblock N-(2-hydroxypropyl methyl) acrylamide (HPMA) copolymer-gadolinium-PTX-Cyanine5.5 nanomedicine [pHPMA-Gd-PTX(GFLG)-Cy5.5]₂-GFLG for short.¹⁶² The GFLG linker was brought in to link PTX into the pHPMA-Gd-Cy5.5 as a spacer and

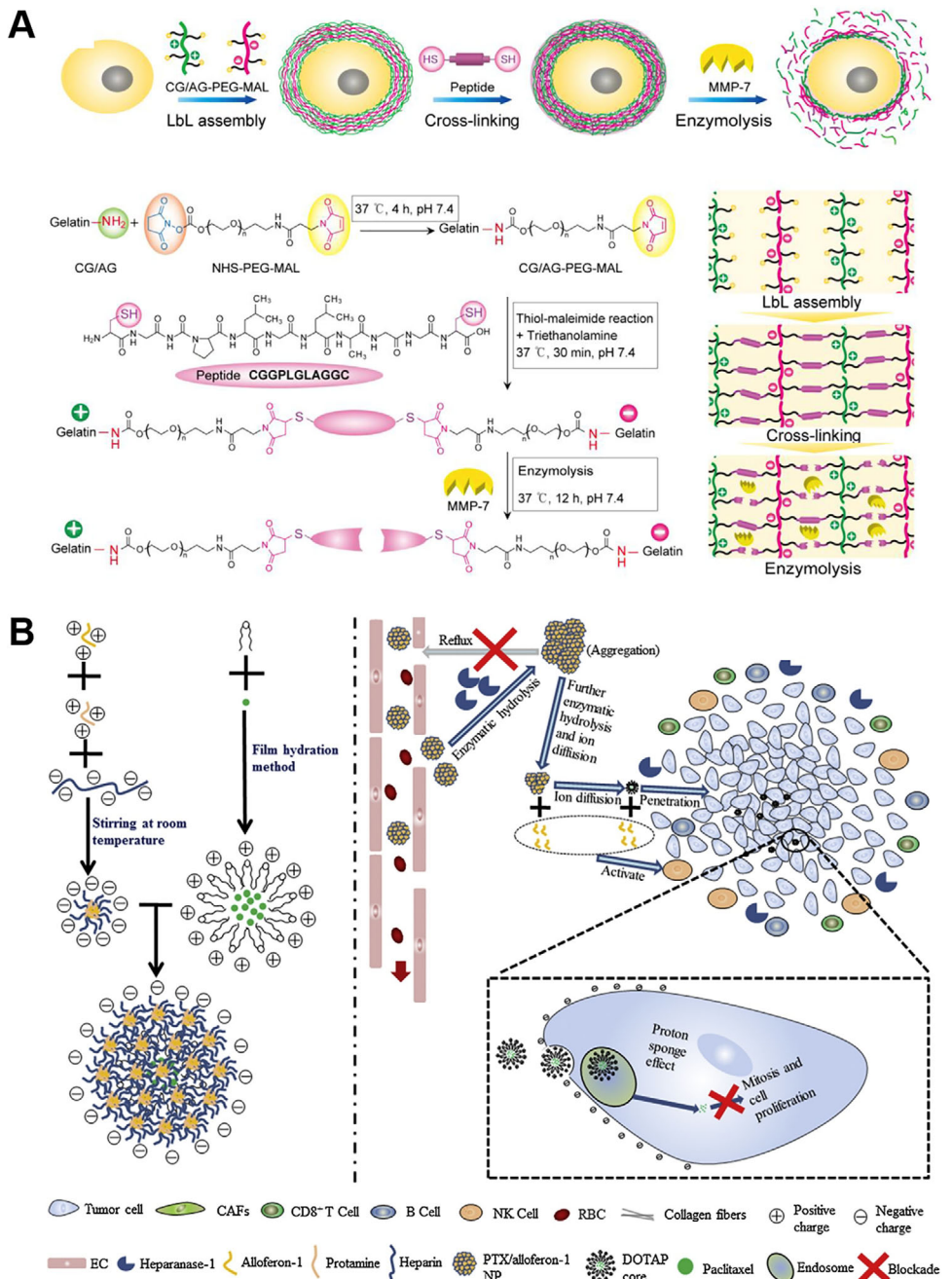


FIGURE 5 (A) Schematic procedures of individual living cell nanoencapsulation and on demand release, including CG-PEG-MAL and AG-PEG-MAL synthesis, LbL assembly, cross-linking, and enzymolysis. Reproduced with permission.¹⁵⁴ Copyright 2019, Elsevier. (B) The preparation process, particle size reduction, charge turnover, and drug distribution in target tumor region of PTX-DOTAP@Alloferon-1-Heparin/Protamine. Reproduced with permission.¹⁷⁷ Copyright 2019, Elsevier

then conjugate with two pHMPMA-Gd-PTX(GFLG)-Cy5.5 as the backbone of the carrier, allowing the high molecular weight conjugate to decompose into the half molecular weight products with drug release in the tumor cells. In addition, cathepsin B detachable gemcitabine (GEM), MMP-9 cleavable PEG, and ligand targeted CycloRGD were conjugated to CdSe/ZnS quantum dots (QDs) to form a dual-enzyme-sensitive nanovector with targeting tumor

therapy.¹⁶³ In this way, these nanovectors would show good stability during bloodstream circulation but crush to exposure the CycloRGD for tumor cellular penetration by overexpressed MMP-9 at TME, with further encouraging GEM release in tumor cells by promotion of cathepsin B degradation. Polytyrosine¹⁶⁴ and the repeats of furin substrates (RVRR)₃¹⁶⁵ were intelligent responsive to proteinase K and protease, respectively. Trypsin positivity

was significantly correlated with tumor progression and its activation ability to matrilysin (MMP-7) will also affect the cancer progression.¹⁶⁶ In a recent work, the poly(casein-g-N-isopropylacrylamide) unimers were synthesized self-assemble into biodegradable micelles for drug delivery.¹⁶⁷ The temperature-responsive property of poly(N-isopropylacrylamide) maintains its graft or block copolymers self-assemble into micelles when the lower critical solution temperature (LCST) like 32°C was achieved, but preserves as unimers below the LCST. Dox was loaded in the micelles by the ionic interaction with casein as a model drug and released by trypsin-triggered casein hydrolyzation.

Esters of carboxylic ester, phospholipids,¹⁶⁸ and acetylcholine¹⁶⁹ are vulnerable to specific enzymatic digestion and have been applied for fabricating materials sensitive to hydrolytic esterase. In the work of Saxena et al, self-assembly nanoparticles of the L-Aspartic amphiphilic polyester containing bis-carboxylic acid ester monomers exhibited excellent encapsulation capability for curcumin and Nile red.¹⁷⁰ These curcumin and Nile red-loaded nanoparticles performed the turn-on theranostic fluorescence resonance energy transfer (FRET) probe function at the extracellular areas, but the turn-off theranostic FRET probe function under the intracellular carboxylic ester hydrolase (CES) hydrolyzation. Because the FRET between the optical donor (curcumin) and acceptor (Nile red) chromophores only occurs when the donor molecules transfer the excitation energy to the acceptor within the nanoconfinement yielding Förster distance of <50 Å. In another study, indomethacin-GFFKEH-bicalutamide was constructed as a CES-sensitive prodrug for prostate cancer treatment.¹⁷¹ Phospholipase A2 catalyzes the hydrolysis of phospholipids at the sn-2 position, for example, 1,2-distearoyl-sn-glycero-3-phosphocholine (DSPC), 1,2-distearoyl-sn-glycero-3-phosphatidylglycerol (DSPG), and their analogs were used to develop phospholipase-sensitive liposomes for cancer drug delivery.^{168,172}

Another class of common hydrolase is HAase,^{173–175} belonging to one of the polysaccharide hydrolase members with heparanase-1 and β-galactosidase. The overexpressed HA receptors such as CD44 and elevated HAase in the TME and the cell liposomes as well as make HA an excellent biodegradable tumor targeted and *in situ* responsive materials. In a recently work, cationic DOX was loaded on the surface of carbonylated-terminated PAMAM dendrimer that encapsulated indocyanine green (ICG) to prepare ICG@PCH@Dox.¹⁷⁶ The ICG@PCH@Dox was further coated with anionic HA as the outer shell with tumor-cell-targeted ability and timely release of the drug. There was a worth mentioning work, which constructed a heparanase-1-sensitive polyelectrolyte complex of PTX-DOTAP@alloferon-1-heparin/protamine

with several biocompatible materials and industrially safe production process.¹⁷⁷ Heparanase-1 displays significant high express level in highly metastatic tumors, especially in melanoma, and it can degrade heparan and heparin in specialty. The preparation and function process of PTX-DOTAP@Alloferon-1-Heparin/Protamine was illustrated in Figure 5B. First, alloferon-1 and protamine with strong positive charge were mixed with negatively charged heparin via electrostatic attraction. Meanwhile, PTX was encapsulated in the DOTAP (1,2-dioleoyl-3-trimethylammonium-propane)-based cationic liposomes as PTX-DOTAP. The PTX-DOTAP was added in the alloferon-1-heparin/protamine polyelectrolyte complex, while the solution is being stirred to finally form PTX-DOTAP@alloferon-1-heparin/protamine polyelectrolyte complex. The final polyelectrolyte complex would experience enzyme-triggered particle size reduction, charge turnover, and step-by-step drug distribution in target tumor region. β-galactosidase is another upregulated glycosidic bond hydrolase in various cancer types. Sharma et al developed a galactose moiety modified prodrug of DOX, and this prodrug could serve as an excellent targeting ligand for asialoglyco-protein receptors, as well as β-galactosidase activated drug with the help of the additional galactose moiety.¹⁷⁸

The remaining hydrolase-responsive material is associated with nuclease. Recently, the nucleic acid-modified metal-organic framework nanoparticles (NMOFs) that were sensitive for four different nucleases respectively, including DNase I, nicking enzyme, endonuclease, and exonuclease III were successfully constructed and effectively loaded with CPT.¹⁷⁹ Attributing to the overexpressed ATP in tumor cells, cooperative ATP biomarker and exonuclease III as dual biocatalytic agents triggered CPT-loaded NMOFs, revealing more effective and selective cytotoxicity to cancer cells than normal cells.

The oxidoreductase overexpressed in tumor region plays an important part in the design of smart materials. And the reductase is generally involved with the GSH and hypoxia sensitive materials and it has been described in the quoted above corresponding content. For instance, azo-bond-linked derivatives and diselenide derivatives were hydrolyzed by azoreductase and thioredoxin reductase, respectively.^{180,181} Indoleamine 2,3-dioxygenase 1 (IDO1) is an intracellular oxidase that promotes the proliferation and immune escape of tumor cells by mediating the metabolism of Trp into kynurenine. In the work of Qiao et al, the hole of MSNs was capped with tryptophan-mediated cucurbit[8]uril complex with Fe₃O₄, upon stimulated by IDO1, the tryptophan was degraded into N-formylkynurenine with “gate open” of the MSNs and intracellular release of DOX.¹⁸²

In addition, a few transferases like upgraded glutathione S-transferases π (GST π) were also applied in the design of enzyme responsive materials. GST π -responsive materials served as NO donor by GST π inspiring the thiol of GSH as an electrophilic center to carry out the nucleophilic attack with NO donor, and then NO release induced tumor cytoplasm-specific disruption.^{175,183}

The last class of enzyme responsive nanosystem is enzyme-triggered carrier geometric transformation. This kind of enzyme-sensitive materials based nanosystem will undergo geometric transformation, always from nanoparticles to nanofibers, with enhanced antitumor activity via different mechanism. The reported enzymes included intracellular cathepsin B,¹⁸⁴ cell surface alkaline phosphatase,^{185,186} and extracellular plasma amine oxidase.¹⁸⁷ As one reported, the prodrug CPT η LVF-FGFLG η PEG η RGD would self-assembled into nanoparticle, being recognized by tumor cell because of the targeting RGD and accumulating in tumor cells, and then it reorganized into nanofiber by cathepsin B hydrolyzation at the peptide GFLG to remove hydrophilic PEG η RGD shell.¹⁸⁴ Thus, this site-specific construction nanosystem enhanced suppression of tumor recurrence by long-term drug depot activity. In the work of Zhou et al, the alkaline phosphatase acts on the phosphate of D-Tyr, causing the tetrapeptide D F D F D F D _pY-based nanoassemblies to dephosphorylate into D F D F D F D Y-based nanofibers.¹⁸⁵ The nanofibers showed fairly strong synergism with NF- κ B targeting inhibitor by the downregulation of three key proteins at upstream NF- κ B pathway in the tumor cells. In another study, (KV)₄ D PPTKV_PYKVK-NH₂, an unfolded, inactive peptide was dephosphorylated (at _pY motif) and shifted (at D PP motif) its conformational bias toward cell-surface alkaline phosphatase to form a facially folded amphiphilic conformer.¹⁸⁶ The facially folded amphiphilic peptide would further affect cell-lytic and cell-penetrating properties via peptide concentration to enhance selective drug delivery.

3 | EXOGENOUS-TRIGGERED SMART MATERIALS

Compared with endogenous stimuli-responsive smart drug delivery materials depended on the TME seriously, exogenous stimuli (mainly including temperature, light, radiation, ultrasound, and magnetic field) are more powerful and effective activation pathways to realize safe and controllable cancer therapeutics by preferably overcoming individual difference-induced different therapeutic effects.^{188–191} Under the assistance of exogenous physical stimuli, drugs loaded in smart materials could be released spatiotemporal controllably, with the physico-

chemical properties change of materials when they reach to tumor site via the EPR effect and/or active targeting performance.¹⁹² Interestingly, the physicochemical change of materials could further accelerate the release rate in return or activate prodrugs in an external controllable way.¹⁹³ Moreover, exogenous stimuli cannot only be applied to prevent premature drug release and minimize unexpected side effects, but also induce additional therapeutic (PTT, PDT, SDT, RT, and so on) and imaging effects (FLI, PAI, US, MRI, and so on).^{15,194}

3.1 | Temperature-responsive smart materials

Temperature or thermoresponsive smart materials-based delivery systems (such as thermosensitive liposomes, polymer micelles, thermal-responsive phase change materials [PCMs], and thermosensitive polypeptide) have been attracted a lot of attentions in the application of drug delivery and cancer treatment that benefit from their structural instability transformation induced by physical and chemical properties change after exposing to high temperature (such as 40–42°C of tumor local temperature or \geq 42°C produced by external energy stimulus-induced hyperthermia).^{195–197} Thus, those nanosystems would release and burst drugs in the tumor tissues, while keeping structural stable in the normal tissues (37°C), resulting in minimal side effect and enhanced enrichment in the tumor. On the other hand, there are some natural or synthetic polymers with liquid phase at room temperature (\sim 25°C or below). They could easily converting into solid phase at the physiological temperature when injected into local diseased region, and could also act as an intelligent drug carrier to persistently control drug release as required.^{198–200}

Here, thermosensitive liposomes entrapped hydrophobic coix seed oil in the hydrophobic layer were developed to controlled drug release with minimal premature leakage (Figure 6A).²⁰¹ Under irritation of external temperature (higher than their phase transition temperature (\sim 42°C)), however, the drugs were released instantly. In addition to thermosensitive liposomes, Cui et al²⁰² synthesized a temperature-sensitive polypeptide brush, poly(g-benzyl-L-glutamate) (PBLG) derivative, acting as “guard” of mesoporous silicon channel to control the release of packages, attributed to its structural transformation from rodlike α -helix conformation to a random coil conformation under exposure of high temperature (Figure 6B). From TEM images, the outstanding encapsulation of PBLG could be observed intuitively compared with that of PBLG-undecorated mesoporous silica, which indicated that PBLG was an expectant gatekeeper (Figure 6C).

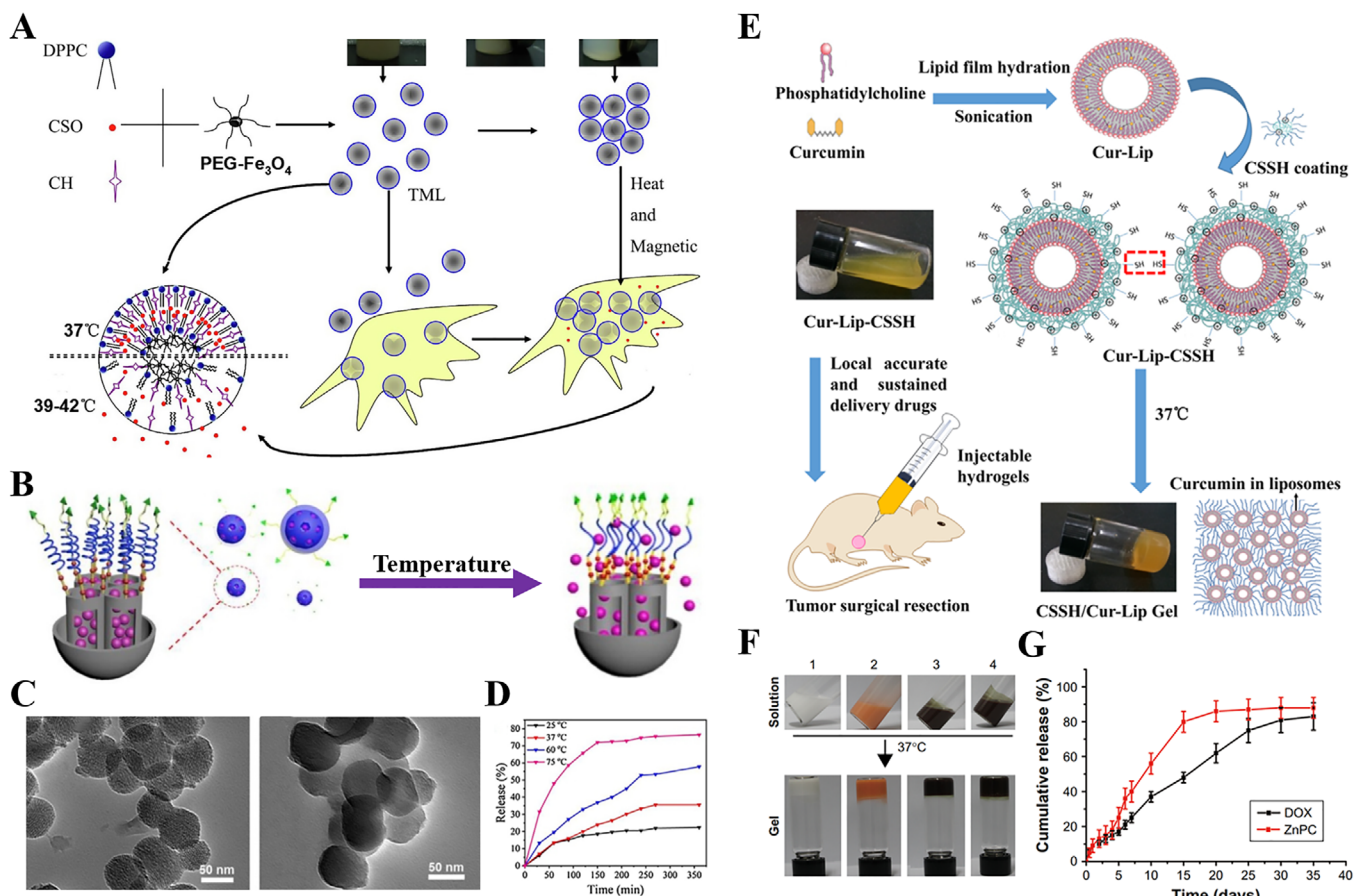


FIGURE 6 (A) Schematic illustration of the formation of TML and its temperature sensitivity. Reproduced with permission.²⁰¹ Copyright 2020, Elsevier. (B) Schematic representation of the temperature-stimuli MSN@PBLGF nanoplatform. (C) TEM images of MSNOH and MSN@PBLGF. (D) The release profiles of the DOX-loaded MSN@PBLGF under temperature stimuli. Reproduced with permission.²⁰² Copyright 2019, Elsevier. (E) Schematic illustrations of preparation of Cur-Lip-CSSH and CSSH/Cur-Lip Gel. Reproduced with permission.²⁰³ Copyright 2020, American Chemical Society. (F) Optical images of blank TNP hydrogel and hydrogels after DOX and/or ZnPC encapsulation and (G) *in vitro* cumulative drug release from TNP/DOX/ZnPC hydrogel within 5 weeks. Reproduced with permission.²⁰⁴ Copyright 2018, IJN

Furthermore, *in vitro* DOX release behavior showed that the release percentage was gradually increased with the elevation of incubated temperature because of damped hydrogen bonding interactions of PBLG after treating with high temperature (Figure 6D). Comparatively, a few smart materials are designed to locate in the tumor tissues by utilizing the physiological temperature to activate their gel state, so as to persistently control drug release over a long period. For instance, Li et al²⁰³ developed thiolated chitosan adsorbed liposomes as thermal-sensitive nanosystems to form gel in situ in tumor site after local injection, and then, the loaded curcumin would start to release slowly and continuously, which not only avoid long-term and frequent administration but also reduce invasiveness to patients (Figure 6E). Moreover, a thermal-responsive hydrogel comprised by PCL-PTSOU-PEG copolymer loading DOX or ZnPC was successfully acquired after injecting into the body (Figure 6F).²⁰⁴ The results of *in vitro* drug release experiments showed the

cumulative release percentage of no matter DOX or ZnPC reached about 80% over 35 days, presenting a gradual and sustaining release process (Figure 6G). Recently, the thermal-responsive PCM possessed the ability to act as a drug carrier or sealant. They have been became a popular medical material due to their phase change performance under stimulation of high temperature, which induced burst release of drugs.³⁹ More importantly, benefitting from commendable biocompatibility, simple preparation, and intravenous administration, PCMs have enormous potential in clinic.

3.2 | Light-responsive smart materials

Light with different wavelength from visible (vis) to NIR is a widespread external physical stimulus used in the biomedicine because of its intrinsic noninvasive performance and ability to modulate the exposure location and dose without interference of individual difference.^{205–208}

In recent decades, numerous researchers have made great efforts to exploit light-responsive smart materials to achieve targeting drug release for cancer treatment, such as vis-responsive composite biomaterials and NIR-responsive photothermal biomaterials.^{209,210}

3.2.1 | Vis

Vis, possessed higher photon energy than NIR, is commonly used to activate photosensitizers in the presence of O₂ to produce abundant ROS for cancer treatment, which induces drug release or prodrug activation at the same time.^{211–213} At present, a mass of smart materials, such as MOFs, mesoporous materials, BP, and so on, is exploited to build up vis laser-responsive drug delivery nanosystems to control drug release precisely and spatiotemporal controllably under irradiation, along with minimal release without toxicity in nonirradiant areas.^{214–216}

MOFs comprised by linking metal ions or clusters with bridging polydentate ligands have been attracted wide attentions for their applications in drug delivery due to their high and tunable porosities, high specific surface area, and versatile functionalities.^{217–219} Under irradiation of vis laser, MOFs, using photosensitizers as framework molecules, would change their physicochemical properties or cause collapse of nanostructure to further promote drug release. For instance, compared with the release amount without illumination, the release rate of CPT from the core of MOFs containing porphyrin ligand dramatically increased under 650-nm laser illumination.²¹⁷ In the same way, Chen et al²²⁰ reported a core-shell nanosystem by encapsulating ZIF-8 shell on photosensitive g-C₃N₄ nanosheets and loading DOX into porous channel of ZIF-8 to realize desirable release of DOX under double stimuli of TME and laser. However, it cannot be ignored that the above strategies, which just simply entrap drugs into the pore of MOFs without any gatekeepers or sealing agent, would cause potential toxicity to normal tissues. To minimize the toxicity, Min et al²¹⁸ designed an intelligent photosensitive porphyritic Zr-MOFs (PCN-224) nanostructure, loading apatinib and subsequently coating with MnO₂ layer. The exterior surface of PCN-224 was further decorated with cell membrane extracted from mouse breast cancer cell line 4T1 (Figure 7A). They found that the integrated nanostructure of 4T1 cell membrane and MnO₂ layer not only wonderfully prevented premature leakage of apatinib in the blood circulation but also increased targeting effect. When the NPs reached tumor site, the release of apatinib from NPs was initiated via the reaction between overexpressed GSH with MnO₂ layer, which was further accelerated with the help of depolymerization of PCN-224 core after 660-nm laser irradiation (Figure 7C). In addition,

Wan et al²²¹ applied CaCO₃ shell as a sealing agent to prevent premature leakage of DHA loaded into the Fe³⁺-based MOFs for tumor-specific therapy with negligible toxicity to normal tissues. Under stimulation of both laser and GSH, the nanostructure of MOFs would collapse to trigger release of loaded DHA, and then DHA would further combine with reduced Fe²⁺ to form toxicity DHA-Fe²⁺ for cancer treatment.

Except for MOFs, hollow MSNs (HMSNs) also could be chosen as smart drug carriers to simultaneously encapsulate DOX and photosensitizer Ce6 and then incorporated with BSA-doped MnO₂ NPs to prevent premature leakage, while the packages would give rise to release under common stimulation of 660-nm laser and TME (Figure 7B).²²² However, the complicated multilayer structures of above nanosystem seriously limited its further clinical transformation and medical application. Therefore, a mesoporous oxygen-generated smart carrier with single structure is urgently needed. To overcome this challenge, our group²²³ and Yang et al²²⁵ constructed a hollow mesoporous MnO₂-based delivery nanosystem, which not only controlled the release of packages under irradiation of 660 nm laser, but also possessed merits including outstanding biocompatibility, biodegradability, and simple nanostructure. Besides, we successfully designed a 660-nm laser-responsive cascaded programmed delivery nanosystem assembled by β-cyclodextrins-modified diblock copolymer (PEG-PGA-β-CD), adamantane-modified BODIPY (Ada-BODIPY), and adamantane-modified paclitaxel (Ada-PTX) via “CD-Ada” coordination interactions to program release payloads (Figure 7E).⁸¹ Upon irradiation, ROS was not only generated for PDT but also induced breakage of ROS-sensitive aminoacrylate group in Ada-PTX to free PTX for chemotherapy (Figure 7D).

3.2.2 | NIR

However, due to limited tissue penetration, vis light is not suitable for further *in vivo* applications, while NIR light with longer wavelengths, lower damage to normal tissues, and deeper tissue penetration is a potential exogenous energy to control drug release for preferably killing distal tumor cells.^{224–227} Meanwhile, most of NIR light-responsive nanomaterials also play an indispensable role in PTT and optical diagnostic imaging. Under exposure of NIR laser, the photothermal nanomaterials with strong NIR absorption, no matter as a wrapper or drug carrier, could convert photon energy into heat, with simultaneously triggering destruction of nanostructure for initial release progress or accelerating the release.²²⁸

Recently, two-dimensional (2D) nanomaterials have been attracted tremendous attention on NIR-triggered

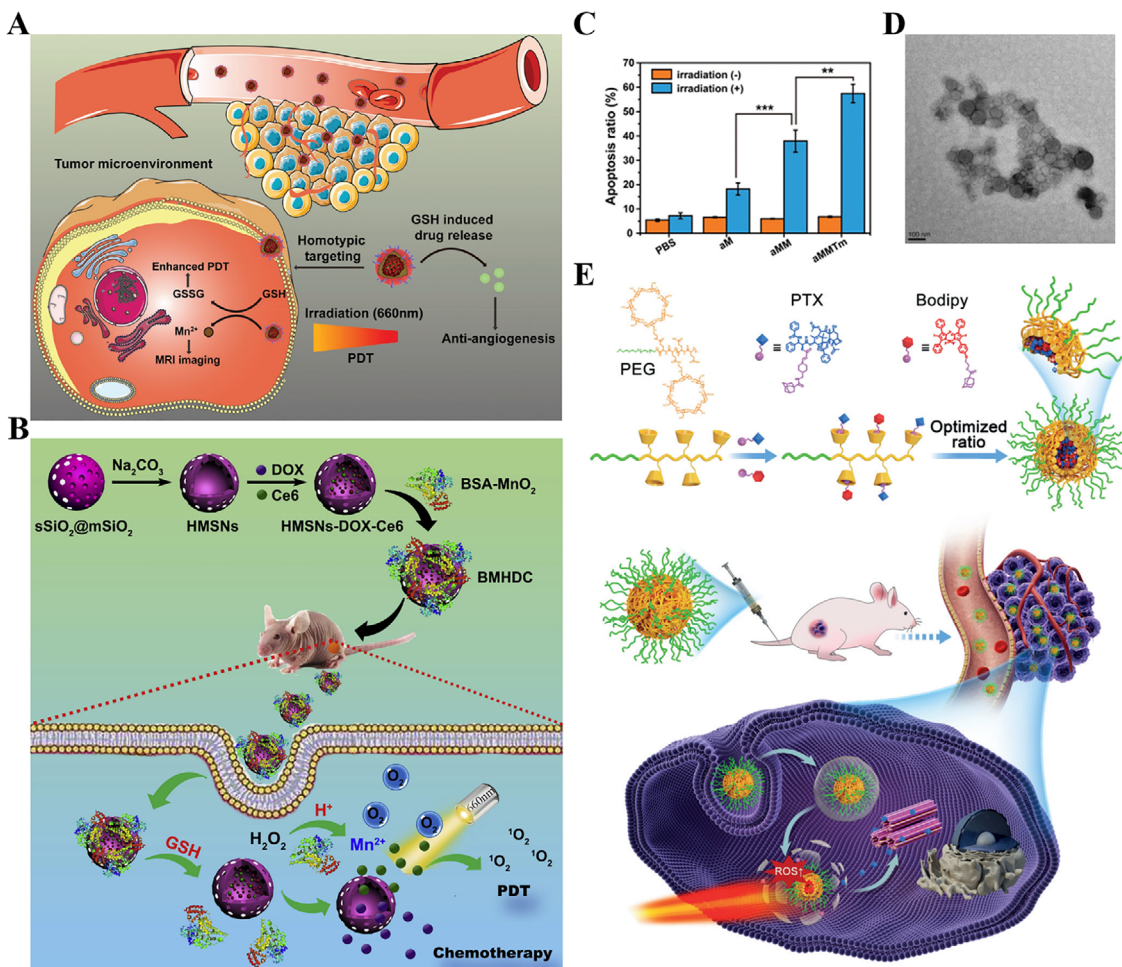


FIGURE 7 (A) Schematic illustration of aMMTm preparation and proposed combination therapy of PDT and antiangiogenesis. Reproduced with permission.²¹⁸ Copyright 2019, Wiley-VCH. (B) Schematic representation for synthetic process and therapeutic mechanism of BMHDC nanoparticle. Reproduced with permission.²²² Copyright 2019, Elsevier. Apoptosis ratios of differently treated cells was quantified in (C). ($n = 3$). (D) TEM images of Ada-PTX (60%)/Ada-BODIPY (40%) under the irradiation of the light with the power of 100 mW. (E) Schematic illustration of the self-assembly process of the nanoparticles with the optimized ratio and the light-activated combination therapy process. Reproduced with permission.⁸¹ Copyright 2019, Wiley-VCH

drug delivery owing to their relatively large surface area, excellent biocompatibility, and insignificant toxicity in dark.^{229–231} Among them, BP with distinct corrugated planes has showed enormous potential in increasing drug loading.²¹⁰ Under stimulation of light, air, or H_2O , it is easy to degrade into nontoxic phosphate and phosphonate, which are essential and safe elements for human body.^{232,233} For example, we have designed a 2D BP NSs with outstanding photothermal conversion performance as promising drug delivery nanosystem for cascaded combined therapy by mechanical exfoliation method. The first example of BP NSs as carriers to entrap anticancer drug (DOX) or dye (Cy7) by electrostatic interaction was reported by our group.²³⁴ The results indicated that the saturation of DOX loading was ~108% (Figure 8A), which was much higher than a majority of conventional delivery nanosystems (~10%–30%).^{235,236} Moreover, with

stimulus of 808 nm laser to control release status of on/off, the accumulated release amount of DOX from BP-PEG/DOX NSs (~54.4%) was much higher than that (~33.4%) without laser stimulus at pH 5.0 over 24 h, demonstrating that NIR laser could distinctly increase the release rate of DOX (Figure 8B). To further improve tumor targeting ability, we fabricated an FA-modified BPQDs-based nanosystem to delivery DOX for NIR-trigger synergistic-combined chemo-PTT (Figure 8E).²³⁷ Owing to active targeting effect of FA, this nanosystem not only greatly reduced toxicity to normal cells but also enhanced DOX accumulation in tumor site. In the nature or physiological environment, however, BP-based carriers without any covering layer may be relatively unstable at air and H_2O , easily inducing undesirable premature degradation and release, thus severely limit their further biological applications. To overtime this challenge, Liu et al²³⁸

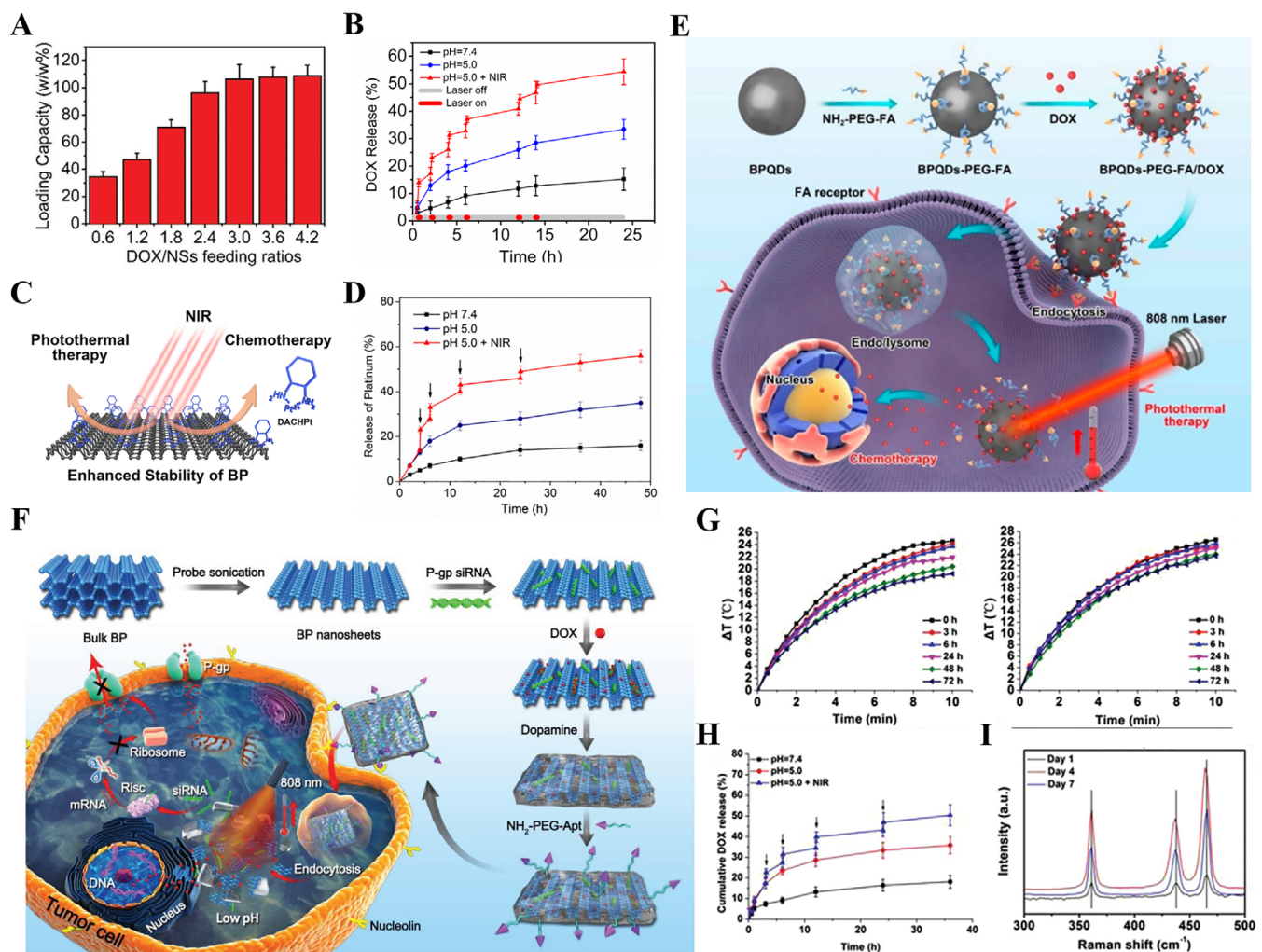


FIGURE 8 (A) DOX loading capacities on BP-PEG NSs (w/w %) with increasing DOX/NS feeding ratios. (B) Drug release kinetics of BP-PEG/DOX NSs at pH = 7.4 and pH = 5.0 (in the absence or presence of 1.0 W/cm² NIR laser). Reproduced with permission.²³⁴ Copyright 2016, Wiley-VCH. (C) Schematic depiction of BP/DACHPt in combined chemo-photothermal therapy. (D) Drug release profiles of BP/DACHPt at pH 7.4 and pH 5.0 (in the absence or presence of NIR irradiation), ↓: NIR irradiation for 10 min. Reproduced with permission.²³⁸ Copyright 2019, Elsevier. (E) Schematic illustration of BP quantum dots (BPQDs)-PEG-FA/DOX for synergistic photothermal/chemotherapy of cancer. Reproduced with permission.²³⁷ Copyright 2019, MDPI. (F) Schematic illustration of the procedure used to fabricate nanostructures and the combined chemo/gene/photothermal targeted therapy of tumor cells. (G) Photothermal heating curves of the BP NSs and BP@PDA, respectively, after storing in water for different periods of time and being irradiated with the 808 nm laser (1.0 W cm⁻²) for 10 min. (H) Drug release kinetics of BP-R-D@PDA at pH = 7.4 and pH = 5.0 (in the absence or presence of 1.0 W cm⁻² NIR laser), ↓: NIR irradiation for 0.1 h. (I) Raman spectra acquired from the BP@PDA after storing in water for different days. Reproduced with permission.⁴⁶ Copyright 2018, Wiley-VCH

tactfully utilized clinical anticancer drugs (oxaliplatin and cisplatin) itself to stabilize BP NSs by coordinating O₂⁻ or H₂O⁻ sensitive lone pair electrons of BP NSs with drugs, which not only commendably protected BP structural integrity, but presented minimal premature drugs leakage in blood circulation. (Figure 8C). In contrast, under laser irradiation, the release rate of drugs was further enhanced at pH 5.0 compared with that without irradiation (Figure 8D). Whereas, extensive surface of BP NSs was directly exposed to air and H₂O without any isolation, still remaining concerns about unexpected degradation and immature release of drug. To further control release more

precisely and protect structural integrity more powerfully, we used acid-sensitive biocompatible PDA shell (PDA) to coat bare BP NSs, simultaneously loading DOX and P-gp siRNA via electrostatic adsorption (Figure 8F).^{46,239} With NIR laser illumination, we found the cumulative DOX release amount was much higher than that (~35%) without illumination, reached 46.9% at 24 h, manifesting NIR-triggered DOX release behavior (Figure 8H). Moreover, the photothermal heating curves of BP and BP@PDA prestored in water for different periods verified that PDA coating could effectively prevent the degradation of BP NSs and maintain physicochemical performance (Figure 8G),

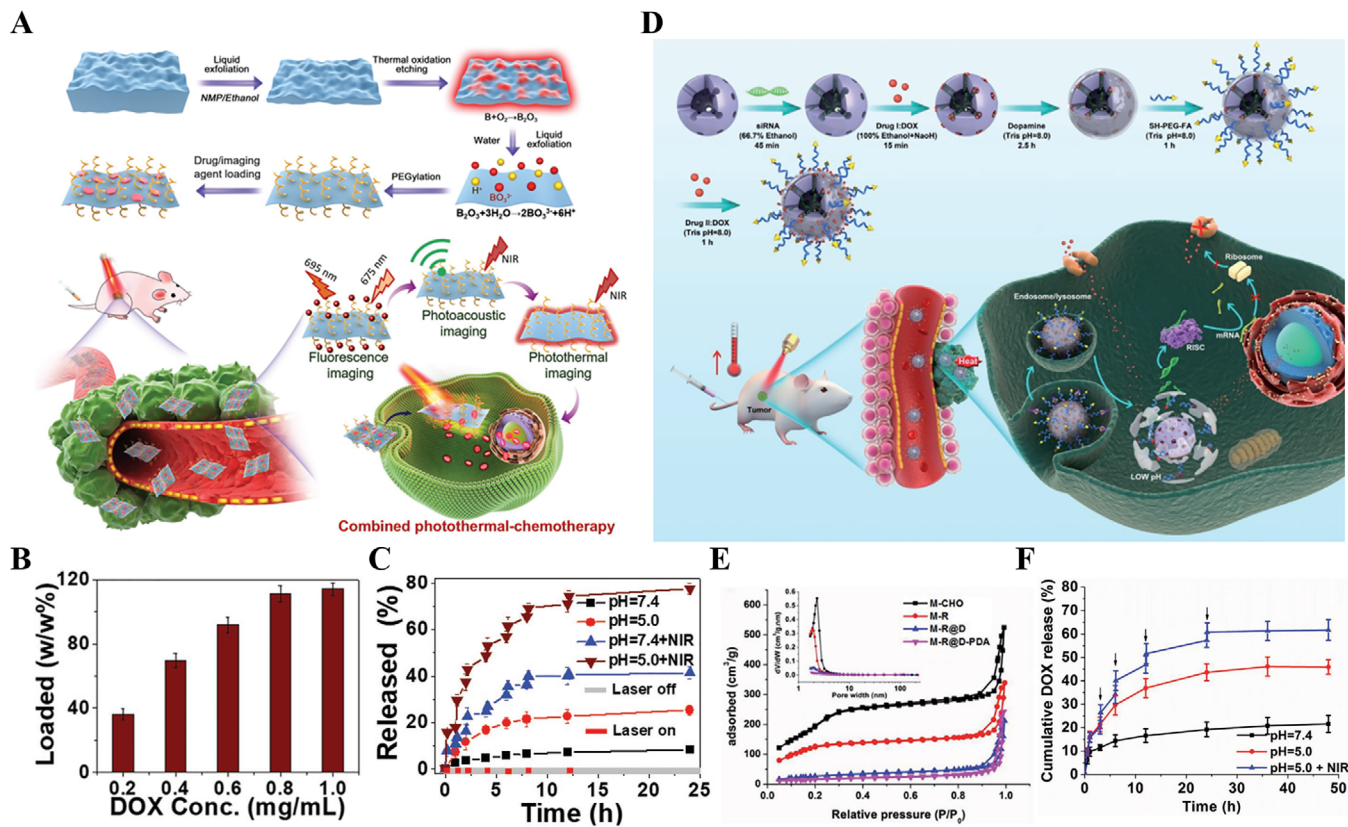


FIGURE 9 (A) Schematic illustration of the preparation of 2D B-PEG/DOX NSs and the systemic delivery of B-PEG/DOX NSs as a photonic nanomedicine for multimodal imaging-guided cancer therapy. (B) DOX loading capacities on B-PEG NSs (w/w %) with increasing DOX feeding concentrations. (C) Release profiles of DOX at different pHs with or without 808 nm NIR laser (1.0 W cm^{-2}). Reproduced with permission.²⁴⁰ Copyright 2018, Wiley-VCH. (D) Schematic illustration of the synthesis route of M-R@D-PDA-PEG-FA-D and the combined photothermal chemo gene targeted therapy of tumors. (E) Nitrogen adsorption–desorption isotherm. Inset: the pore size distribution. (F) Drug release kinetics of M-R@D-PDA-PEG-FA-D at pH = 7.4 and pH = 5.0 (in the absence or presence of 1.0 W cm^{-2} NIR laser) ↓: NIR irradiation for 0.1 h. Reproduced with permission.⁴³ Copyright 2017, Wiley-VCH

which was consistent with the Raman spectra results (Figure 8I).

Inspired by 2D BP NSs, our group first exploited a novel ultrathin high-quality 2D boron (B) NSs, served as a new photonic drug delivery nanoplatform by coupling liquid exfoliating and thermal oxidation etching (Figure 9A).²⁴⁰ The saturation of DOX loading in B NSs was ~114% by weight due to high surface-to-mass ratio of B NSs, corresponding to BP NSs (Figure 9B). The results showed that the DOX release amount from B-PEG/DOX NSs was only ~8.3% at pH 7.4 after 24 h because of their inherent leakage in blood circulation (Figure 9C). While for pH 5.0, ~24.0% of released DOX was detected owing to protonation of DOX in acid environment accorded with TME. In sharp contrast, under 808-nm laser irradiation, the NIR-responsive release amount drastically increased to ~41.4% and ~77.6% at pH 7.4 and 5.0, respectively. Because NIR-induced local hyperthermia further blocked electrostatic interaction between B-PEG NSs and DOX, thus triggered burst release of DOX. In general, B NSs-based drug delivery

nanoplatform has potential clinical applications. In addition, 2D biomaterials-based prodrug delivery nanosystem also attracts a lot of attention. Recently, Zhang et al²⁴¹ synthesized a novel ultrathin biocompatible SnTe NSs coated with MnO₂ shell to prevent undesirable degradation of SnTe NSs. When NSs reached tumor site, stimulated by NIR laser, SnTe@MnO₂-SP NSs not only produced heat to burn tumor, but also simultaneously generated toxicity TeO₃²⁻, which could act as an anticancer drug to kill tumor cells.

The materials we mentioned above, PDA, as a mussel-inspired material, not only possesses acid-responsive ability, but also has potential to delivery drugs due to characteristic of NIR-triggered structural collapse.^{41,44,242} For instance, Liu et al²⁴³ designed a core-shell structure-based delivery nanosystem formed by coating dynamic PEGylated borate-based coordination polymer with porous structure into NIR-responsive PDA core (termed PDA@CP-PEG). The polymer containing phenylboronic acid (PBA) groups could be used to load DOX with

considerable loading efficiency (~80%) and further to connect with catechol-capped PEG by forming an acid-cleavable PBA/catechol bond. When this nanoplatform reached tumor site, it started to release DOX and further accelerated release process under NIR laser irradiation. Although porous structure-based delivery nanoplatform could commendably increase drug package efficiency, there were still considerable concerns about the exposed pore canal that could not prevent premature leakage-induced toxicity absolutely and powerfully. Therefore, we developed a multifunctional DDS (M@D-PDA-PEG-FA-D) formed by capping the pores of P-gp siRNA-encapsulated MSNs with DOX and then coating PDA film to control the release (Figures 9D and 9E).^{43,244} After that, in order to achieve minimal toxicity to tissues, active tumor-targeted molecule FA was linked to the surface of PDA shell. At pH 5.0, ~45.9% of DOX from M@D-PDA-PEG-FA-D NPs was released over 48 h, while the release amount of DOX significantly increased to ~60% with the aid of 808 nm laser (6 min) over the same time period, attributed to acid- and NIR-sensitive property of PDA (Figure 9F).

3.3 | Ultrasound-responsive smart materials

In comparison with light, US, acting as a noninvasive and nonionic mechanical wave, has higher tissue-penetration ability with lower tissue attenuation. The US has been applied to control drug release with higher spatial precision in recent years.^{208,245,246} Furthermore, US-triggered cavitation, mechanical, or thermal effects can result in disassembly or even collapse of US-responsive smart materials mainly including inorganic sonosensitizers and organic sonosensitizers, and further give rise to release the payloads and concurrently exert SDT, US-triggered chemotherapy, and US-stimulated imaging.^{247–251}

For instance, Yue et al¹⁹ constructed an FDA-approved liposome-based delivery nanoplatform simultaneously coloading with two hydrophobic molecules, US-responsive sonosensitizer hematoporphyrin monomethyl ether, and immune adjuvant imiquimod (R837). The US-responsive sonosensitizer would produce ROS to induce tumor cell apoptosis and concurrently destroy nanostructure of liposomes to release R837 under stimulation of US. To further enhance cascaded interaction between US-responsive drug release and oxygen-dependent SDT, Li et al²⁵² flexibly employed fluorinated chitosan with self-assembled ability to coat sonosensitizer-conjugated catalase (CAT), forming US-activated delivery nanoplatform for orthotopic bladder tumors treatment. Under exogenous US irradiation, its nanostructure would give rise to rupture, thus triggering release of CAT. Subsequently, overexpressed H₂O₂ in

the TME immediately reacted with CAT to generate O₂, which facilitated SDT in return. This drug delivery strategy commendably achieved cascaded reaction in the tumor site with single stimulus.

Except for organic sonosensitizers-based delivery nanosystem, inorganic sonosensitizers (titanium dioxide [TiO₂]) also attracted lots of attention of researchers. Currently, Liang et al²⁵³ synthesized a DOX-loaded hollow Pt-TiO₂ Janus nanostructure and its loading capacity could reach 20.2% (Figure 10A). Moreover, the drug release results demonstrated that about 52% of DOX was released from this nanoplatform over 72 h with double stimulation of pH 5.5 and US irradiation (1.0 MHz, 1.5 W cm⁻², 5 min), while the release percent was only ~43% with single stimulation of pH 5.5 (Figure 10B). To improve drug release sensitivity to US and minimize toxicity to healthy tissues, a PEI-FA conjugation decorated curcumin (CUR)-loaded core-shell nanostructure (CUR@FA-PEI-DSTNs) based on TiO₂-coated MSNs was exploited with considerable loading capacity (~25.37%) (Figure 10D).²⁵⁴ The US-controlled drug release experiment showed that about 90% CUR from CUR@DSTNs leaked at pH 7.4 without the aid of gatekeepers PEI-FA conjugation after 48 h, while the cumulative release percentage from CUR@PEI-FA-DSTNs was below 20% at the same period time, indicating that PEI-FA-conjugated nanoplatform was quite safety in blood circulation without US irradiation (Figure 10E). In contrast, the release amount of CUR from CUR@PEI-FA-DSTNs reached up to ~50%, ~61%, and ~78%, respectively, under US irradiation ((1 MHz, 2 W cm⁻²) for 30, 60, and 120 s at the beginning of the drug release experiments. Manifesting the release behavior of CUR is US irradiation time-dependence and badly US-sensitivity.

Thanks to cavitation, the US irradiation could also be used to transform the morphology size of smart delivery nanoplatform from big size to small size, so as to promote penetration in tumor and enhance treatment efficacy for deep-seated tumors. Lin et al²⁵⁵ constructed a US and GSH dual-responsive delivery nanomicelle with self-assembly capacity formed by Janus Au-MnO NPs grafted with hydrophilic PEG-SH and hydrophobic ROS-sensitive sulphydryl-capped polymers (PPADTS) via Au-S chemical bond (Figure 10F). Owing to the breakage of PPADTS induced by produced-ROS upon US irradiation, this nanomicelle (~100 nm) would disassemble into smaller monomer Janus Au-MnO NPs (~20 nm). Then, the monomer NPs further exerted chemodynamic therapy with deeper penetration in GSH-overexpressed TME for treatment of orthotopic liver tumor (Figure 10G). Moreover, Meng et al utilized US stimulation to achieve the morphological transformation from microbubbles simultaneously containing Au NPs and sulfur hexafluoride gas to

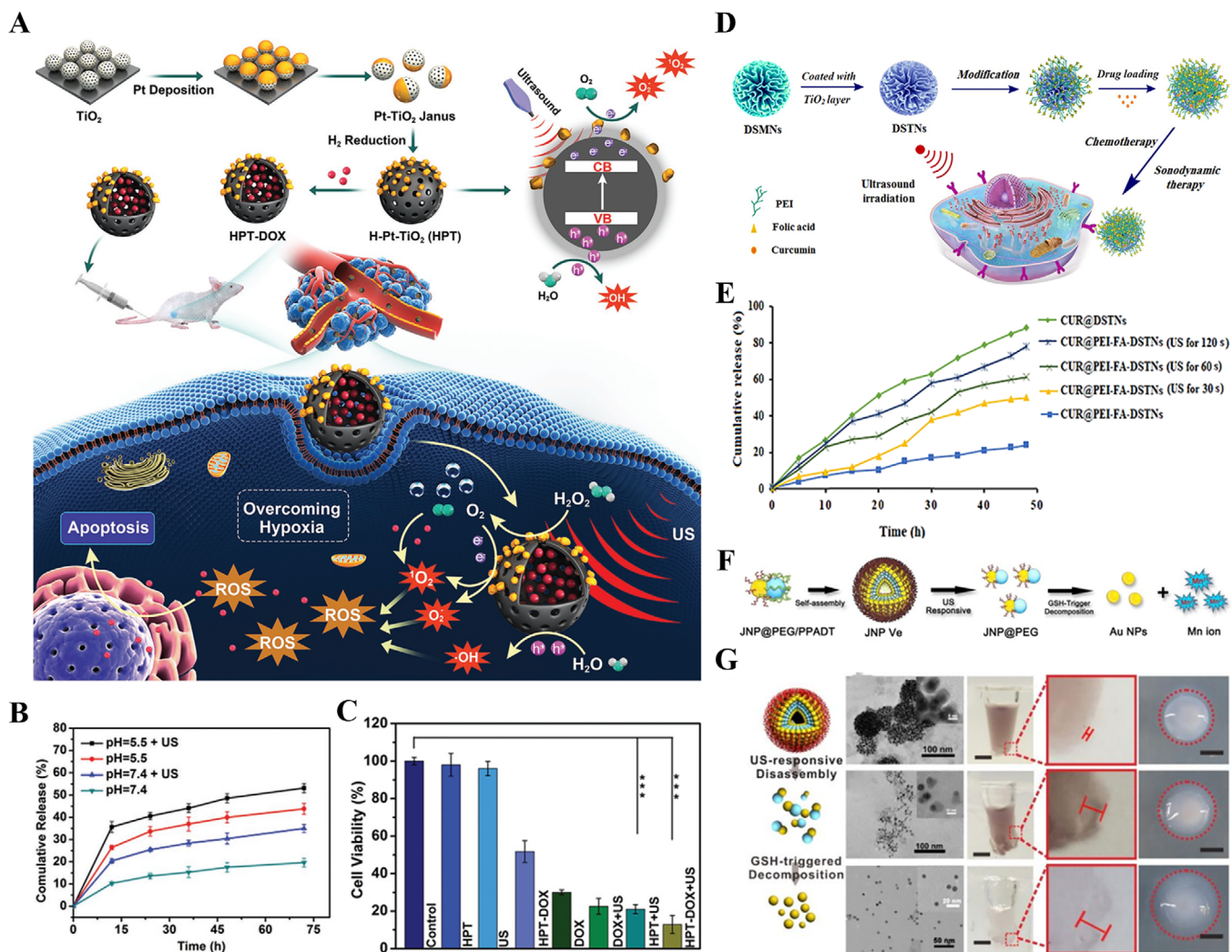


FIGURE 10 (A) Schematic illustration for the preparation and the anticancer mechanism of HPT-DOX. (B) The drug release from HPT-DOX triggered by US irradiation in different conditions ($\text{pH} = 7.4$ and 5.5), $n = 3$. (C) Cell survival rates of 4T1 cells incubation for 24 h after different treatments including control, HPT, US, HPT-DOX, DOX, DOX + US, and HPT-DOX + US ($*** p < .001$). Reproduced with permission.²⁵³ Copyright 2020, Wiley-VCH. (D) Synthetic route for the preparation of CUR@FA-PEI-DSTNs and its sonodynamic therapy. (E) *In vitro* release profiles of CUR@DSTNs and CUR@PEI-FA-DSTNs in PBS at different release conditions. Reproduced with permission.²⁵⁴ Copyright 2019, American Chemical Society. (F) Schematic illustration of self-assembly of amphiphilic Janus Au-MnO NPs into functional vesicles. (G) The schematic diagram of dissociation process of the vesicle. (d-f) TEM images of JNP Ves, Janus Au-MnO NPs, and single Au NPs. (g-i) Images showing penetration of JNP Ves, Janus Au-MnO NPs, and Au NPs. Reproduced with permission.²⁵⁵ Copyright 2019, Wiley-VCH

nanobubbles because of the strong cavitation properties of gas, in order to dramatically enhance PA signals *in vivo* and *in vitro*.²⁵⁶

3.4 | X-ray-responsive smart materials

As the main source of radiation, X ray, which is wildly used in clinical cancer treatment for several years, can penetrate into deeper solid tumor with higher energy compared with light.²⁵⁷ However, on account of the low radiation absorption of tumor tissues and hypoxia in the TME, O₂-dependent radiotherapy (RT) in clinical

always requires exogenous X-ray radiation with superior doses, frequently resulted in unexpected damages to surrounding normal tissue.^{258,259} Therefore, researchers developed a mass of high atomic number (Z) elements contained smart nanosystems with higher X-ray absorbing capability and/or O₂-generated property to precisely deposit radiation energy in tumor cells, in order to decrease toxicity to normal tissues and augment therapeutic efficacy as far as possible.^{260–262} Furthermore, X-ray-triggered various emissions in those nanosystems could also be applied to trigger cascade reaction for cancer treatment, such as photoelectrons, Auger electrons, and Compton electrons.²⁶³

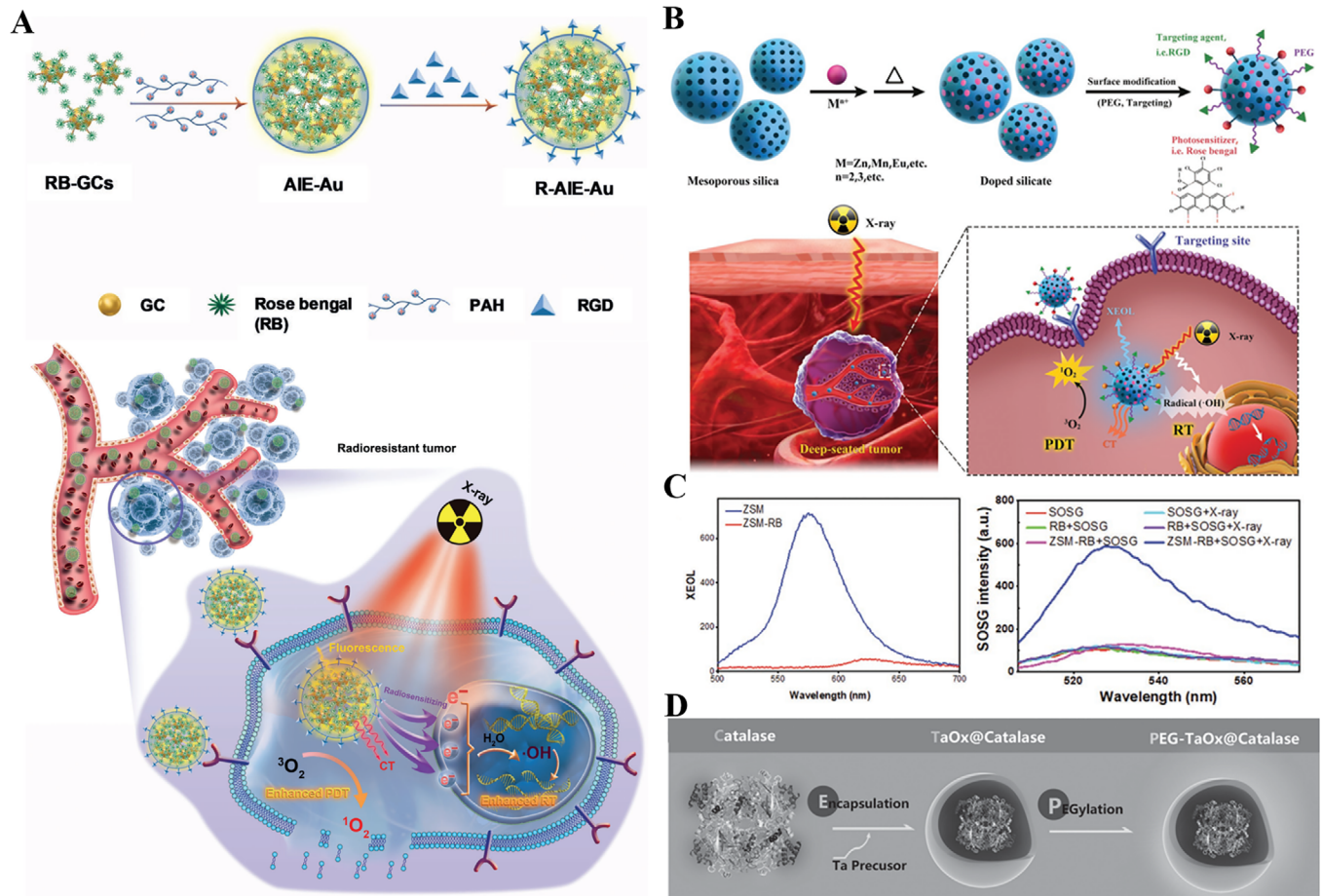


FIGURE 11 (A) Schematics showing the preparation of R-AIE-Au nanosensitizers and a working model of R-AIE-Au for fluorescence and CT imaging-guided X-ray-induced enhanced RT and PDT. Reproduced with permission.²⁶⁴ Copyright 2019, Wiley-VCH. (B) Schematic illustrations of the process of the preparation of RGD-ZSM-RB nanosensitizers and of the mechanisms of RGD-ZSMRB-mediated X-PDT. (C) The luminescence spectra of ZSM (blue curve) and ZSM-RB activated by X-ray irradiation (red line). The SOSG fluorescence spectra in different solutions with or without X-ray irradiation. Reproduced with permission.²⁶⁵ Copyright 2019, Wiley-VCH. (D) A scheme showing *in situ* encapsulation of catalase into hollow nanospheres of TaOx and the subsequent PEGylation. Reproduced with permission.²⁶⁶ Copyright 2016, Wiley-VCH

Among those high atomic number elements, Au, possessed wonderful performance of considerable radiosensitization, satisfactory biocompatibility, and easily secondary modification, is generally applied in establishing X-ray-sensitive drug delivery nanosystems. For instance, an aggregation-induced emission gold clustoluminogens (AIE-Au)-based nanoparticle, which not only augments absorption of X ray (lower than the dose used in clinical) to produce abundant ROS, but also enhances the X-ray-excited optical luminescence (XEOL) by 5.2-fold due to photoelectron effect, was successfully prepared (Figure 11A).²⁶⁴ Interestingly, under single X-ray stimulation, the luminescence immediately excited conjugated photosensitizers to further generate ROS with cascaded amplification. Except for Au element, Sun et al.²⁶⁵ reported a bio-compatible silicate scintillators doped Zn, Mn, and Eu also had XEOL effect to excited photosensitizer (rose bengal,

containing four iodine atoms) loaded in the pore canal to exert PDT effect and enhance RT therapeutic effect at the same time due to X-ray strong absorbing ability of I atoms under low-dose X-ray irradiation (Figures 11B-6C). In summary, X-ray-responsive smart delivery nanoplatforms with XEOL effect not only reduce side effect to normal tissues by using harmless dose of X ray, but also overcome the challenge that external light-induced PDT with limited penetration depth could not completely clear out the solid tumor. Because X-ray-activated XEOL effect *in situ* could transmitted energy to photosensitizers collocated in tumor tissues for PDT.

However, the complex nanostructure and severe synthesis process seriously limited the potential clinical application of Z elements' doped delivery nanosystems. Therefore, a new delivery nanosystem formed by loading catalase within tantalum oxide (TaOx) nanoshells was assembled

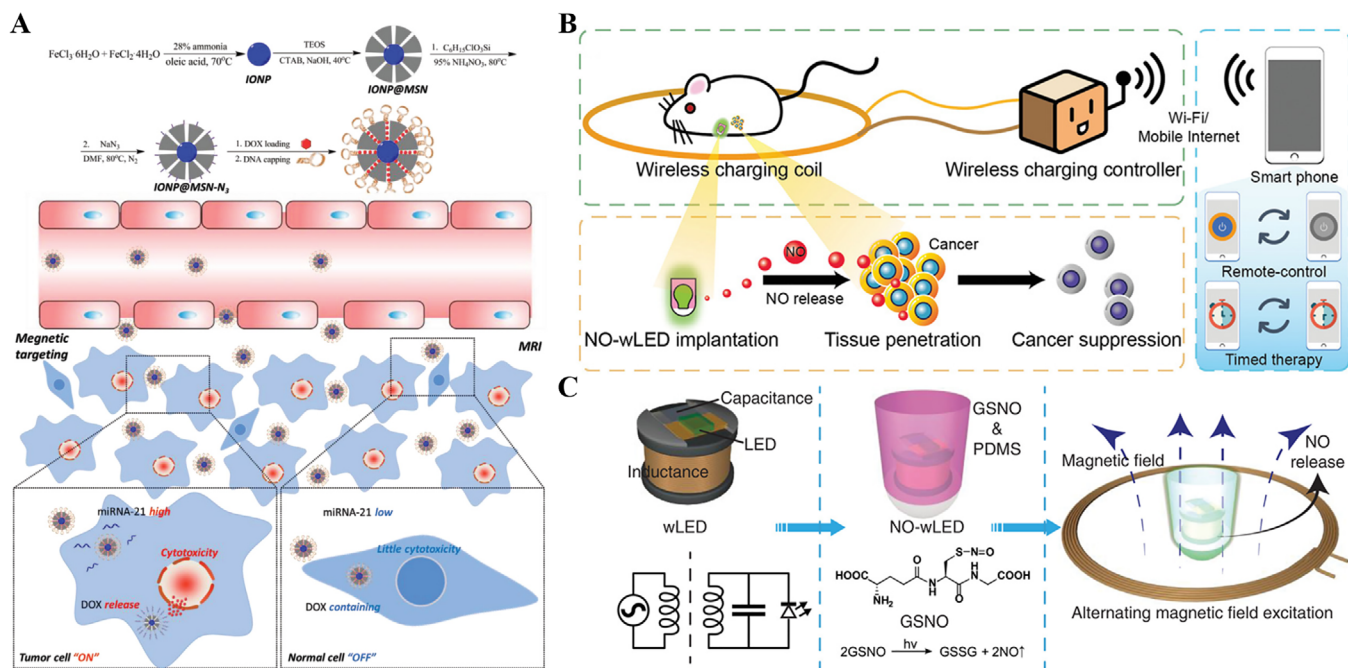


FIGURE 12 (A) Scheme for the synthesis of nanostructures of IONP@MSN/DOX-DNA and its tumor cell-activated therapy under the magnetic irritation. Reproduced with permission.²⁷⁰ Copyright 2020, American Chemical Society. (B) Cancer therapy by remote-controlled NO release from wirelessly charged NO-wLED. (C) Construction and simplified circuit diagram of wLED (left), the structure of NO-wLED and NO release reaction from GSNO under irradiation (middle), and illumination of NO-wLED by alternating magnetic field excitation in wirelessly charged coil (right). Reproduced with permission.²⁷² Copyright 2020, Wiley-VCH

via a simple and mild one-step method (Figure 11D).²⁶⁶ Upon exposure to X-ray and overexpressed H_2O_2 concentration in the TME, TaOx NSs would be destroyed to produce ROS, accelerate release of CAT, and further facilitate O_2 generation for improving O_2 -dependent RT. In addition, except for used to excite high atomic number elements, X-ray irradiation is also applied to break low-energy chemical bond to promote drug release, which is different from conventional RT. Fan et al designed a *tert*-butyl hydroperoxide (TBHP) and iron pentacarbonyl ($\text{Fe}(\text{CO})_5$) coloaded hollow mesoporous organosilica (HMNs) nanoplatform with biodegradability.²⁹ The former drug (TBHP) contained unstable peroxy bond would be cleavable to produce highly toxic hydroxyl ($\cdot\text{OH}$) under X-ray radiation, and then the latter drug ($\text{Fe}(\text{CO})_5$) with ROS-responsive feature would be activated to release CO for gas therapy. Such a single stimulation-activated smart drug delivery nanoplatform with programmed release capacity has potential medicinal applications in clinic.

3.5 | Magnetic-responsive smart materials

Magnetic field, as a powerful external stimulation, plays crucial role in on-demand drug delivery, real-time

MRI, and other biomedical applications, on account of its outstanding temporal-spatial resolution, noninvasive, deep penetration, and quantitative evaluation of disease pathogenesis.^{208,267} Up to now, three magnetic-responsive delivery strategies have been developed by the investigators primarily: (a) magnetic field-directed drug targeting delivery strategy; (b) magnetic hyperthermia-triggered drug release strategy; and (c) magnetic-field-controlled on-demand and repeating drug release strategy.

As is known to all, the paramagnetic or superparamagnetic materials with strong magnetically targeted capacity have broadly been investigated to delivery toxicity drugs to tumor. Among these materials, superparamagnetic iron oxide nanoparticles (SPIONs) have gained widespread popularity because of their excellent magnetic targeting ability and magnetic thermal performance.^{268,269} For example, Liu et al employed SPIONs to accurately delivery DOX-loaded MSNs to tumor site with minimal toxicity to healthy tissues in the guidance of magnetic field (Figure 12A).²⁷⁰ Besides, a SPIONs-based core-shell nanostucture loading DOX into the thermoresponsive copolymer shell was successfully established.²⁷¹ They found that the DOX cumulative release percent from this nanostucture incubated at 37°C was almost 0% after 10 h, while the release amount encouragingly reached to 100% at 42°C after 54 h. It is interesting to note that the increased temperature of SPIONs, possessing magnetic

hyperthermia effect, was high enough ($>42^{\circ}\text{C}$) to initial burst release of DOX under magnetic stimulation. Although above-mentioned nanosystems effectively control the release of drugs in tumor site, the limited loading capacity and restricted magnetic stimulation for once is unable to meet the requirements of clinical patients. Inspiringly, Li et al²⁷² designed an implantable nitric oxide (NO)-release nanocarrier, which could be activated by simultaneously implantable wirelessly powered light-emitting diode (wLED) nearly closed to nanocarrier to release NO with artificially controllable and long-term release pattern under the stimulation of external wireless charging (Figure 12B). It is worth noting that wLED would transmit light with wavelength of 335 or 545 nm, which was accorded with the absorption wavelength of NO precursor molecules GSNO. The electrical energy from wireless charging was converted into magnetic energy first. Then, the magnetic energy was immediately converted into electrical energy to illuminate the wLED (termed wireless power transmission), when the wireless charging was supplied power controlled by a smart phone through wifi or mobile internet (Figure 12C). This magnetic-field-controlled on-demand and repeating drug release strategy has been initiated a new vision on magnetic-responsive smart delivery systems. It may be activated through inductive coupling effect using magnetic as intermediate energy medium or directly energy output source to control the release of drugs artificially and intelligently.

4 | MULTIPLE-TRIGGERED SMART MATERIALS

TME is a relatively independent and complex system. In general, the extremely harsh microenvironment, for example, pH, GSH, and enzyme, may coexist simultaneously but present spatial heterogeneity. These characteristics provide the possibility for engineering of multiple endogenous sensitive smart materials. Moreover, comparing to endogenous responsive smart materials alone, those composite materials that are sensitive to both endogenous and exogenous stimulus might possess higher treatment efficiency. Rational design of multiple-responsive smart materials for either endogenous or exogenous conditions can facilitate multistage drug delivery and synergistic effect of multiple functions, achieving higher specificity and efficacy of chemotherapy by overall prolonging blood circulation, improving tumor accumulation, strengthening cell penetration, increasing internalization with cancer cells, etc.

The multiple endogenous sensitive smart materials were common in many works, such as dual responsive materials to pH and GSH,^{273–277} pH and hypoxia,¹³¹ pH and

enzyme,¹⁷³ ROS and GSH,^{60,278,279} GSH and hypoxia,^{280,281} as well as GSH and enzyme.¹⁸³ There were also examples of triple responsive materials which were sensitive to pH, GSH, and enzyme.^{161,282} These materials are usually single polymer with dual or multiple endogenous sensitive linkers and polymer complexes for dual or multiple endogenous responses, forming nanosystems as carriers or prodrugs. For achieving multistage drug delivery and release in tumor regions, in a recent study, PEG-Azo-PLGA and DATAT-PEG-PLGA (dimethylmaleic anhydride [DA]-terminated TAT-PEG-PLGA) were constructed and self-assembled to nanomicelles loaded with Ce6 and TPZ.¹³¹ These nanomicelles would experience stepwise-activatable destinies in tumor regions among the five stages *in vivo*. Initially, the TAT-functionalized nanoparticles were protected by DA to prolong blood circulation and then degraded the DA protectors in tumor acidic environment. Thus, tumoral accumulation and further cellular uptake were improved with Ce6 release. With exogenous laser treatment, Ce6 produced cytotoxic ROS with consumption of O₂ supply. The subsequently generated hypoxic microenvironment induced the Azo-benzene bonds breakage of the nanomicelles with hypoxia activatable prodrug TPZ release. Finally, TPZ was activated by PDT-triggered hypoxia to achieve synergistic PDT and bioreductive chemotherapy. In another creative study, a unique type of dual-responsive human serum albumin (HSA)-based nanosystem was reported.²⁸⁰ As shown in Figure 13A, the Ce6-conjugated HSA and Pt (IV) prodrug-conjugated HSA were cross linked by the hypoxia-sensitive azobenzene group to form the dual endogenous sensitive nanosystem. Under hypoxic conditions, hypoxia-responsive azobenzene moiety of the nanosystem would be cleaved with nanosystem dissociating into ultra-small Ce6-conjugated HSA and Pt (IV) prodrug-conjugated HSA, resulting in deep tumor penetration enhancement and further intracellular GSH-responsive chemotherapy. A smart unimolecular micelle-based polyprodrug with dual endogenous redox-response, starlike polymer β -CD-*b*-P(CPT_{GSH}-co-CPT_{ROS}-co-OEGMA), was synthesized and proved to equip with higher anticancer activity than the single ROS- or GSH-responsive polyprodrug.²⁷⁹ Because the dual redox-response polyprodrug could be triggered to release CPT completely and intelligently by the dynamic equilibrium high GSH concentration and ROS levels in the TME.

Multiple exogenous sensitive smart materials can also be seen in some works. For instance, Li et al²⁸³ developed a chiral Cu_xCo_yS nanoplateform to selectively eliminate senescent cells with insignificant damaging the activities of normal cells in the meantime under stimulation of both an alternating magnetic field and an NIR laser. In another example, an innovative delivery nanoplateform made by red

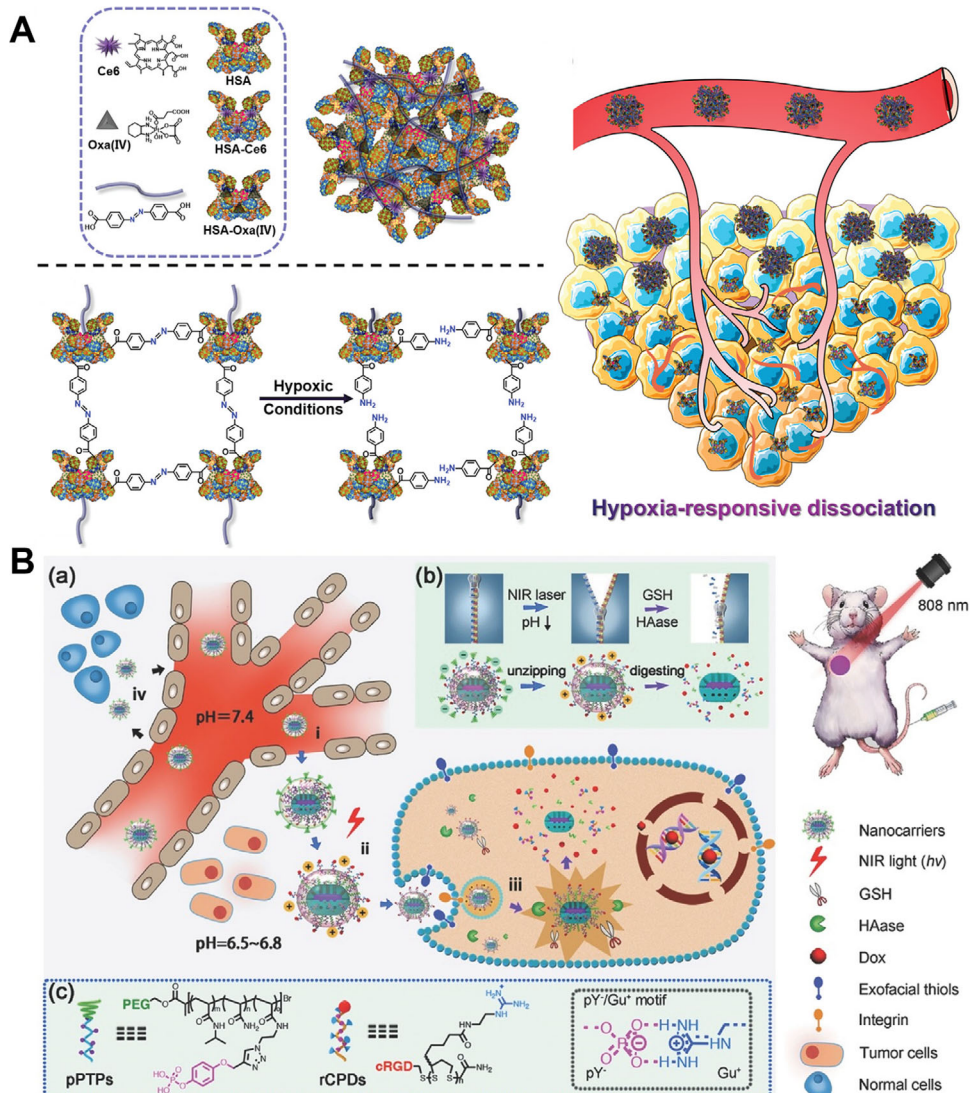


FIGURE 13 (A) Synthesis, hypoxia-responsive dissociation, the increase tumor penetrating ability induced by hypoxia-responsive dissociation of HSA-based complexes. Reproduced with permission.²⁸⁰ Copyright 2019, WILEY-VCH. (B) Schematic design of smart nanocarriers coated with pH-/thermal-/GSH-responsive polymer zippers for precision tumor treatment. (a) NIR-/pH-guided cellular uptake and GSH/HAase-controlled release in vivo. (b) The surface state variations during drug delivery (the polymer zipper decoding and the sandwich protective shell degradation). (c) The composition of the pPTP/CPD polymer zipper with multiple pY⁻/Gu⁺ salt bridges. Reproduced with permission.²⁸⁹ Copyright 2017, WILEY-VCH

blood cell membrane modified engineered *Chlorella vulgaris* was developed.²⁸⁴ First, the nanoplatform could successfully delivered to tumor tissues with the protection of red blood cell membrane, and then, generated O₂ *in situ* to alleviate tumor hypoxia under illumination of red light due to the photosynthesis of *C. vulgaris*, leading to improved RT induced by X ray. Subsequently, the release of chlorophyll from *C. vulgaris* could response to 650 nm laser irradiation to produce ROS, resulting in further enhanced cancer cell killing. Such a multiple stimulus-responsive nanoplateform (red light/X ray/Vis light) with cascade anticancer reactions has huge potential to promote the further development of nanomedicine.

Many exogenous response materials that were sensitive to temperature, light, radiation, ultrasound, and magnetic, as mentioned above, were combined with endogenous sensitive smart materials for cooperative action of chemotherapy and PDT/PTT,^{46,119,285} controlled multistage drug delivery,^{286–290} cooperative action of chemotherapy and SDT,²⁹¹ sequentially triggered excellent RT,²⁹² PAI-guided synergistic chemo-PTT,^{156,290} MRI-guided combinatorial chemotherapy,^{95,120,121} etc. In a typical example, a pH-/thermal-/GSH-responsive polymer zipper was engineered as the smart surface of nanocarriers.²⁸⁹ In detail, RGD-tailed poly(disulfide)s bearing guanidinium (Gu⁺) residues (rCPDs) and the PEG-tailed thermosensitive

polymers bearing phosphate (pY^-) residues (pPTPs), seen in Figure 13Bc, were adhered to each other by multiple salt bridges of the efficient molecular glues between Gu^+ and pY^- groups as a smart polymer zipper for controlled multistage drug delivery. Under low pH in the tumor environment and exogenous NIR laser, the pY^-/Gu^+ binding was weakened and unzipped by phase transition to exposure the positive surface charges of Gu^+ motifs. And with the assistance of cell-penetrating RGD, these nanocarriers exercised rapid cellular uptake and endosome escape. At last, endogenous GSH could digest the RGD-tailed poly(disulfide)s bearing Gu^+ residues and collapse the zipper with drug release. Moreover, in another recent study, Zhu et al developed the PAI-guided concurrent chemo-immunotherapy system by the self-assembled PEG-grafted nanogapped gold nanoparticles (AuNNPs) and poly(SN38-co-4-vinylpyridine) (a dual pH/GSH-responsive polyprodrug).²⁹⁰ The AuNNPs encapsulated immune inhibitor BLZ-945 to achieve targeted pH-responsive immunotherapy. In detail, the acidic environment induced nanogapped AuNNPs dissociation into single AuNNP, whereupon the single AuNNP equipped with excellent cell-penetrating ability and intracellular GSH-responsive chemotherapy. Thus, controlled multi-stage DDS under PAI guide and endogenous pH/GSH induction was established.

5 | PRESENT AND OUTLOOK

Thanks to the advances in materials science, molecular pharmaceutics, and nanobiotechnology, the first two decades of the new century have witnessed the flourishing growth of stimuli-responsive materials. Although there are enormous efforts in scientific publications, few technologies have practiced successfully in clinical translation.

Only two tapes of exogenous-triggered smart materials own commercialized products, including thermal-responsive liposomes and magnetic-responsive iron oxide nanoparticles.²⁹³ The listed magnetic-responsive iron oxide nanoparticle (Nanotherm®, MagForce AG) was first approved by FDA in 2010. And the commercialized thermal-responsive liposome (ThermoDox, Celsion Corp.) had finished the Phase III study in HCC treatment for 3 years (NCT00617981) but has not got the approval of FDA yet. At present, ThermoDox® involved clinical trials (NCT02536183 and NCT03749850) are still ongoing.

Part of clinical trials of stimuli-responsive materials-based nanocarriers was summarized in the work of Peng Mi. However, some of them stopped at Phase I or Phase II like MTC-DOX (DOX adsorbed to magnetic targeted carriers). And there is no existing clinical trial of thermosensitive nanoparticles for disease

diagnosis earning profits from the thermosensitive characteristics of these nanomaterials.²⁹⁴ The ongoing clinical trials of endogenous-triggered smart materials-based nanocarriers including LiPlaCis (NCT01861496), CRLX101 (NCT03531827 and NCT02769962), and NC6300 (NCT03168061). CRLX101 is a pH-responsive nano polyprodrug that was first formed by self-assembly polymer of PEGylated β -cyclodextrin-CPT conjugates in 2003.^{295,296} The preclinical data confirm the superiority of CRLX101 in solubility, formulation, toxicity, and pharmacokinetic challenges when compared with other CPT administrations, but clinical trials have not yet found enough competitiveness for its clinical use. NC6300 is another pH-responsive nano polyprodrug of HDZ bond-linked epirubicin and PEG polyaspartate block copolymer.²⁹⁷ Furthermore, the LiPlaCis liposomes are designed to release the encapsulated cisplatin under the hydrolysis of phospholipase A2.²⁹⁸ In brief, the clinical study of either endogenous or exogenous sensitive smart materials is still in its infancy, far from for extensive clinical application.

But why are the stimuli-responsive smart materials stepping into troubles in clinical translation? First, biocompatibility and biodegradability. In drug delivery, the systematic toxicity and immunogenicity of the formulations will result in poor clinical performance. Meanwhile, the higher molecular weights of smart polymer carriers are supposed to more effective in reaching their cellular targets, resulting in accumulative toxicity in the body. Thus, it is urgent to use or design materials with excellent biocompatibility and biodegradability. Second, high sensitivity. Many materials like thermosensitive materials cannot provide enough advantages in clinical use based on its thermosensitive characteristics. Third, application range. The triggered delivery systems are always associated with specific disease states, such as specific tape of tumor, making their poor clinical reality from a pharmacoeconomic perspective. Finally, large-scale manufacturing. The structural and physicochemical complexity of the materials and its formed nanocarriers act as an impenetrable barrier for pharmaceutically manufacture on a large scale, limiting their clinical translation potential. Besides, other considerations such as the drug nature, components stability, components cost, pharmacokinetics, pharmacodynamics, whether the airport scanners or ambient conditions or fever will trigger it, and so on, are equally important for clinical translation of stimuli-responsive smart materials.

As we have seen, numerous stimuli-responsive smart materials have been explored for drug delivery as nanocarriers in the preclinical state. In that regard, it is time for clinical translation-oriented exploration of these materials. It does not mean that the research in this field must own potential of clinical translation immediately, but

considering the importance of practicality of them at the beginning of design. And more efforts should be focused on addressing the dilemma of stimuli-responsive smart materials in translation development.

Many clinical trials of single smart materials-based drug delivery were failure in the clinical studies. Combination with tumor target drugs such as Olaparib (NCT02769962) or tumor immunotherapy antibodies might the new development opportunity. Overall, the nanocarrier of stimuli-responsive smart materials bring novel strategy for tumor drug delivery. They have been gifted with multiple functions such as controlled drug release, increased tumor accumulation, “ON-OFF” switch activities, as well as enhanced diagnostic accuracy and therapeutic efficacy. The future development prospects of smart materials in drug delivery can be expected with the innovations of materials chemistry, biomolecular engineering, pharmaceutical science, and so on.

CONFLICT OF INTEREST

The authors declare no conflict of interest.

ACKNOWLEDGMENTS

Y.Y. and W.Z. contributed equally to this work. We are grateful for the financial support from the National Natural Science Foundation of China (31922042, 81771966, and 32071342), Guangdong Special Support Program (2019TQ05Y209), and the Fundamental Research Funds for the Central Universities (19ykzd31).

ORCID

Lin Mei  <https://orcid.org/0000-0001-6503-5149>

REFERENCES

- R. J. Deshaies, *Nature*. **2020**, *580*, 329.
- A. S. Hoffman, *Adv Drug Del Rev*. **2013**, *65*, 10.
- M. E. Calderera-Moore, W. B. Liechty, N. A. Peppas, *Acc Chem Res*. **2011**, *44*, 1061.
- S. M. Park, A. Aalipour, O. Vermesh, J. H. Yu, S. S. Gambhir, *Nat Rev Mater*. **2017**, *2*, 17014.
- M. S. Muthu, D. T. Leong, L. Mei, S. S. Feng, *Theranostics* **2014**, *4*, 660.
- Z. Li, N. Song, Y. W. Yang, *Matter* **2019**, *1*, 345.
- E. Blanco, H. Shen, M. Ferrari, *Nat. Biotechnol*. **2015**, *33*, 941.
- S. Wang, P. Huang, X. Chen, *ACS Nano* **2016**, *10*, 2991.
- Y. Liu, C. F. Xu, S. Iqbal, X. Z. Yang, J. Wang, *Adv. Drug Del. Rev*. **2017**, *115*, 98.
- Y. Dang, J. Guan, *Smart Mater Med*. **2020**, *1*, 10.
- H. Chen, D. Liu, Z. Guo, *Chem. Lett*. **2016**, *45*, 242.
- R. Mo, Z. Gu, *Mater. Today* **2016**, *19*, 274.
- Z. Fang, L. Y. Wan, L. Y. Chu, Y. Q. Zhang, J. F. Wu, *Expert Opinion on Drug Delivery* **2015**, *12*, 1943.
- Y. Wang, D. S. Kohane, *Nat Rev Mater*. **2017**, *29*, 1606596.
- W. Feng, X. Han, R. Wang, X. Gao, P. Hu, W. Yue, Y. Chen, J. Shi, *Adv Mater*. **2019**, *31*, e1805919.
- M. J. Webber, E. A. Appel, E. W. Meijer, R. Langer, *Nat Mater*. **2015**, *15*, 13.
- P. Mi, *Theranostics* **2020**, *10*, 4557.
- A. E. Allen, J. W. Locasale, *Cancer Cell*. **2018**, *33*, 337.
- L. Wang, X. Niu, Q. Song, et al, *J. Controlled Release* **2020**, *318*, 197.
- P. E. Saw, H. Yao, C. Lin, W. Tao, O. C. Farokhzad, X. Xu, *Nano Lett*. **2019**, *19*, 5967.
- X. Zhang, M. Zhao, N. Cao, W. Qin, M. Zhao, J. Wu, D. Lin, *Biomater. Sci*. **2020**, *8*, 1885.
- G. Liu, H. Tsai, X. Zeng, Y. Zuo, W. Tao, J. Han, L. Mei, *Theranostics* **2017**, *7*, 1192.
- D. Zheng, J. Zhao, Y. Tao, J. Liu, L. Wang, J. He, J. Lei, K. Liu, *Chem. Eng. J*. **2020**, *389*.
- T. Zhang, Y. Wang, X. Ma, C. Hou, S. Lv, D. Jia, Y. Lu, P. Xue, Y. Kang, Z. Xu, *Biomater Sci*. **2020**, *8*, 473.
- S. Zhong, C. Chen, G. Yang, Y. Zhu, H. Cao, B. Xu, Y. Luo, Y. Gao, W. Zhang, *ACS Appl Mater Interf*. **2019**, *11*, 33697.
- Y. Li, Y. Miao, M. Chen, X. Chen, F. Li, X. Zhang, Y. Gan, *Theranostics* **2020**, *10*, 3722.
- B. Ma, W. Zhuang, H. Xu, G. Li, Y. Wang, *ACS Appl Mater Interf*. **2019**, *11*, 47259.
- W. Cheng, C. Liang, X. Wang, H. I. Tsai, G. Liu, Y. Peng, J. Nie, L. Huang, L. Mei, X. Zeng, *Nanoscale* **2017**, *9*, 17063.
- L. Fang, H. Lin, Z. Wu, Z. Wang, X. Fan, Z. Cheng, X. Hou, D. Chen, *Carbohydr. Polym*. **2020**, *234*, 115930.
- Z. Fang, S. Pan, P. Gao, H. Sheng, L. Li, L. Shi, Y. Zhang, X. Cai, *Int. J. Pharm*. **2020**, *575*, 118841.
- S. Liu, L. Wang, M. Zhang, K. Tao, B. Wang, M. Lin, X. Zhang, Y. Liu, Y. Hou, H. Zhang, B. Yang, *ACS Appl Mater Interf* **2019**, *11*, 25730.
- D. Qu, M. Jiao, H. Lin, C. Tian, G. Qu, J. Xue, L. Xue, C. Ju, C. Zhang, *Carbohydr. Polym*. **2020**, *229*, 115498.
- Y. Feng, Y. Cheng, Y. Chang, H. Jian, R. Zheng, X. Wu, K. Xu, L. Wang, X. Ma, X. Li, H. Zhang, *Biomaterials* **2019**, *217*, 119327.
- X. Han, K. Cheng, Y. Xu, Y. Wang, H. Min, Y. Zhang, X. Zhao, R. Zhao, G. J. Anderson, L. Ren, G. Nie, Y. Li, *J. Am. Chem. Soc*. **2020**, *142*, 2490.
- H. Tian, J. Zhang, H. Zhang, Y. Jiang, A. Song, Y. Luan, *Chem. Eng. J*. **2020**, *382*, 123043.
- X. Yuan, S. Peng, W. Lin, J. Wang, L. Zhang, *J. Colloid Interface Sci*. **2019**, *555*, 82.
- X. Li, Q. Xu, P. Zhang, X. Zhao, Y. Wang, *J. Controlled Release* **2019**, *314*, 72.
- L. H. Liu, W. X. Qiu, Y. H. Zhang, B. Li, C. Zhang, F. Gao, L. Zhang, X. Z. Zhang, *Adv. Funct. Mater*. **2017**, *27*, 1700220.
- N. Deirram, C. Zhang, S. S. Kermanian, A. P. R. Johnston, G. K. Such, *Macromol. Rapid Commun*. **2019**, *40*, e1800917.
- H. R. Jia, Y. X. Zhu, X. Liu, G. Y. Pan, G. Gao, W. Sun, X. Zhang, Y. W. Jiang, F. G. Wu, *ACS Nano* **2019**, *13*, 11781.
- W. Cheng, X. Zeng, H. Chen, Z. Li, W. Zeng, L. Mei, Y. Zhao, *ACS Nano* **2019**, *13*, 8537.
- F. Ponzio, J. Barthès, J. Bour, M. Michel, P. Bertani, J. Hemmerlé, M. D'Ischia, V. Ball, *Chem. Mater*. **2016**, *28*, 4697.
- W. Cheng, J. Nie, N. Gao, G. Liu, W. Tao, X. Xiao, L. Jiang, Z. Liu, X. Zeng, L. Mei, *Adv. Funct. Mater*. **2017**, *27*, 1704135.

44. W. Cheng, C. Liang, L. Xu, G. Liu, N. Gao, W. Tao, L. Luo, Y. Zuo, X. Wang, X. Zhang, X. Zeng, L. Mei, *Small* **2017**, *13*, 1700623.
45. J. Nie, W. Cheng, Y. Peng, G. Liu, Y. Chen, X. Wang, C. Liang, W. Tao, Y. Wei, X. Zeng, L. Mei, *Drug Deliv* **2017**, *24*, 1124.
46. X. Zeng, M. Luo, G. Liu, X. Wang, W. Tao, Y. Lin, X. Ji, L. Nie, L. Mei, *Adv Sci.* **2018**, *5*, 1800510.
47. W. Zeng, H. Zhang, Y. Deng, A. Jiang, X. Bao, M. Guo, Z. Li, M. Wu, X. Ji, X. Zeng, L. Mei, *Chem. Eng. J.* **2020**, *389*, 124494.
48. W. Cheng, J. Nie, L. Xu, C. Liang, Y. Peng, G. Liu, T. Wang, L. Mei, L. Huang, X. Zeng, *ACS Appl Mater Interf* **2017**, *9*, 18462.
49. G. Liu, N. Gao, Y. Zhou, J. Nie, W. Cheng, M. Luo, L. Mei, X. Zeng, W. Deng, *Pharmaceutics* **2019**, *11*, 507.
50. J. An, Y. G. Hu, K. Cheng, C. Li, X. L. Hou, G. L. Wang, X. S. Zhang, B. Liu, Y. D. Zhao, M. Z. Zhang, *Biomaterials* **2020**, *234*, 119761.
51. T. Finkel, *J. Cell Biol.* **2011**, *194*, 7.
52. W. Tao, Z. He, *Asian J Pharm. Sci.* **2018**, *13*, 101.
53. H. Pelicano, D. Carney, P. Huang, *Drug Res Updates* **2004**, *7*, 97.
54. W. Wu, M. Chen, T. Luo, Y. Fan, J. Zhang, Y. Zhang, Q. Zhang, A. Sapin-Minet, C. Gaucher, X. Xia, *Acta Biomater.* **2020**, *103*, 259.
55. Y. H. Gong, M. Shu, J. H. Xie, C. Zhang, Z. Cao, Z. Z. Jiang, J. Liu, *J. Mater. Chem. B* **2019**, *7*, 651.
56. Y. Cheng, X. Jiao, T. Xu, W. Wang, Y. Cao, Y. Wen, X. Zhang, *Small* **2017**, *13*.
57. B. Yang, K. Wang, D. Zhang, B. Sun, B. Ji, L. Wei, Z. Li, M. Wang, X. Zhang, H. Zhang, Q. Kan, C. Luo, Y. Wang, Z. He, J. Sun, *Biomater. Sci.* **2018**, *6*, 2965.
58. M. Li, L. Zhao, T. Zhang, Y. Shu, Z. He, Y. Ma, D. Liu, Y. Wang, *Acta Pharmaceutica Sin B* **2019**, *9*, 421.
59. K. Wang, B. Yang, H. Ye, X. Zhang, H. Song, X. Wang, N. Li, L. Wei, Y. Wang, H. Zhang, Q. Kan, Z. He, D. Wang, J. Sun, *ACS Appl. Mater. Interfaces* **2019**, *11*, 18914.
60. W. Yin, W. Ke, N. Lu, Y. Wang, A. A. W. M. M. Japir, F. Mohammed, Y. Wang, Y. Pan, Z. Ge, *Biomacromolecules* **2020**, *21*, 921.
61. Z. Luo, L. Jiang, S. Yang, Z. Li, W. M. W. Soh, L. Zheng, X. J. Loh, Y. L. Wu, *Adv Healthcare Mater.* **2019**, *8*, e1900406.
62. L. Yu, H. L. Ke, F. S. Du, Z. C. Li, *Biomacromolecules* **2019**, *20*, 2809.
63. F. Li, T. Li, W. Cao, L. Wang, H. Xu, *Biomaterials* **2017**, *133*, 208.
64. J. Wang, H. He, X. Xu, X. Wang, Y. Chen, L. Yin, *Biomaterials* **2018**, *171*, 72.
65. C. Y. Sun, Z. Cao, X. J. Zhang, R. Sun, C. S. Yu, X. Yang, *Theranostics* **2018**, *8*, 2939.
66. Y. Li, J. Hu, X. Liu, Y. Liu, S. Lv, J. Dang, Y. Ji, J. He, L. Yin, *Nano Res.* **2019**, *12*, 999.
67. M. Wang, Y. Zhai, H. Ye, Q. Lv, B. Sun, C. Luo, Q. Jiang, H. Zhang, Y. Xu, Y. Jing, L. Huang, J. Sun, Z. He, *ACS Nano* **2019**, *13*, 7010.
68. C. Wang, B. Huang, G. Yang, Y. Ouyang, J. Tian, W. Zhang, *Biomacromolecules* **2019**, *20*, 4218.
69. H. Jin, T. Zhu, X. Huang, M. Sun, H. Li, X. Zhu, M. Liu, Y. Xie, W. Huang, D. Yan, *Biomaterials* **2019**, *211*, 68.
70. Y. Zhang, Q. Guo, S. An, Y. Lu, J. Li, X. He, L. Liu, Y. Zhang, T. Sun, C. Jiang, *ACS Appl. Mater. Interfaces* **2017**, *9*, 12227.
71. P. Pei, C. Sun, W. Tao, J. Li, X. Yang, J. Wang, *Biomaterials* **2019**, *188*, 74.
72. Q. Pei, X. Hu, X. Zheng, S. Liu, Y. Li, X. Jing, Z. Xie, *ACS Nano* **2018**, *12*, 1630.
73. L. Xu, M. Zhao, W. Gao, Y. Yang, J. Zhang, Y. Pu, B. He, *Colloids Surf B Biointerfaces* **2019**, *181*, 252.
74. Y. Zhang, P. He, X. Liu, H. Yang, H. Zhang, C. Xiao, X. Chen, *Biomater. Sci.* **2019**, *7*, 3898.
75. Y. Wang, H. Liu, W. Jiang, Q. Wang, L. Hang, Y. Wang, *Biomater. Sci.* **2019**, *7*, 3706.
76. C. Dong, Q. Zhou, J. Xiang, F. Liu, Z. Zhou, Y. Shen, *J. Controlled Release* **2020**, *321*, 529.
77. D. Zhu, H. Yan, X. Liu, J. Xiang, Z. Zhou, J. Tang, X. Liu, Y. Shen, *Adv. Funct. Mater.* **2017**, *27*, 1606826.
78. T. Li, S. Pan, H. Zhuang, S. Gao, H. Xu, *ACS Appl. Bio Mater.* **2020**, *3*, 1283.
79. H. Li, Q. Li, W. Hou, J. Zhang, C. Yu, D. Zeng, G. Liu, F. Li, *ACS Appl. Mater. Interfaces* **2019**, *11*, 43581.
80. Y. He, S. Guo, L. Wu, P. Chen, L. Wang, Y. Liu, H. Ju, *Biomaterials* **2019**, *225*, 119501.
81. H. Chen, X. Zeng, H. P. Tham, S. Z. F. Phua, W. Cheng, W. Zeng, H. Shi, L. Mei, Y. Zhao, *Angew Chem - Int Ed* **2019**, *58*, 7641.
82. H. Zhu, Y. Fang, Q. Miao, X. Qi, D. Ding, P. Chen, K. Pu, *ACS Nano* **2017**, *11*, 8998.
83. S. Uthaman, S. Pillarisetti, A. P. Mathew, Y. Kim, W. K. Bae, K. M. Huh, I. K. Park, *Biomaterials* **2020**, *232*, 119702.
84. J. Lee, R. Jenjob, E. Davaa, S. G. Yang, *J. Controlled Release* **2019**, *305*, 120.
85. F. Q. Schafer, G. R. Buettner, *Free Radical Biol Med.* **2001**, *30*, 1191.
86. G. Wu, Y. Z. Fang, S. Yang, J. R. Lupton, N. D. Turner, *J. Nutr.* **2004**, *134*, 489.
87. P. Kuppusamy, H. Li, G. Ilangoan, A. J. Cardounel, J. L. Zweier, K. Yamada, M. C. Krishna, J. B. Mitchell, *Cancer Res.* **2002**, *62*, 307.
88. P. Mi, H. Yanagie, N. Dewi, H. C. Yen, X. Liu, M. Suzuki, Y. Sakurai, K. Ono, H. Takahashi, H. Cabral, K. Kataoka, N. Nishiyama, *J. Controlled Release* **2017**, *254*, 1.
89. P. Laskar, S. Somani, S. J. Campbell, M. Mullin, P. Keating, R. J. Tate, C. Irving, H. Y. Leung, C. Dufès, *Nanoscale* **2019**, *11*, 20058.
90. C. Maiti, S. Parida, S. Kayal, S. Maiti, M. Mandal, D. Dhara, *ACS Applied Materials and Interfaces* **2018**, *10*, 5318.
91. P. Huang, G. Wang, Y. Su, Y. Zhou, W. Huang, R. Zhang, D. Yan, *Theranostics* **2019**, *9*, 5755.
92. L. Qiu, L. Zhao, C. Xing, Y. Zhan, *Chin. Chem. Lett.* **2018**, *29*, 301.
93. F. Behroozi, M. J. Abdkhodaie, H. S. Abandansari, L. Satarian, M. Molazem, K. T. Al-Jamal, H. Baharvand, *Acta Biomater.* **2018**, *76*, 239.
94. Y. Liu, W. Zhen, L. Jin, S. Zhang, G. Sun, T. Zhang, X. Xu, S. Song, Y. Wang, J. Liu, H. Zhang, *ACS Nano* **2018**, *12*, 4886.
95. Q. Ren, K. Yang, R. Zou, Z. Wan, Z. Shen, G. Wu, Z. Zhou, Q. Ni, W. Fan, J. Hu, Y. Liu, *Nanoscale* **2019**, *11*, 23021.
96. X. Ling, X. Chen, I. A. Riddell, W. Tao, J. Wang, G. Hollett, S. J. Lippard, O. C. Farokhzad, J. Shi, J. Wu, *Nano Lett.* **2018**, *18*, 4618.
97. X. Ji, R. Zhang, Z. Wang, S. Niu, C. Ding, *ACS Appl. Bio Mater.* **2019**, *2*, 370.

98. W. W. Guo, Z. T. Zhang, Q. Wei, Y. Zhou, M. T. Lin, J. J. Chen, T. T. Wang, N. N. Guo, X. C. Zhong, Y. Y. Lu, Q. Y. Yang, M. Han, J. Gao, *Biomacromolecules* **2020**, *21*, 444.
99. T. Yin, Y. Wang, X. Chu, Y. Fu, L. Wang, J. Zhou, X. Tang, J. Liu, M. Huo, *ACS Appl. Mater. Interfaces* **2018**, *10*, 35693.
100. H. Deng, Z. Zhou, W. Yang, L. S. Lin, S. Wang, G. Niu, J. Song, X. Chen, *Nano Lett.* **2020**, *20*, 1928.
101. R. Iyer, T. Nguyen, D. Padanilam, C. Xu, D. Saha, K. T. Nguyen, Y. Hong, *J. Controlled Release* **2020**, *321*, 363.
102. S. Li, P. E. Saw, C. Lin, Y. Nie, W. Tao, O. C. Farokhzad, L. Zhang, X. Xu, *Biomaterials* **2020**, *234*, 119760.
103. D. Wang, Y. Ren, Y. Shao, L. Meng, *Polym. Chem.* **2017**, *8*, 6938.
104. Q. Tang, X. Ma, Y. Zhang, X. Cai, W. Xue, D. Ma, *Acta Biomater.* **2018**, *69*, 277.
105. Y. Shang, N. Zheng, Z. Wang, *Biomacromolecules* **2019**, *20*, 4602.
106. Y. Cheng, Y. Ji, *J. Controlled Release* **2020**, *318*, 38.
107. J. Tang, Z. Zeng, J. Yan, C. Chen, J. Liu, X. Feng, *J. Controlled Release* **2019**, *307*, 90.
108. S. P. Hadipour Moghaddam, J. Saikia, M. Yazdimamaghani, H. Ghandehari, *ACS Appl. Mater. Interfaces* **2017**, *9*, 21133.
109. Y. Lu, Y. Yang, Z. Gu, J. Zhang, H. Song, G. Xiang, C. Yu, *Biomaterials* **2018**, *175*, 82.
110. S. P. Hadipour Moghaddam, M. Yazdimamaghani, H. Ghandehari, *J. Controlled Release* **2018**, *282*, 62.
111. H. Mekaru, A. Yoshigoe, M. Nakamura, T. Doura, F. Tamanoi, *ACS Appl. Nano Mater.* **2019**, *2*, 479.
112. P. Venkatesan, N. Thirumalaivasan, H. P. Yu, P. S. Lai, S. P. Wu, *ACS Appl. Bio Mater.* **2019**, *2*, 1623.
113. X. He, J. Zhang, C. Li, Y. Zhang, Y. Lu, Y. Zhang, L. Liu, C. Ruan, Q. Chen, X. Chen, Q. Guo, T. Sun, J. Cheng, C. Jiang, *Theranostics* **2018**, *8*, 4884.
114. B. Sun, C. Luo, X. Zhang, M. Guo, M. Sun, H. Yu, Q. Chen, W. Yang, M. Wang, S. Zuo, P. Chen, Q. Kan, H. Zhang, Y. Wang, Z. He, J. Sun, *Nat Commun.* **2019**, *10*, 3211.
115. Y. X. Lin, Y. Wang, H. W. An, B. Qi, J. Wang, L. Wang, J. Shi, L. Mei, H. Wang, *Nano Lett.* **2019**, *19*, 2968.
116. C. Liang, H. Wang, M. Zhang, W. Cheng, Z. Li, J. Nie, G. Liu, D. Lian, Z. Xie, L. Huang, X. Zeng, *J. Colloid Interface Sci.* **2018**, *525*, 1.
117. H. Huang, Y. Dong, Y. Zhang, D. Ru, Z. Wu, J. Zhang, M. Shen, Y. Duan, Y. Sun, *Theranostics* **2019**, *9*, 1047.
118. X. Ling, J. Tu, J. Wang, A. Shajii, N. Kong, C. Feng, Y. Zhang, M. Yu, T. Xie, Z. Bharwani, B. M. Aljaeid, B. Shi, W. Tao, O. C. Farokhzad, *ACS Nano* **2019**, *13*, 357.
119. S. Wang, L. Yang, H. Y. Cho, S. T. Dean Chueng, H. Zhang, Q. Zhang, K. B. Lee, *Biomaterials* **2019**, *224*, 119498.
120. S. Wang, F. Li, R. Qiao, X. Hu, H. Liao, L. Chen, J. Wu, H. Wu, M. Zhao, J. Liu, R. Chen, X. Ma, D. Kim, J. Sun, T. P. Davis, C. Chen, J. Tian, T. Hyeon, D. Ling, *ACS Nano* **2018**, *12*, 12380.
121. X. Sun, G. Zhang, R. Du, R. Xu, D. Zhu, J. Qian, G. Bai, C. Yang, Z. Zhang, X. Zhang, D. Zou, Z. Wu, *Biomaterials* **2019**, *194*, 151.
122. G. Helmlinger, F. Yuan, M. Dellian, R. K. Jain, *Nat. Med.* **1997**, *3*, 177.
123. P. Vaupel, A. Mayer, *Cancer Metastasis Rev.* **2007**, *26*, 225.
124. F. Kallinowski, R. Zander, M. Hoeckel, P. Vaupel, *Int J Radiat Oncol Biol Phys* **1990**, *19*, 953.
125. R. Kumari, D. Sunil, R. S. Ningthoujam, *J. Controlled Release* **2020**, *319*, 135.
126. Y. Wang, Y. Xie, J. Li, Z. H. Peng, Y. Sheinin, J. Zhou, D. Oupický, *ACS Nano* **2017**, *11*, 2227.
127. P. Yuan, H. Zhang, L. Qian, X. Mao, S. Du, C. Yu, B. Peng, S. Q. Yao, *Angew Chem - Int Ed* **2017**, *56*, 12481.
128. C. Huang, W. Tan, J. Zheng, C. Zhu, J. Huo, R. Yang, *ACS Applied Materials and Interfaces* **2019**, *11*, 25740.
129. S. Son, N. V. Rao, H. Ko, S. Shin, J. Jeon, H. S. Han, V. Q. Nguyen, T. Thambi, Y. D. Suh, J. H. Park, *Int. J. Biol. Macromol.* **2018**, *110*, 399.
130. H. Li, W. Yan, X. Suo, H. Peng, X. Yang, Z. Li, J. Zhang, D. Liu, *Biomaterials* **2019**, *200*, 1.
131. K. M. Ihsanullah, B. N. Kumar, Y. Zhao, H. Muhammad, Y. Liu, L. Wang, H. Liu, W. Jiang, *Biomaterials* **2020**, *245*, 119982.
132. X. Si, S. Ma, Y. Xu, D. Zhang, N. Shen, H. Yu, Y. Zhang, W. Song, Z. Tang, X. Chen, *J. Controlled Release* **2020**, *320*, 83.
133. W. Wang, L. Lin, X. Ma, B. Wang, S. Liu, X. Yan, S. Li, H. Tian, X. Yu, *ACS Appl. Mater. Interfaces* **2018**, *10*, 19398.
134. X. Zhang, M. Wu, J. Li, S. Lan, Y. Zeng, X. Liu, J. Liu, *ACS Appl. Mater. Interfaces* **2018**, *10*, 21909.
135. S. Im, J. Lee, D. Park, A. Park, Y. M. Kim, W. J. Kim, *ACS Nano* **2019**, *13*, 476.
136. N. Ding, Z. Li, X. Tian, J. Zhang, K. Guo, P. Wang, *Chem. Commun.* **2019**, *55*, 13172.
137. W. Yin, M. Qiang, W. Ke, Y. Han, J. F. Mukerabigwi, Z. Ge, *Biomaterials* **2018**, *181*, 360.
138. L. Hua, Z. Wang, L. Zhao, H. Mao, G. Wang, K. Zhang, X. Liu, D. Wu, Y. Zheng, J. Lu, R. Yu, H. Liu, *Theranostics* **2018**, *8*, 5088.
139. H. He, R. Zhu, W. Sun, K. Cai, Y. Chen, L. Yin, *Nanoscale* **2018**, *10*, 2856.
140. Y. Li, A. Lu, M. Long, L. Cui, Z. Chen, L. Zhu, *Acta Biomater.* **2019**, *83*, 334.
141. S. J. Tseng, I. M. Kempson, K. Y. Huang, H. J. Li, Y. C. Fa, Y. C. Ho, Z. X. Liao, P. C. Yang, *ACS Nano* **2018**, *12*, 9894.
142. J. Zhen, S. Tian, Q. Liu, C. Zheng, Z. Zhang, Y. Ding, Y. An, Y. Liu, L. Shi, *Biomater. Sci.* **2019**, *7*, 2986.
143. N. Shen, J. Wu, C. Yang, H. Yu, S. Yang, T. Li, J. Chen, Z. Tang, X. Chen, *Nano Lett.* **2019**, *19*, 8021.
144. Z. Wang, Z. M. Chang, D. Shao, F. Zhang, F. Chen, L. Li, M. F. Ge, R. Hu, X. Zheng, Y. Wang, W. F. Dong, *ACS Appl. Mater. Interfaces* **2019**, *11*, 34755.
145. A. P. Bidkar, P. Sanpui, S. S. Ghosh, *ACS Appl. Bio Mater.* **2019**, *2*, 4077.
146. Y. Li, J. Dang, Q. Liang, L. Yin, *Biomaterials* **2019**, *209*, 138.
147. S. B. Reddy, S. K. Williamson, *Expert Opinion on Investigational Drugs* **2009**, *18*, 77.
148. K. B. Peters, J. M. Brown, *Cancer Res.* **2002**, *62*, 5248.
149. J. M. Brown, M. J. Lemmon, *Int J Radiat Oncol Biol Phys* **1991**, *20*, 457.
150. D. Chen, Y. Tang, J. Zhu, J. Zhang, X. Song, W. Wang, J. Shao, W. Huang, P. Chen, X. Dong, *Biomaterials* **2019**, *221*, 119422.
151. W. Wang, Y. Cheng, P. Yu, H. Wang, Y. Zhang, H. Xu, Q. Ye, A. Yuan, Y. Hu, J. Wu, *Nat. Commun.* **2019**, *10*, 1580.
152. Z. Sun, R. Li, J. Sun, Y. Peng, L. Xiao, X. Zhang, Y. Xu, M. Wang, *ACS Appl. Mater. Interfaces* **2017**, *9*, 40614.
153. F. H. Liu, C. Y. Hou, D. Zhang, W. J. Zhao, Y. Cong, Z. Y. Duan, Z. Y. Qiao, H. Wang, *Biomater. Sci.* **2018**, *6*, 604.
154. J. Yang, Y. Yang, N. Kawazoe, G. Chen, *Biomaterials* **2019**, *197*, 317.

155. G. Iaccarino, M. Profeta, R. Vecchione, P. A. Netti, *Acta Biomater.* **2019**, *89*, 265.
156. K. Yang, Y. Liu, Y. Wang, Q. Ren, H. Guo, J. B. Matson, X. Chen, Z. Nie, *Biomaterials* **2019**, *223*, 119460.
157. C. Battistella, C. E. Callmann, M. P. Thompson, S. Yao, A. V. Yeldandi, T. Hayashi, D. A. Carson, N. C. Gianneschi, *Adv. Healthcare Mater.* **2019**, *8*, e1901105.
158. J. Jiang, N. Shen, T. Ci, Z. Tang, Z. Gu, G. Li, X. Chen, *Adv. Mater.* **2019**, *31*, e1904278.
159. Y. Chau, F. E. Tan, R. Langer, *Bioconj Chem* **2004**, *15*, 931.
160. N. Li, H. Cai, L. Jiang, J. Hu, A. Bains, J. Hu, Q. Gong, K. Luo, Z. Gu, *ACS Appl. Mater. Interfaces* **2017**, *9*, 6865.
161. Z. Duan, H. Cai, H. Zhang, K. Chen, N. Li, Z. Xu, Q. Gong, K. Luo, *ACS Appl. Mater. Interfaces* **2018**, *10*, 35770.
162. H. Cai, X. Wang, H. Zhang, L. Sun, D. Pan, Q. Gong, Z. Gu, K. Luo, *Appl. Mater. Today* **2018**, *11*, 207.
163. H. Han, D. Valdepérez, Q. Jin, B. Yang, Z. Li, Y. Wu, B. Pelaz, W. J. Parak, J. Ji, *ACS Nano* **2017**, *11*, 1281.
164. X. Gu, M. Qiu, H. Sun, J. Zhang, L. Cheng, C. Deng, Z. Zhong, *Biomater. Sci.* **2018**, *6*, 1526.
165. C. Cao, D. Sheng, X. Li, F. Xue, L. Liu, Y. Zhong, P. Wei, R. Li, T. Yi, *Chem. Commun.* **2019**, *55*, 11872.
166. H. Yamamoto, S. Iku, Y. Adachi, A. Imsumran, H. Taniguchi, K. Noshio, Y. Min, S. Horiuchi, M. Yoshida, F. Itoh, K. Imai, *J. Pathol.* **2003**, *199*, 176.
167. J. C. Cuggino, F. E. Ambrosioni, M. L. Picchio, M. Nicola, Á. F. Jiménez Kairuz, G. Gatti, R. J. Minari, M. Calderón, C. I. Alvarez Igartzabal, L. M. Gugliotta, *Int. J. Biol. Macromol.* **2020**, *154*, 446.
168. M. Ghavami, T. Shiraishi, P. E. Nielsen, *ACS Appl. Bio Mater.* **2020**, *3*, 1018.
169. X. Guan, Y. Chen, X. Wu, P. Li, Y. Liu, *Chem. Commun.* **2019**, *55*, 953.
170. S. Saxena, A. Pradeep, M. Jayakannan, *ACS Appl. Bio Mater.* **2019**, *2*, 5245.
171. S. He, L. Mei, C. Wu, M. Tao, Z. Zhai, K. Xu, W. Zhong, *Nanoscale* **2019**, *11*, 5030.
172. R. G. Østrem, L. Parhamifar, H. Pourhassan, G. Clergeaud, O. L. Nielsen, A. Kjær, A. E. Hansen, T. L. Andresen, *J. Controlled Release* **2017**, *262*, 212.
173. Q. Ren, Z. Liang, X. Jiang, P. Gong, L. Zhou, Z. Sun, J. Xiang, Z. Xu, X. Peng, S. Li, W. Li, L. Cai, J. Tang, *Int. J. Biol. Macromol.* **2019**, *130*, 845.
174. X. Dong, W. Yin, X. Zhang, S. Zhu, X. He, J. Yu, J. Xie, Z. Guo, L. Yan, X. Liu, Q. Wang, Z. Gu, Y. Zhao, *ACS Appl. Mater. Interfaces* **2018**, *10*, 4271.
175. L. Hou, Y. Zhang, X. Yang, C. Tian, Y. Yan, H. Zhang, J. Shi, H. Zhang, Z. Zhang, *ACS Appl. Mater. Interfaces* **2019**, *11*, 255.
176. P. Wu, Y. Sun, W. Dong, H. Zhou, S. Guo, L. Zhang, X. Wang, M. Wan, Y. Zong, *Nanoscale* **2019**, *11*, 11470.
177. Y. Huang, Y. Shi, Q. Wang, T. Qi, X. Fu, Z. Gu, Y. Zhang, G. Zhai, X. Zhao, Q. Sun, G. Lin, *J. Controlled Release* **2019**, *316*, 208.
178. A. Sharma, E. J. Kim, H. Shi, J. Y. Lee, B. G. Chung, J. S. Kim, *Biomaterials* **2018**, *155*, 145.
179. W. H. Chen, G. F. Luo, Y. S. Sohn, R. Nechushtai, I. Willner, *Adv. Funct. Mater.* **2019**, *29*, 1805341.
180. L. Zhang, Y. Wang, X. Zhang, X. Wei, X. Xiong, S. Zhou, *ACS Appl. Mater. Interfaces* **2017**, *9*, 3388.
181. J. Yang, S. Pan, S. Gao, Y. Dai, H. Xu, *Biomaterials* **2020**, *249*, 120054.
182. H. Qiao, J. Jia, H. Shen, S. Zhao, E. Chen, W. Chen, B. Di, C. Hu, *Adv. Healthcare Mater.* **2019**, *8*, e1900174.
183. X. Jia, Y. Zhang, Y. Zou, Y. Wang, D. Niu, Q. He, Z. Huang, W. Zhu, H. Tian, J. Shi, Y. Li, *Adv. Mater.* **2018**, *30*, 1704490.
184. D. B. Cheng, X. H. Zhang, Y. J. Gao, D. Wang, L. Wang, H. Chen, Z. Y. Qiao, H. Wang, *Small* **2019**, *15*, e1901813.
185. J. Zhou, X. Du, X. Chen, J. Wang, N. Zhou, D. Wu, B. Xu, *J. Am. Chem. Soc.* **2018**, *140*, 2301.
186. J. Shi, J. P. Schneider, *Angew Chem - Int Ed* **2019**, *58*, 13706.
187. Z. Gong, Y. Shi, H. Tan, L. Wang, Z. Gao, B. Lian, G. Wang, H. Sun, P. Sun, B. Zhou, J. Bai, *ACS Appl. Mater. Interfaces* **2020**, *12*, 4323.
188. Z. Gu, S. Zhu, L. Yan, F. Zhao, Y. Zhao, *Adv. Mater.* **2019**, *31*, e1800662.
189. A. P. Blum, J. K. Kammeyer, A. M. Rush, C. E. Callmann, M. E. Hahn, N. C. Gianneschi, *J. Am. Chem. Soc.* **2015**, *137*, 2140.
190. J. Yao, J. Feng, J. Chen, *Asian J Pharm. Sci.* **2016**, *11*, 585.
191. W. Cai, J. Wang, C. Chu, W. Chen, C. Wu, G. Liu, *Adv. Sci.* **2019**, *6*, 1801526.
192. X. Li, J. Kim, J. Yoon, X. Y. Chen, *Adv. Mater.* **2017**, *29*, 24.
193. Y. Zhang, D. Yang, H. Chen, W. Q. Lim, F. S. Z. Phua, G. An, P. Yang, Y. Zhao, *Biomaterials* **2018**, *163*, 14.
194. M.-X. Wu, Y.-W. Yang, *Adv. Mater.* **2017**, *29*, 1606134.
195. M. Liu, H. Du, W. Zhang, G. Zhai, *Mater Sci Eng C-Mater Biol Appl.* **2017**, *71*, 1267.
196. D. Liu, F. Yang, F. Xiong, N. Gu, *Theranostics* **2016**, *6*, 1306.
197. S. Geng, H. Zhao, G. Zhan, Y. Zhao, X. Yang, *ACS Appl. Mater. Interfaces* **2020**, *12*, 7995.
198. L. Thai Minh Duy, B.-K. Jung, Y. Li, D. Huu Thuy Trang, N. Thanh Loc, J. W. Hong, C.-O. Yun, D. S. Lee, *Biomater. Sci.* **2019**, *7*, 4195.
199. Z. Wang, J. Guo, J. Sun, P. Liang, Y. Wei, X. Deng, W. Gao, *Adv. Sci.* **2019**, *6*, 1900586.
200. Y. Wen, Y. Liu, H. Zhang, M. Zou, D. Yan, D. Chen, Y. Zhao, *Nanoscale* **2019**, *11*, 2687.
201. J. Zheng, C. Bai, H. Peng, L. Zhao, H. Xiong, *J. Magn. Magn. Mater.* **2020**, *497*, 166012.
202. Y. Cui, R. Deng, X. Li, X. Wang, Q. Jia, E. Bertrand, K. Meguelati, Y.-W. Yang, *Chin. Chem. Lett.* **2019**, *30*, 2291.
203. R. Li, Z. Lin, Q. Zhang, Y. Zhang, Y. Liu, Y. Lyu, X. Li, C. Zhou, G. Wu, N. Ao, L. Li, *ACS Appl. Mater. Interfaces* **2020**, *12*, 17948.
204. Z. Huang, H. Xiao, X. Lu, W. Yan, Z. Ji, *Int. J. Nanomed.* **2018**, *13*, 7623.
205. M. Luo, T. Fan, Y. Zhou, H. Zhang, L. Mei, *Adv. Funct. Mater.* **2019**, *29*, 1808306.
206. A. Jhaveri, P. Deshpande, V. Torchilin, *J. Controlled Release* **2014**, *190*, 352.
207. C. Thang Do, Z. Wang, X. Lu, B. Xing, *Theranostics* **2019**, *9*, 3308.
208. M. Karimi, A. Ghasemi, P. S. Zangabad, R. Rahighi, S. M. M. Basri, H. Mirshekari, M. Amiri, Z. S. Pishabad, A. Aslani, M. Bozorgomid, D. Ghosh, A. Beyzavi, A. Vaseghi, A. R. Aref, L. Haghani, S. Bahrami, M. R. Hamblin, *Chem. Soc. Rev.* **2016**, *45*, 1457.

209. Z. Meng, X. Zhou, J. Xu, X. Han, Z. Dong, H. Wang, Y. Zhang, J. She, L. Xu, C. Wang, Z. Liu, *Adv. Mater.* **2019**, *31*, e1900927.
210. M. Qiu, D. Wang, W. Liang, L. Liu, Y. Zhang, X. Chen, D. K. Sang, C. Xing, Z. Li, B. Dong, F. Xing, D. Fan, S. Bao, H. Zhang, Y. Cao, *Proc. Natl. Acad. Sci. USA* **2018**, *115*, 501.
211. T. J. Dougherty, G. B. Grindey, R. Fiel, K. R. Weishaupt, D. G. Boyle, *J. Natl. Cancer Inst.* **1975**, *55*, 115.
212. S. S. Lucky, K. C. Soo, Y. Zhang, *Chem. Rev.* **2015**, *115*, 1990.
213. X. Li, S. Lee, J. Yoon, *Chem. Soc. Rev.* **2018**, *47*, 1174.
214. S.-Y. Li, H. Cheng, B.-R. Xie, W.-X. Qiu, J.-Y. Zeng, C.-X. Li, S.-S. Wan, L. Zhang, W.-L. Liu, X.-Z. Zhang, *ACS Nano* **2017**, *11*, 7006.
215. Y. Dou, Y. Liu, F. Zhao, Y. Guo, X. Li, M. Wu, J. Chang, C. Yu, *Theranostics* **2018**, *8*, 5870.
216. Q. Wu, G. Chen, K. Gong, J. Wang, X. Ge, X. Liu, S. Guo, F. Wang, *Matter* **2019**, *1*, 496.
217. W. Zhang, J. Lu, X. Gao, P. Li, W. Zhang, Y. Ma, H. Wang, B. Tang, *Angew Chem - Int Ed* **2018**, *57*, 4891.
218. H. Min, J. Wang, Y. Qi, Y. Zhang, X. Han, Y. Xu, J. Xu, Y. Li, L. Chen, K. Cheng, G. Liu, N. Yang, Y. Li, G. Nie, *Adv. Mater.* **2019**, *31*, e1808200.
219. X.-G. Wang, Z.-Y. Dong, H. Cheng, S.-S. Wan, W.-H. Chen, M.-Z. Zou, J.-W. Huo, H.-X. Deng, X.-Z. Zhang, *Nanoscale* **2015**, *7*, 16061.
220. R. Chen, J. Zhang, Y. Wang, X. Chen, J. A. Zapien, C.-S. Lee, *Nanoscale* **2015**, *7*, 17299.
221. X. Wan, H. Zhong, W. Pan, Y. Li, Y. Chen, N. Li, B. Tang, *Angew Chem - Int Ed* **2019**, *58*, 14134.
222. J. Fang, Q. Wang, G. Yang, X. Xiao, L. Li, T. Yu, *Colloids Surfaces B-Biointerfaces* **2019**, *179*, 250.
223. W. Zeng, H. Zhang, Y. Deng, A. Jiang, X. Bao, M. Guo, Z. Li, M. Wu, X. Ji, X. Zeng, L. Mei, *Chem Eng J* **2020**, *389*, 124494.
224. Q. Zhang, J. Zhang, S. Wan, W. Wang, L. Fu, *Adv. Funct. Mater.* **2018**, *28*, 1802500.
225. X. Li, J. Shan, W. Zhang, S. Su, L. Yuwen, L. Wang, *Small* **2017**, *13*, 1602660.
226. A. R. Rastinehad, H. Anastos, E. Wajswol, J. S. Winoker, J. P. Sfakianos, S. K. Doppalapudi, M. R. Carrick, C. J. Knauer, B. Taouli, S. C. Lewis, A. K. Tewari, J. A. Schwartz, S. E. Canfield, A. K. George, J. L. West, N. J. Halas, *Proc. Natl. Acad. Sci. USA* **2019**, *116*, 18590.
227. H. Lin, S. Gao, C. Dai, Y. Chen, J. Shi, *J. Am. Chem. Soc.* **2017**, *139*, 16235.
228. Y.-H. Chien, K. K. Chan, T. Anderson, K. V. Kong, B. K. Ng, K.-T. Yong, *Adv. Ther.* **2019**, *2*, 1800090.
229. X. Ji, Y. Kang, J. Ouyang, Y. Chen, D. Artzi, X. Zeng, Y. Xiao, C. Feng, B. Qi, N. Y. Kim, P. E. Saw, N. Kong, O. C. Farokhzad, W. Tao, *Adv. Sci.* **2019**, *6*, 1901211.
230. Z. Liu, S. Zhang, H. Lin, M. Zhao, H. Yao, L. Zhang, W. Peng, Y. Chen, *Biomaterials* **2018**, *155*, 54.
231. W. Tao, X. Ji, X. Zhu, L. Li, J. Wang, Y. Zhang, P. E. Saw, W. Li, N. Kong, M. A. Islam, T. Gan, X. Zeng, H. Zhang, M. Mahmodi, G. J. Tearney, O. C. Farokhzad, *Adv. Mater.* **2018**, *30*, e1802061.
232. J. Shao, H. Xie, H. Huang, Z. Li, Z. Sun, Y. Xu, Q. Xiao, X.-F. Yu, Y. Zhao, H. Zhang, H. Wang, P. K. Chu, *Nat. Commun.* **2016**, *7*, 12967.
233. L. Chen, M. Qian, H. Jiang, Y. Zhou, Y. Du, Y. Yang, T. Huo, R. Huang, Y. Wang, *Biomaterials* **2020**, *236*, 119770.
234. W. Tao, X. Zhu, X. Yu, X. Zeng, Q. Xiao, X. Zhang, X. Ji, X. Wang, J. Shi, H. Zhang, L. Mei, *Adv. Mater.* **2017**, *29*, 1603276.
235. W. Tao, X. Zeng, J. Wu, X. Zhu, X. Yu, X. Zhang, J. Zhang, G. Liu, L. Mei, *Theranostics* **2016**, *6*, 470.
236. X. Zeng, W. Tao, L. Mei, L. Huang, C. Tan, S.-S. Feng, *Biomaterials* **2013**, *34*, 6058.
237. M. Luo, W. Cheng, X. Zeng, L. Mei, G. Liu, D. W., *Pharmaceutics* **2019**, *11*, 342.
238. G. Liu, H.-I. Tsai, X. Zeng, J. Qi, M. Luo, X. Wang, L. Mei, W. Deng, *Chem. Eng. J.* **2019**, *375*, 121917.
239. N. Gao, C. Xing, H. Wang, L. Feng, X. Zeng, L. Mei, Z. Peng, *Frontiers Pharmacol* **2019**, *10*, 270.
240. X. Ji, N. Kong, J. Wang, W. Li, Y. Xiao, S. T. Gan, Y. Zhang, Y. Li, X. Song, Q. Xiong, S. Shi, Z. Li, W. Tao, H. Zhang, L. Mei, J. Shi, *Adv. Mater.* **2018**, *30*, e1803031.
241. H. Zhang, W. Zeng, C. Pan, L. Feng, M. Ou, X. Zeng, X. Liang, M. Wu, X. Ji, L. Mei, *Adv. Funct. Mater.* **2019**, *29*, 1903791.
242. W. Cheng, J. Nie, L. Xu, C. Liang, Y. Peng, G. Liu, T. Wang, L. Mei, L. Huang, X. Zeng, *ACS Appl. Mater. Interfaces* **2017**, *9*, 18462.
243. S. Liu, J. Pan, J. Liu, Y. Ma, F. Qiu, L. Mei, X. Zeng, G. J. S. Pan, *Small* **2018**, *14*, 1703968.
244. G. Liu, N. Gao, Y. Zhou, J. Nie, W. Cheng, M. Luo, L. Mei, X. Zeng, W. Deng, *Pharmaceutics* **2019**, *11*, 507.
245. A. Shanei, A. Sazgarnia, *Iranian J Basic Med Sci* **2019**, *22*, 848.
246. Y. Zhou, X. Han, X. Jing, Y. Chen, *Adv Healthc Mater* **2017**, *6*, 1700646.
247. F. Gong, L. Cheng, N. Yang, O. Betzer, L. Feng, Q. Zhou, Y. Li, R. Chen, R. Popovtzer, Z. Liu, *Adv. Mater.* **2019**, *31*, e1900730.
248. C. Yang, Y. Li, M. Du, Z. Chen, *J. Drug Targeting* **2019**, *27*, 33.
249. T. Mainprize, N. Lipsman, Y. Huang, Y. Meng, A. Bethune, S. Ironside, C. Heyn, R. Alkins, M. Trudeau, A. Sahgal, J. Perry, K. Hyynnen, *Sci. Rep.* **2019**, *9*, 321.
250. Y. Liu, W. Zhen, Y. Wang, J. Liu, L. Jin, T. Zhang, S. Zhang, Y. Zhao, S. Song, C. Li, J. Zhu, Y. Yang, H. Zhang, *Angew Chem - Int Ed* **2019**, *58*, 2407.
251. Z. Shi, Y. Zhou, T. Fan, Y. Lin, H. Zhang, L. Mei, *Smart Mater Med* **2020**, *1*, 32.
252. G. Li, S. Wang, D. Deng, Z. Xiao, Z. Dong, Z. Wang, Q. Lei, S. Gao, G. Huang, E. Zhang, G. Zeng, Z. Wen, S. Wu, Z. Liu, *ACS Nano* **2020**, *14*, 1586.
253. S. Liang, X. Deng, G. Xu, X. Xiao, M. Wang, X. Guo, P. a. Ma, Z. Cheng, D. Zhang, J. Lin, *Adv. Funct. Mater.* **2020**, *30*, 1908598.
254. S. Malekmohammadi, H. Hadadzadeh, S. Rezakhani, Z. Amirghofran, *ACS Biomater. Sci. Eng.* **2019**, *5*, 4405.
255. X. Lin, S. Liu, X. Zhang, R. Zhu, S. Chen, X. Chen, J. Song, H. Yang, *Angew Chem - Int Ed* **2020**, *59*, 1682.
256. Z. Meng, X. Zhou, J. She, Y. Zhang, L. Feng, Z. Liu, *Nano Lett.* **2019**, *19*, 8109.
257. G. Song, L. Cheng, Y. Chao, K. Yang, Z. Liu, *Adv. Mater.* **2017**, *29*, 1700996.
258. J. Beik, M. Khateri, Z. Khosravi, S. K. Kamrava, S. Kooranifar, H. Ghaznavi, A. Shakeri-Zadeh, *Coordination Chem Rev* **2019**, *387*, 299.
259. D. De Ruysscher, G. Niedermann, N. G. Burnet, S. Siva, A. W. M. Lee, F. Hegi-Johnson, *Nat. Rev. Dis. Primers* **2019**, *5*, 13.
260. T. I. Kostelnik, C. Orvig, *Chem. Rev.* **2019**, *119*, 902.

261. K. Lu, C. He, N. Guo, C. Chan, K. Ni, G. Lan, H. Tang, C. Pelizzari, Y.-X. Fu, M. T. Spiotto, R. R. Weichselbaum, W. Lin, *Nat. Biomed. Eng.* **2018**, *2*, 600.
262. Y. Yong, X. Cheng, T. Bao, M. Zu, L. Yan, W. Yin, C. Ge, D. Wang, Z. Gu, Y. Zhao, *ACS Nano* **2015**, *9*, 12451.
263. J. Xie, L. Gong, S. Zhu, Y. Yong, Z. Gu, Y. Zhao, *Adv. Mater.* **2019**, *31*, e1802244.
264. W. Sun, L. Luo, Y. Feng, Y. Cai, Y. Zhuang, R.-J. Xie, X. Chen, H. Chen, *Angew Chem - Int Ed* **2020**, *59*, 9914.
265. W. Sun, T. Shi, L. Luo, X. Chen, P. Lv, Y. Lv, Y. Zhuang, J. Zhu, G. Liu, X. Chen, H. Chen, *Adv. Mater.* **2019**, *31*, e1808024.
266. G. Song, Y. Chen, C. Liang, X. Yi, J. Liu, X. Sun, S. Shen, K. Yang, Z. Liu, *Adv. Mater.* **2016**, *28*, 7143.
267. N. Lee, D. Yoo, D. Ling, M. H. Cho, T. Hyeon, J. Cheon, *Chem. Rev.* **2015**, *115*, 10637.
268. Z.-Q. Zhang, S.-C. Song, *Biomaterials* **2016**, *106*, 13.
269. J.-X. Fan, M.-Y. Peng, H. Wang, H.-R. Zheng, Z.-L. Liu, C.-X. Li, X.-N. Wang, X.-H. Liu, S.-X. Cheng, X.-Z. Zhang, *Adv. Mater.* **2019**, *31*, 1808278.
270. J. Liu, W. Liu, K. Zhang, J. Shi, Z. Zhang, *Adv. Healthcare Mater.* **2020**, *9*, e1901316.
271. Z. Ferjaoui, E. J. Al Dine, A. Kulmukhamedova, L. Bezdetnaya, C. S. Chan, R. Schneider, F. Mutelet, D. Mertz, S. Begin-Colin, F. Quiles, E. Gaffet, H. Alem, *ACS Appl. Mater. Interfaces* **2019**, *11*, 30610.
272. B. Li, P. Ji, S.-Y. Peng, P. Pan, D.-W. Zheng, C.-X. Li, Y.-X. Sun, X.-Z. Zhang, *Adv. Mater.* **2020**, *32*, 2000376.
273. J. Hu, Y. Xu, Y. Zhang, *Chin. Chem. Lett.* **2019**, *30*, 2039.
274. X. Jing, Z. Zhi, L. Jin, F. Wang, Y. Wu, D. Wang, K. Yan, Y. Shao, L. Meng, *Nanoscale* **2019**, *11*, 9457.
275. A. Ibrahim, E. Twizeyimana, N. Lu, W. Ke, J. F. Mukerabigwi, F. Mohammed, A. A. W. M. M. Japir, Z. Ge, *ACS Appl. Bio Mater.* **2019**, *2*, 5099.
276. F. Lin, D. Wen, X. Wang, R. I. Mahato, *Biomaterials* **2019**, *192*, 95.
277. Y. Qu, B. Chu, X. Wei, M. Lei, D. Hu, R. Zha, L. Zhong, M. Wang, F. Wang, Z. Qian, *J. Controlled Release* **2019**, *296*, 93.
278. D. Chen, G. Zhang, R. Li, M. Guan, X. Wang, T. Zou, Y. Zhang, C. Wang, C. Shu, H. Hong, L. J. Wan, *J. Am. Chem. Soc.* **2018**, *140*, 7373.
279. S. Bai, X. Ma, X. Shi, J. Shao, T. Zhang, Y. Wang, Y. Cheng, P. Xue, Y. Kang, Z. Xu, *ACS Appl. Mater. Interfaces* **2019**, *11*, 36130.
280. G. Yang, S. Z. F. Phua, W. Q. Lim, R. Zhang, L. Feng, G. Liu, H. Wu, A. K. Bindra, D. Jana, Z. Liu, Y. Zhao, *Adv. Mater.* **2019**, *31*, e1901513.
281. D. Guo, S. Xu, W. Yasen, C. Zhang, J. Shen, Y. Huang, D. Chen, X. Zhu, *Biomaterials Science* **2020**, *8*, 694.
282. X. Jiang, X. Fan, W. Xu, C. Zhao, H. Wu, R. Zhang, G. Wu, *Controlled Release* **2019**, *316*, 196.
283. S. Li, M. Sun, C. Hao, A. Qu, X. Wu, L. Xu, C. Xu, H. Kuang, *Angew. Chem.* **2020**, *59*, 13915.
284. Y. Qiao, Y. Qiao, F. Yang, T. Xie, Z. Du, D. Zhong, Y. Qi, Y. Li, W. Li, W. Li, Z. Lu, J. Rao, Y. Sun, Y. Sun, M. Zhou, M. Zhou, M. Zhou, *Sci. Adv.* **2020**, *6*, eaba5996.
285. W. Xu, J. Qian, G. Hou, Y. Wang, J. Wang, T. Sun, L. Ji, A. Suo, Y. Yao, *Acta Biomater.* **2019**, *83*, 400.
286. Y. Cui, R. Deng, X. Li, X. Wang, Q. Jia, E. Bertrand, K. Meguelati, Y. W. Yang, *Chin. Chem. Lett.* **2019**, *30*, 2291.
287. Y. Gao, C. M. Dong, *Chin. Chem. Lett.* **2018**, *29*, 927.
288. P. Wei, M. Sun, B. Yang, J. Xiao, J. Du, *J. Controlled Release* **2020**, *322*, 81.
289. P. Zhang, Y. Wang, J. Lian, Q. Shen, C. Wang, B. Ma, Y. Zhang, T. Xu, J. Li, Y. Shao, F. Xu, J. J. Zhu, *Adv. Mater.* **2017**, *29*.
290. R. Zhu, L. Su, J. Dai, Z. W. Li, S. Bai, Q. Li, X. Chen, J. Song, H. Yang, *ACS Nano* **2020**, *14*, 3991.
291. J. An, Y. G. Hu, C. Li, X. L. Hou, K. Cheng, B. Zhang, R. Y. Zhang, D. Y. Li, S. J. Liu, B. Liu, D. Zhu, Y. D. Zhao, *Biomaterials* **2020**, *230*, 119636.
292. L. Chan, P. Gao, W. Zhou, C. Mei, Y. Huang, X. F. Yu, P. K. Chu, T. Chen, *ACS Nano* **2018**, *12*, 12401.
293. Y. Lu, A. A. Aimetti, R. Langer, Z. Gu, *Nature Rev Mater* **2016**, *2*, 16075.
294. S. Nardecchia, P. Sánchez-Moreno, J. de Vicente, J. A. Marchal, H. Boulaiz, *Nanomaterials* **2019**, *9*, 191.
295. J. Cheng, K. T. Khin, G. S. Jensen, A. Liu, M. E. Davis, *Bioconj. Chem* **2003**, *14*, 1007.
296. C. Young, T. Schluep, J. Hwang, S. Eliasof, *Curr. Bioact. Compd.* **2011**, *7*, 8.
297. A. Takahashi, Y. Yamamoto, M. Yasunaga, Y. Koga, J. I. Kuroda, M. Takigahira, M. Harada, H. Saito, T. Hayashi, Y. Kato, T. Kinoshita, N. Ohkohchi, I. Hyodo, Y. Matsumura, *Cancer Sci.* **2013**, *104*, 920.
298. M. J. A. De Jonge, M. Slingerland, W. J. Loos, E. A. C. Wiemer, H. Burger, R. H. J. Mathijssen, J. R. Kroep, M. A. G. Den Hollander, D. Van Der Biessen, M. H. Lam, J. Verweij, H. Gelderblom, *Eur J Cancer* **2010**, *46*, 3016.
299. H. Chen, F. Li, Y. Yao, Z. Wang, Z. Zhang, N. Tan, *Theranostics* **2019**, *9*, 90.
300. J. H. Shi, T. R. Wang, Y. Q. You, M. L. Akhtar, Z. J. Liu, F. Han, Y. Li, Y. Wang, *Nanoscale* **2019**, *11*, 13078.

AUTHOR BIOGRAPHIES



Yao Yang received her BSc (2015) and MSc (2019) degrees in School of Pharmaceutical Sciences at Sun Yat-Sen University (SYSU). In 2019, she started her PhD study under the supervision of Dr. Xiaowei Zeng in School of Pharmaceutical Sciences (Shenzhen) at Sun Yat-sen University (SYSU). Her research focuses on the design and synthesis of multifunctional smart biomaterials for cancer theranostics.



Xiaowei Zeng received his PhD degree from Nankai University in 2011 and carried out his postdoctoral work at Tsinghua University. Currently, he is an associate professor in the School of Pharmaceutical Sciences (Shenzhen), Sun Yat-sen University. His research mainly focuses on biomaterials, molecular pharmaceutics, and nanocarriers for biomedical applications.



Lin Mei received his BS degree from Fudan University in 2003 and PhD degree from Peking Union Medical College, Tsinghua University, in 2007. He is a professor and Assistant Dean of the School of Pharmaceutical Sciences (Shenzhen), Sun Yat-sen University. His research interests are focused on biomaterials, molecular pharmaceuticals, and drug delivery systems.

How to cite this article: Yang Y, Zeng W, Huang P, Zeng X, Mei L. Smart Materials for Drug Delivery and Cancer Therapy. *VIEW*. 2021;2:20200042.

<https://doi.org/10.1002/VIW.20200042>